

RELATIONSHIP BETWEEN FLUID FLOW  
IN CELLULOSE AND THE GENERATED  
ELECTRIC ENERGY WITH APPLICATION  
TO WATER MOVEMENT IN PLANTS

Thesis for the Degree of Ph. D.  
MICHIGAN STATE UNIVERSITY  
MOUNIR A. MORCOS  
1969



This is to certify that the

thesis entitled

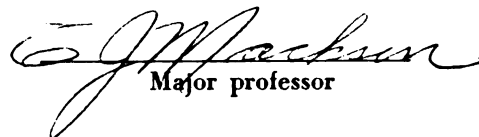
RELATIONSHIP BETWEEN FLUID FLOW IN CELLULOSE AND  
THE GENERATED ELECTRIC ENERGY WITH APPLICATION  
TO WATER MOVEMENT IN PLANTS

presented by

Mounir A. Morcos

has been accepted towards fulfillment  
of the requirements for

Ph.D. degree in Agr. Eng.

  
Major professor

Date 31 Oct 69

## ABSTRACT

### RELATIONSHIP BETWEEN FLUID FLOW IN CELLULOSE AND THE GENERATED ELECTRIC ENERGY WITH APPLICATION TO WATER MOVEMENT IN PLANTS

by Mounir A. Morcos

The concept of electro-osmotic flow in plants was examined. The engineering bases of fluid flow inside xylem vessels were studied, and the nature and the role of the electric potential and current in plants were investigated.

A review of the fundamental bases of plant anatomy and physiology was done to examine the limits imposed by them on the vascular tissues and the whole intact plant. The finding of many of the early and latest experiments in the area of electro-osmosis, was interpreted by the zeta potential concept.

A model representing xylem vessels was developed. The flow of energy through this model was analyzed mathematically. The energy balance equation for the model was solved for dissipated energy, which was considered to be the source of the generated electric energy.

The relationship between the dissipated energy and the electric energy was examined by forcing water to pass through a cellulose pad of filter papers. Different water heads were applied, and voltage, current, flow rate were measured and recorded. The tested fluids were: distilled deionized water at 23.8<sup>o</sup>c and at 30.0<sup>o</sup>c, CO<sub>2</sub>-saturated water, (0.005M) and (0.01M) KCl solution.

Mounir A. Morcos

The results showed that the source of electric energy may not be an "intrinsic constant quantity" of the material and the liquid such as zeta potential. The electric energy may be a product of the flow process itself.

A theory "The Electron Accumulation Theory" was developed to relate the generated electric energy to energy losses due to the dynamics of water flow through porous materials.

Applying these results to the plant, showed that "electro-osmosis", according to its definition, does not play a role in sap movement in xylem vessels.

Physiological processes in plants which may be explained by the "Electron Accumulation Theory" include a negative charge existing on root hair surfaces as a result of the flow of soil water to the cortex of the root.

The structure of xylem vessels permits xylem sap to keep high tensile stresses. These tensile stresses, combined with the electric behavior of the flow, may cause the xylem sap to act as a communication system along the whole height of the plant.

Equations for energy dissipation which can be solved by using numerical techniques were developed.

Approved

  
Major Professor

Approved

  
Department Chairman

RELATIONSHIP BETWEEN FLUID FLOW IN CELLULOSE AND  
THE GENERATED ELECTRIC ENERGY WITH APPLICATION  
TO WATER MOVEMENT IN PLANTS

By

Mounir A. Morcos

A THESIS

Submitted to  
Michigan State University  
in partial fulfillment of the requirements  
for the degree of

DOCTOR OF PHILOSOPHY  
Department of Agricultural Engineering

1969

661751  
4-27-70

## ACKNOWLEDGMENTS

The author is grateful for the assistance of all who helped him in this study. He is extremely appreciative for Dr. Chester J. Mackson (Agricultural Engineering) for his continuous assistance and encouragement, and for the suggestion of the topic of this research.

To Dr. Klaus Raschke (Atomic Energy Commission), the author expresses his gratitude for the time, instrumentation, and his constructive criticisms.

To Dr. Bill A. Stoute (Agricultural Engineering), Dr. George E. Merva (Agricultural Engineering), Dr. Harold Davidson (Horticulture), and Dr. Rolland T. Hinkle (Mechanical Engineering), the author expresses his sincere appreciation for their guidance, encouragement, and helpful suggestions.

The author wishes to thank Dr. Carl W. Hall, Chairman of the Agricultural Engineering Department for his assistance in so many ways.

Special thanks are due the people of U.A.R. Cultural and Educational Bureau for their help whenever needed. Appreciations are extended to many graduate students at Michigan State University, especially Mr. Samir Mansy and Mr. John Gerrish for their valuable suggestions.

The author also appreciates the help of Mrs. Sharyon Morgan in the typing of the manuscript.

To:

My family, my wife Eugeni, and my daughter

Hanan, for their many sacrifices.

## TABLE OF CONTENTS

	Page
ACKNOWLEDGMENTS .....	ii
DEDICATION .....	iii
LIST OF FIGURES .....	vi
LIST OF APPENDICES .....	viii
 Chapter	
I INTRODUCTION.....	1
I.A Nature of the Problem.....	1
I.B Objectives.....	2
II REVIEW OF LITERATURE.....	4
II.A The Structure of the Plant.....	4
II.A-1 The Structural Unit of Plant Tissue.....	4
II.A-2 The Conducting Tissues of the Plant.....	8
II.B Sap Translocation.....	14
II.B-1 Root Pressure Theory.....	14
II.B-2 The Cohesion Theory.....	15
II.C Assimilates Translocation.....	18
II.D Electrical Potential in Plants.....	22
II.E Background Theories.....	28
III MATHEMATICAL ANALYSIS OF FLUID TRANSLOCATION INSIDE XYLEM TISSUE.....	39
IV EXPERIMENTAL ANALYSIS.....	57
V DISCUSSION OF RESULTS.....	64
V.A The Source of the Natural Electrical Potential	64
V.A-1 First Theory.....	65
V.A-2 Second Theory "Electron Accumulation Theory"	68
V.A-3 The Validity of "Electron Accumulation Theory"	69
V.B The Relationship Between Fluid Flow and The Electric Phenomenon.....	72
V.B-1 Electric Responses to the Tested Fluids....	72
V.B-2 Numerical Evaluation of Electric Responses to the Tested Fluids.....	87
V.B-3 The Role of Electric Energy in Plant.....	97



Chapter	Page
V.C The Role of Xylem Vessel Wall Structure in Plant.....	103
V.C-1 The Generation of Electric Energy.....	103
V.C-2 The Existence of High Tensile Stresses in Xylem Sap.....	104
V.C-3 The Existence of a Communication System in Plants.....	108
VI SUMMARY AND CONCLUSIONS.....	112
VI.A Summary.....	112
VI.B Conclusions.....	113
VII RECOMMENDATIONS FOR FURTHER STUDY.....	115
SELECTED REFERENCES.....	117
APPENDICES.....	122

## LIST OF FIGURES

Figure		Page
1	The Major Parts of the Plant.....	5
2	Plant Cell.....	7
3	The Pit.....	7
4	Cell Wall Construction.....	7
5	Xylem Tissue.....	10
6	Phloem Tissue.....	11
7	Sieve Plate.....	11
8	The Microstructure of the Root.....	12
9	The Microstructure of the Stem.....	12
10	The Microstructure of the Leaf.....	13
11	Root Pressure Theory.....	17
12	The Cohesion Theory.....	17
13	Patterns of Water Uptake.....	17
14	Effect of Cuts on Water Path.....	17
15	Cytoplasm Streaming.....	19
16	Münch Mechanism.....	19
17	Pressure Flow Mechanism (Münch Mech) in Plant.....	19
18	The Physiological Processes in Plant.....	40
19	Xylem Tube Model.....	42
20	Energy Flow Through Tube Wall.....	42
21	Flow Work Through a Tube Section.....	42
22	Schematic Diagram of the Used Apparatus.....	58

Figure	Page
23	A. The Apparatus Used To Determine The Electrical Current and Voltage. Showing The General Set Up Instrumentation, and Faraday Cage..... 59
	B. A Close Up of the Cellulose Pad in the Plexi-glass container..... 59
24	Effect of Water Flow Through Cellulose Pad..... 66
25	Effect of Pressure Head on Electrical Potential.... 66
26	Schematic Diagram Represents The Source of Electrical Potential in the Cellulose Pad..... 70
27	The Effects of the Flow of Distilled Deionized Water (23.8 <sup>o</sup> c) in Cellulose Pad, on the Voltage, Current and Electric Energy..... 77
28	The Effects of the Flow of Warm Water (30.0 <sup>o</sup> c) in Cellulose Pad, on the Voltage, Current and Electric Energy..... 78
29	The Effects of the Flow of CO <sub>2</sub> -Saturaged Water in Cellulose Pad, on the <sup>2</sup> Voltage, Current and Electric Energy..... 79
30	The Effects of the Flow of (0.005M) KCl Solution in Cellulose Pad, on Voltage, Current, and Electric Energy..... 80
31	The Effects of the Flow of (0.01M) KCl Solution in Cellulose Pad on the Voltage, Current and Electric Energy..... 81
32	Electric Energy and Dissipated Energy as Function of $(\Delta p)^2$ ..... 82
33	The Generated Electric Energy of the Fluid Tested.. 83
34	The Effect of the Distance Between Downstream Electrode and Pad Surface, on Voltage and Current..... 84
35	The Effects of Flow of Distilled Deionized Water (22.6 <sup>o</sup> c) in a Glass Fiber Pad on Voltage, Current, and Dissipated and Electric Energy... 86
36	Flow Pattern During the 24 Hours of the Day..... 98
37	Vapor Bubble Formation..... 109
38	The Apparatus Used in Testing the Existence of Tensile Stress in Water Column..... 109

## LIST OF APPENDICES

Appendix		Page
	Table A.1	
	The Effect of Flow of Deionized Distilled Water Through Cellulose Pad (23.8 <sup>o</sup> c) ..	123
	Table A.2	
	The Effect of Flow of Warm Deionized Dis- tilled Water Through Cellulose Pad (30.0 <sup>o</sup> c).....	124
	Table A.3	
	The Effect of Flow of CO <sub>2</sub> Saturated Water Through Cellulose Pad (23.4 <sup>o</sup> c).....	125
	Table A.4	
	The Effect of Flow of (.005M) KCl Solution Through Cellulose Pad (23.8 <sup>o</sup> c) .....	126
	Table A.5	
	The Effect of Flow of (.01 M) KCl Solution Through Cellulose Pad (23.8 <sup>o</sup> c) .....	127
	Table A.6	
	The Effect of the Distance of Down Stream Electrode From the Pad .....	128
	Table A.7	
	The Effect of Flow of Deionized Distilled Water Through Glass Fiber Pad (22.6 <sup>o</sup> c)	129

## I. INTRODUCTION

### I-A. Nature of the Problem:

Fluid translocation in plants is one of the topics which receives a lot of interest and research in the field of plant biology. The nature of this process is still not completely understood. The translocation of sap in trees explained by many theories: capillarity, imbibition, vital pumping, and finally the cohesion theory. The translocation of assimilates has been explained by: diffusion, protoplasmic streaming, changing turgidity, and finally by mass flow along a gradient of hydrostatic pressure.

The natural electric current which was observed in living plants, has attracted the attention of many scientists. Some investigators related this current to translocation of sap, and tried to force the sap to move inside the tissues of the plant by applying an external electric current or potential. Others offered new theories about the role of electro-osmosis in the translocation of sap and assimilates. To study this electro-osmosis concept, or the use of electrical potential in general, many experiments have been performed. However many of the investigators attacked the problem with little considerations of either the limits imposed by both the anatomy of vascular tissues and the whole intact living plant, or the physical laws controlling any process of fluid translocation. To determine the role of electro-osmosis in fluid translocation inside the plant, the study must be based on both these limits and

those physical laws which have been extensively studied in other fields of science. The role of electro-osmosis may have great potential and may make many contributions in plant production, as many scientists have predicted. However, this study is intended to investigate this role from the engineering point of view. It will investigate the engineering bases of fluid flow inside the plant, and try to determine if there is, in fact, any significant role of the electrical potential in the flow of fluids inside the plant.

Since sap and assimilates translocation is a fluid flow process, a physical model representing plant vascular tissues will help in studying this fluid flow process which might take place in this model, and will help in constructing the physical equations which can represent these processes.

The degree of agreement between these equations and the result of experiments performed will show the validity of the model, and at the same time, the role of electro-osmosis in fluid translocation in plants.

I-B. Objectives:

1. Constructing a physical model representing the plant tissues.
2. Studying the physical processes of fluid flow in that model.
3. Constructing the equations which describe the flow process.

4. Evaluating these equations experimentally to determine their validity and the validity of the concept of electro-osmotic flow in plants.

## II. REVIEW OF LITERATURE

### II-A. The Structure of the Plant:

According to Fuller (1963), the body of most flowering plants is composed of four kinds of structures: roots, stems, leaves, and flowers. The first three are the vegetative parts and their functions center upon the intake of raw materials, the manufacture of food, and the utilization of food for growth and development. The flowers are the reproductive parts and are concerned with the formation of seeds, Figure 1.

The roots are non-green in color and their principal functions are the absorption of water and nutrients from the soil, the anchorage of the plant body in the soil, the conduction of materials upward into the stem and downward from the stem and leaves, and sometimes, the storage of considerable quantities of food. Stems arise usually as branched continuations of the root system and their primary functions are the conduction of materials upward, downward and transversely, the production and support of leaves and flowers, and sometimes, the storage of food. The chief function of leaves is the manufacture of food. This process is known as photosynthesis.

#### II-A-1. The Structure Unit of Plant Tissue:

The smallest structural unit of plants is the cell. Plant cells are extremely varied in size, structure and functions. In general, a plant cell, figure 2, is constructed of:

1. The cell wall which enclose the living substance.



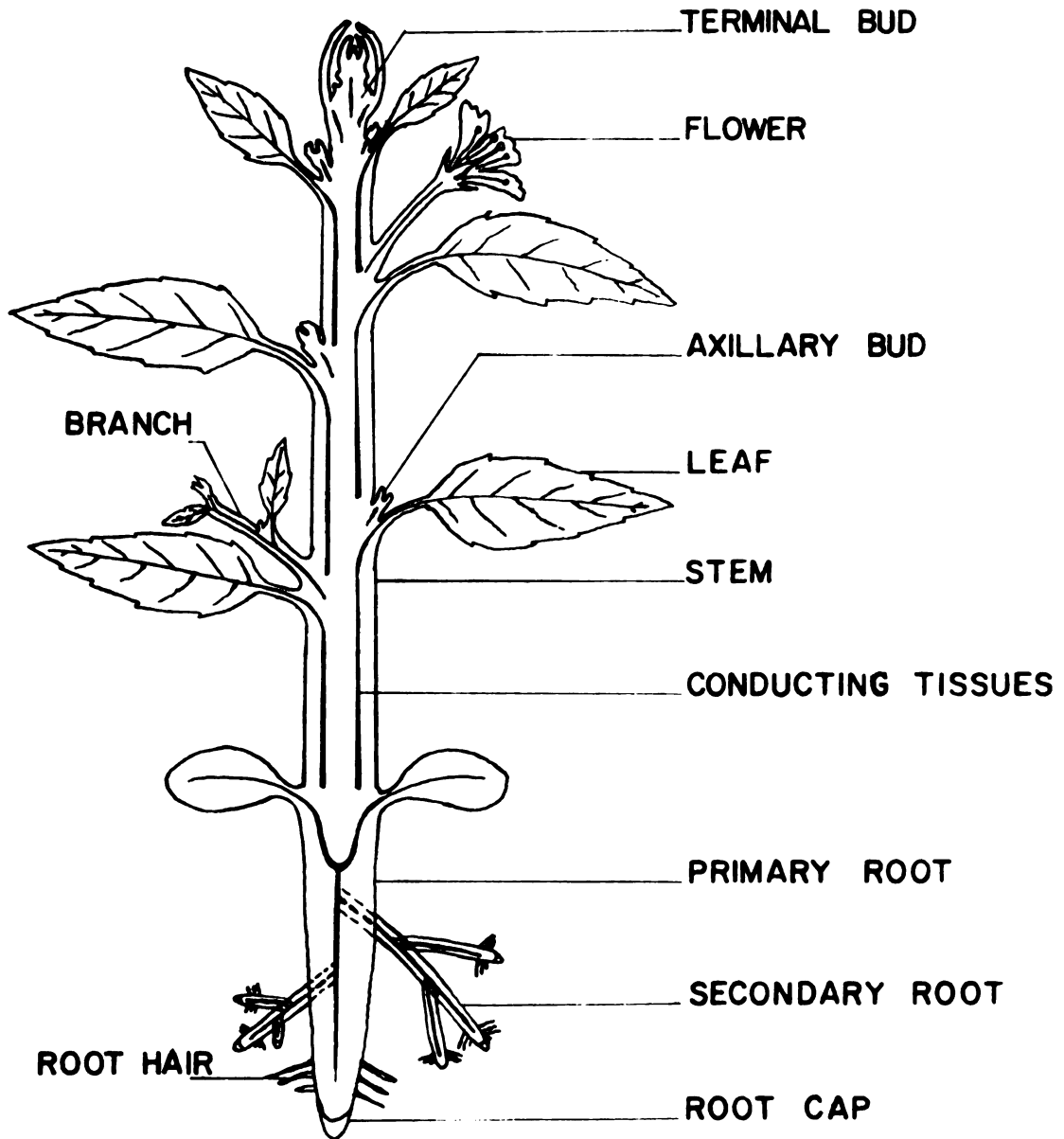


FIG. I. THE MAJOR PARTS OF THE PLANT.

FULLER, (1963)

2. The protoplast, or the living component of a single cell, which consists of the cytoplasm with the nucleus and other component embedded in it.
3. The ergastic substances, which are the nonliving materials present within the cell, such as liquids, crystals and other solid bodies.

#### 1. The Cell Wall

Cell walls have a layered structure: the middle lamella which is a pectic substance, the primary wall which consists chiefly of cellulose, hemicellulose and pectic materials, and the secondary wall which is deposited upon the primary wall after the cell attains its final size and consists chiefly of cellulose. The secondary wall layers do not develop at certain points to form the pits, Figure 3, which facilitate the passage of water and dissolved materials. Lignin, which is a polymer of high carbon content, may be present in all three wall layers, Esau (1965).

Cellulose occurs in the form of long chain molecules with length as great as five microns. A cellulose molecule has a maximum width of  $8 \text{ \AA}$ . Cellulose molecules are combined into micelle with diameter of  $100 \text{ \AA}$  and contains about 100 cellulose molecules in a transection. The micelles form a bundle called microfibril which is  $250 \text{ \AA}$  wide and contains about 2000 cellulose molecules. Microfibrils are combined into macrofibrils  $0.4 \text{ micron}$  wide and containing 500,000 cellulose molecules in a transection, Figure 4. These macrofibrils are oriented into

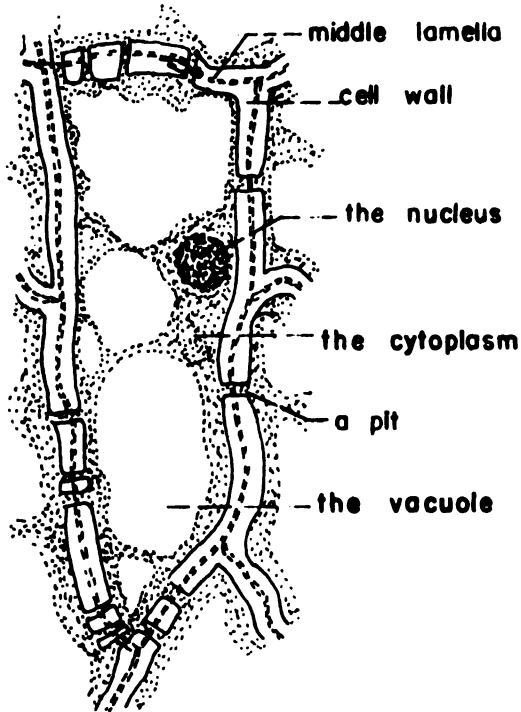


FIG. 2 - PLANT CELL

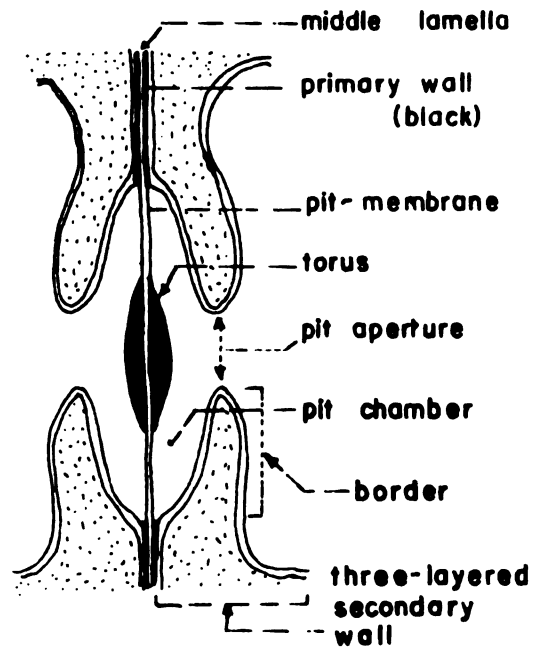


FIG. 3 - THE PIT

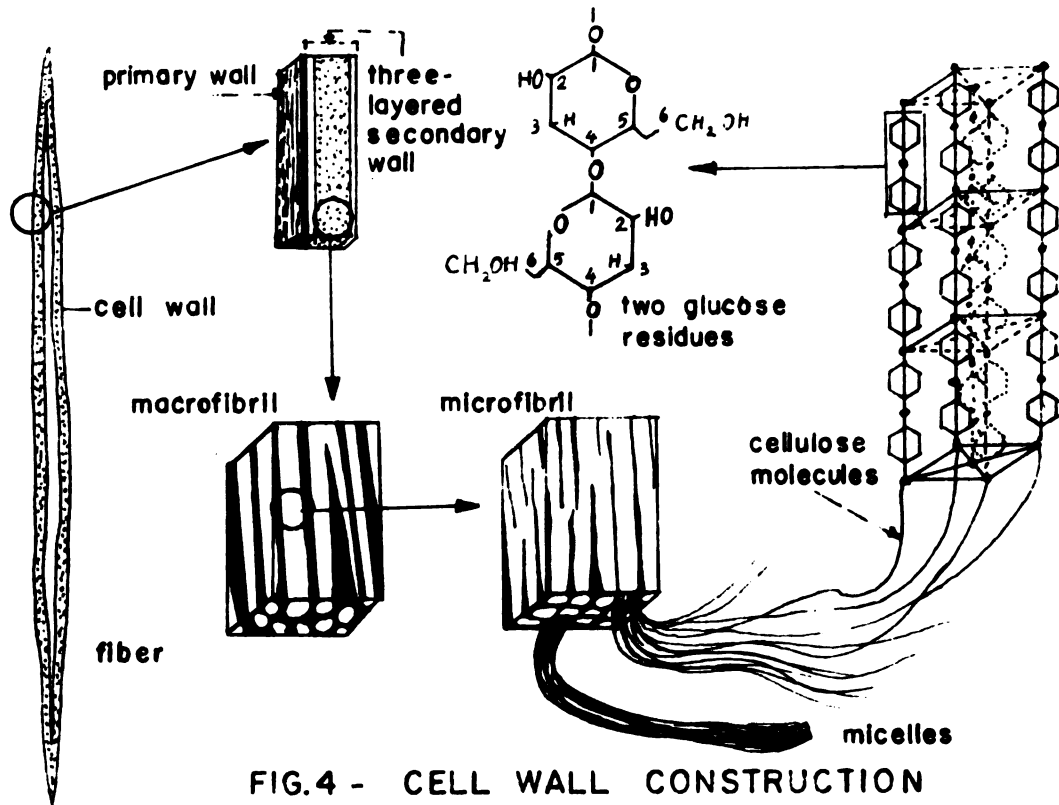


FIG. 4 - CELL WALL CONSTRUCTION

ESAU, (1965)

two or three layers, almost perpendicular on each other, Preston (1965).

Cellulose does not dissolve in water, but it absorbs water in large quantities and therefore, most all walls are in a highly hydrated or saturated condition.

## 2. Protoplast:

Consists of many components: the nucleus embedded in the cytoplasm, the cytoplasm layer, and a vacuole filled with cell sap inside the cytoplasm layer. The cytoplasm layer is surrounded by two membranes, the endoplast around the vacuole, and the ectoplast between the cytoplasm and the cell wall. Both membranes control the passage of materials into and out of the living protoplast.

There are cytoplasmic connections between cells. The cell walls possess minute pores through which extend fine thread of cytoplasm called plasmodesmata. These plasmodesmata provide a means for the interchanging of materials of adjoining cells.

## 3. Ergastic Substance

These were previously mentioned.

## II-A-2. The Conducting Tissues of the Plant:

The conducting tissues of plants are, the xylem and the phloem tissues.

### 1. Xylem Tissue:

The function of xylem tissue is mainly to translocate water

and dissolved materials from the soil to the leaves. The components of this tissue are the tracheids, vessels, ray parenchyma cells, fibers, and xylem parenchyma, Figure 5. The vessels and tracheids are constructed of dead cells which lack protoplasm at maturity. The inside diameter of xylem vessel ranges from  $20\mu$  to  $400\mu$  in trees. In vines it may be as much as  $700\mu$  in diameter.

## 2. Phloem Tissue:

The function of phloem tissue is to conduct food from the leaves to other parts of plants. The components of this tissue are the sieve tube members, companion cells, phloem parenchyma, ray parenchyma cells, and phloem fibers, Figure 6.

Sieve tubes, like xylem vessels, are vertically elongated rows of cylindrical cells. However, the end walls of the sieve tubes contain numerous perforations, and the cells contain living protoplasm, but the nuclei are absent at maturity, and the cytoplasm is continuous from cell to cell through the sieve plates of the end walls.

The length of sieve tube ranges from 550 micron with pitted fine-porous plates, to short membered tubes have a length of about 135 microns with transverse wide-meshed plates. The average diameter of sieve tube is  $23\mu$ . The diameter of the pores in the sieve plates ranges from a fraction of a micron to 15 micron, and are associated with callose, a polymer of glucose residues, Figure 7. Figures 8, 9, and 10 show the location of these tissues in the root, stem and leaf respectively.

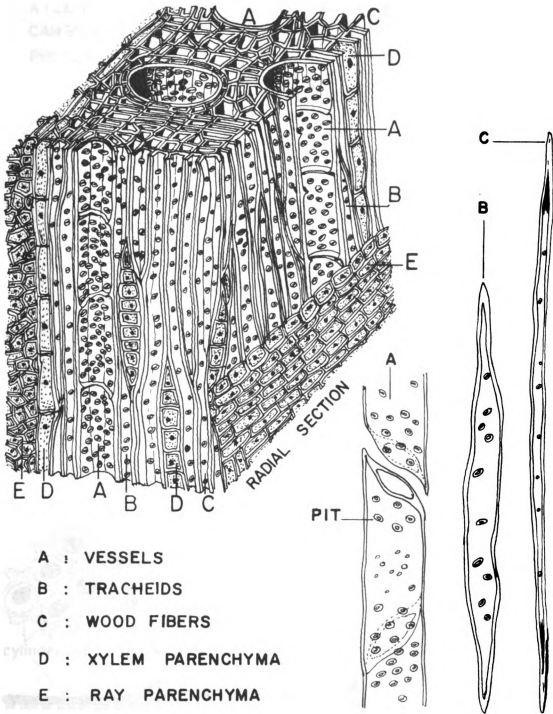


**FIG. 5 XYLEM TISSUE.**

FULLER, (1963)

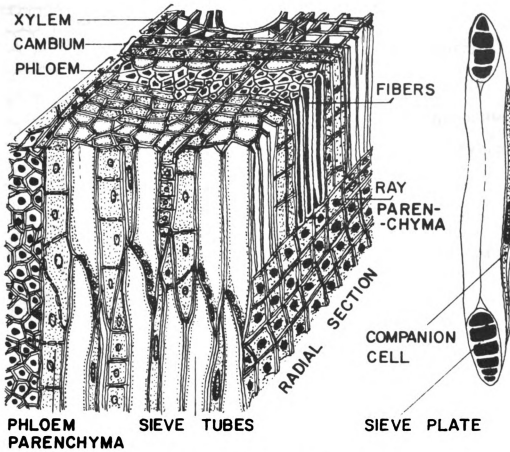


FIG. 6 - PHLOEM TISSUE  
FULLER, (1963)

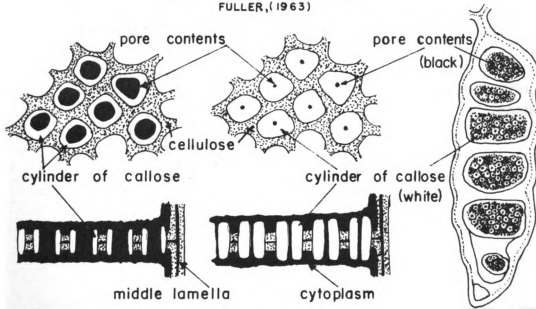
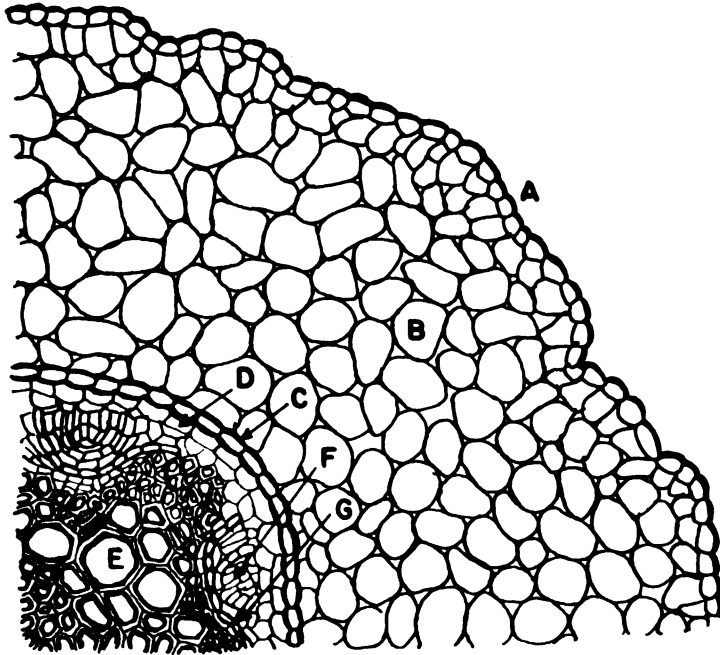
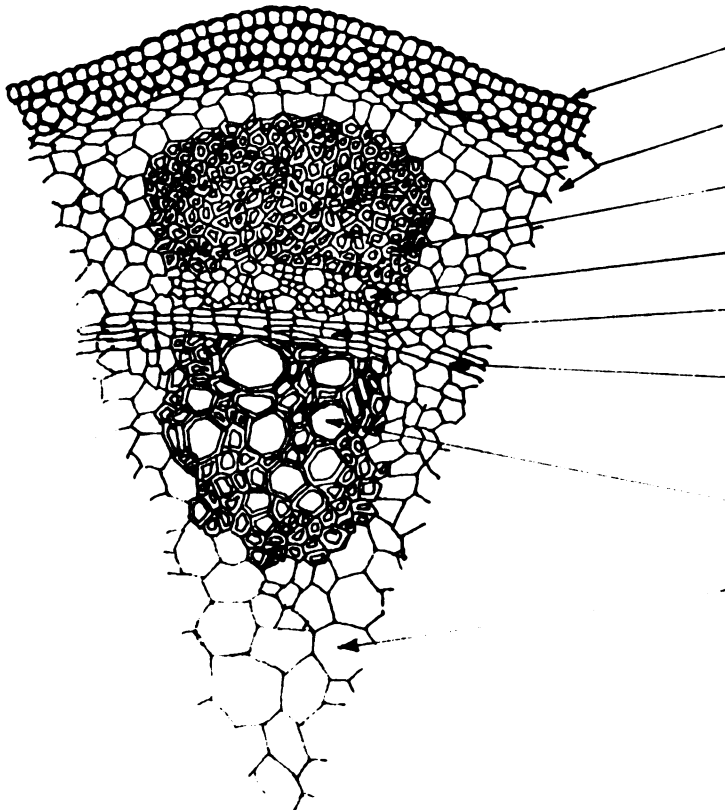


FIG. 7 - SIEVE PLATE  
ESAU, (1965)



- A EPIDERMIS
- B CORTEX
- C ENDODERMIS
- D PERICYCLE
- E XYLEM
- F PHLOEM
- G CAMBIUM

FIG. 8 - THE MICROSTRUCTURE OF THE ROOT

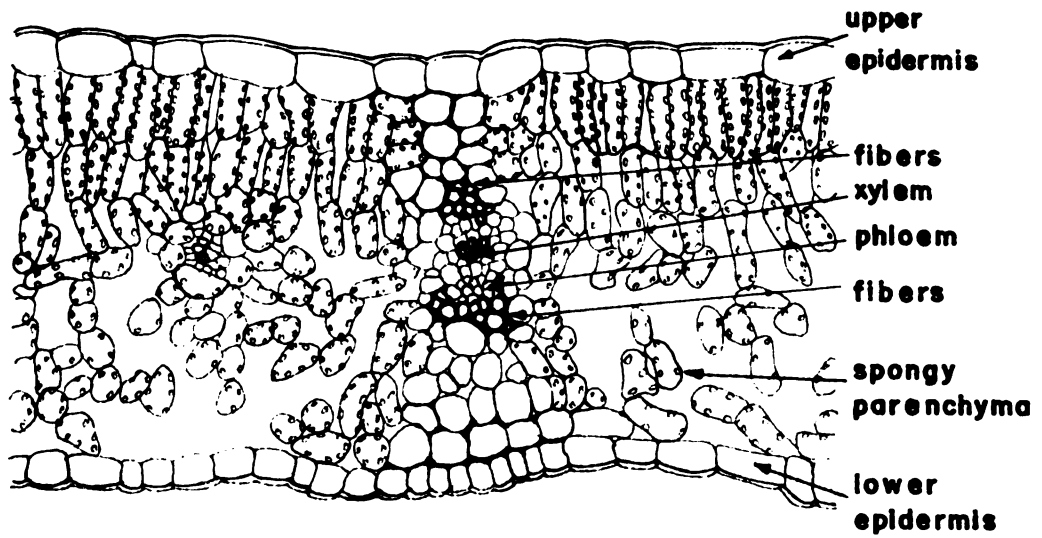


- EPIDERMIS
- CORTEX
- BUNDLE CAP FIBERS
- PHLOEM
- FASCICULAR CAMBIUM
- INTERFASCICULAR CAMBIUM
- XYLEM
- PITH

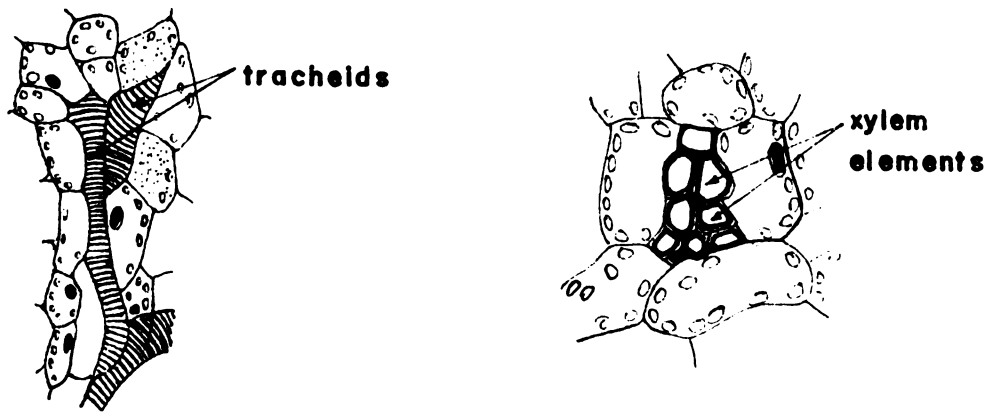
FIG. 9 - THE MICROSTRUCTURE OF THE STEM

"SUNFLOWER"- FULLER, (1963)





A. cross section in the leaf



B. the ends of xylem elements

FIG. 10 - THE MICROSTRUCTURE OF THE LEAF

"PEAR LEAF" - ESAU, (1965)

## II-B. Sap Translocation:

Salisbury (1966), summarized the two main theories of sap translocation: the root pressure theory, and the cohesion theory.

### II-B-1. Root Pressure Theory:

In this theory, the dissolved salts from the soil solution diffuse through the apoplast of the cortex of the root. The apoplast includes the cell walls and the intercellular spaces. The symplast, which is the living part of the cell, then accumulates these ions actively by moving them across the actoplast by its metabolic processes. This metabolic activity is due to the ample amount of available oxygen in the cells nearest the surface of the cortex tissues of the root. These ions can move via the symplast toward the inside root, where the oxygen tension is much lower and the processes of accumulation are much less efficient. These ions then begin to leak out into the surrounding apoplast and into the water-filled xylem tubes. Such an increase in concentration would then put into effect the process of osmosis, with the semi-permeable endodermal layer of cells acting as the semipermeable membrane of an osmometer, Figure 11.

Crafts (1961) pointed out that sap exudation from root pressure is not abnormal flow contingent upon cutting, for if the atmosphere was allowed to become saturated, solution would appear in droplets at the hydathodes and drips from the plant. However, Fisher (1949), suggested that the pressure in the trunk

of a tree is sub-atmospheric since when holes were bored at the base of a tree, sap flow did not occur but water poured into the hole was absorbed.

Kozlowski (1964) pointed out that there still are many arguments against the importance of root pressure to sap ascent, and it is generally considered not to play a primary role in ascent of sap.

#### II-B-2. The Cohesion Theory:

If water evaporates from the leaves at a fairly rapid rate, root pressures are not expected to develop at all, and the plant seems to act simply as a water conduit between the soil and the air. The actual movement of water through the stem is in response to hydraulic gradients, but these in turn are established by the free-energy gradient. Under atmospheric pressure, there is a steep gradient from low to high, "Diffusion Pressure Deficite", "DPD", and from high to low free energy, going from the soil water through the plant into the atmosphere, Figure 12. The term, "DPD", is defined as the difference between the osmotic pressure, "OP", and the Turgor pressure, "TP", which is that pressure exerted against the cytoplasm and hence the cell wall as a result of osmosis.

$$DPD = OP - TP$$

As water evaporates and is removed from the leaf, it will be pulled up in the xylem elements. Rather high tensions may be

developed in holding the column of water together between the roots and the leaves. Kozlowski (1964), indicated that the cohesion theory has been re-examined and re-evaluated in the light of recent data, and many objections have been raised. These objections include the impossibility of existence of tensile channels in presence of free air bubbles, inadequacy of tensile strength of water, failure of stem pressures to decrease proportionally with increase in height, and insufficient evidence for existence of continuous water columns.

Preston (1938), pointed out that many vessels were found filled with gas, and Scholander (1955), has proved that vapor bubbles in the vine did not prevent the movement of the transpiration stream. On the other hand, the existence of continuous columns of water has been acknowledged by many investigators as Haines (1935), and Gibbs (1935).

Dealing with the pattern of water movement, Rudinsky (1959), showed that patterns of water uptakes in unilaterally injected conifers varied greatly among species. He gave five distinct patterns, and attributed them to anatomical differences in xylem structure. The most complete distribution of water into the crown was provided by a system of spiral ascent and the least effective by a vertical ascent, Figure 13. Kozlowski (1963) showed that patterns of dye uptake varied greatly with species.

Greenidge (1955), observed that dye solutions moved up to horizontal saw cut in tree stems, and then were transferred laterally into regions above the incisions, Figure 14.

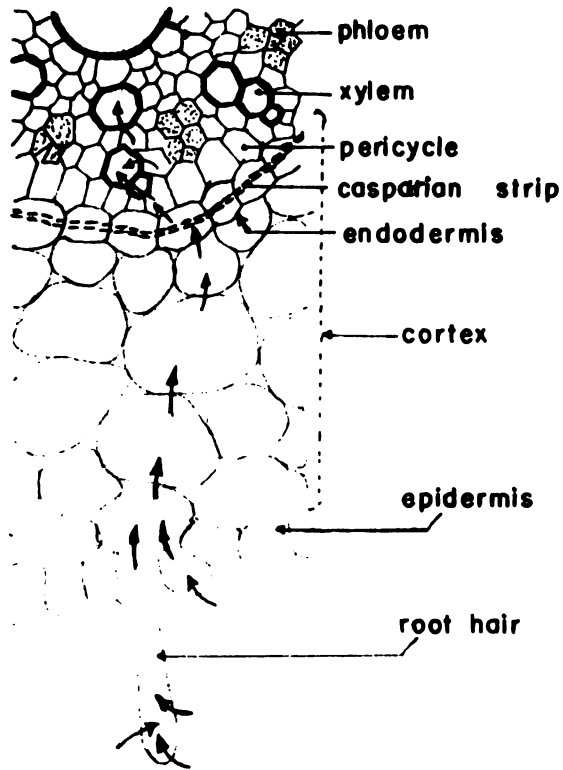


**FIG. 11 - ROOT PRESSURE THEORY**

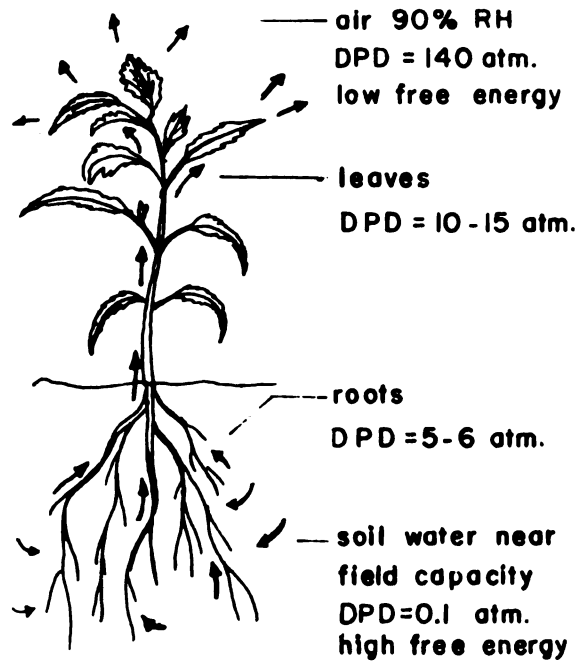


**FIG. 12 - THE COHESION THEORY**

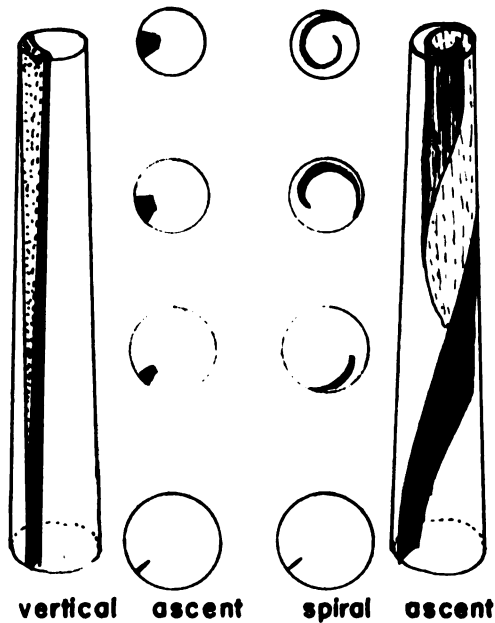


**FIG. 13 - PATTERNS OF WATER UPTAKE**

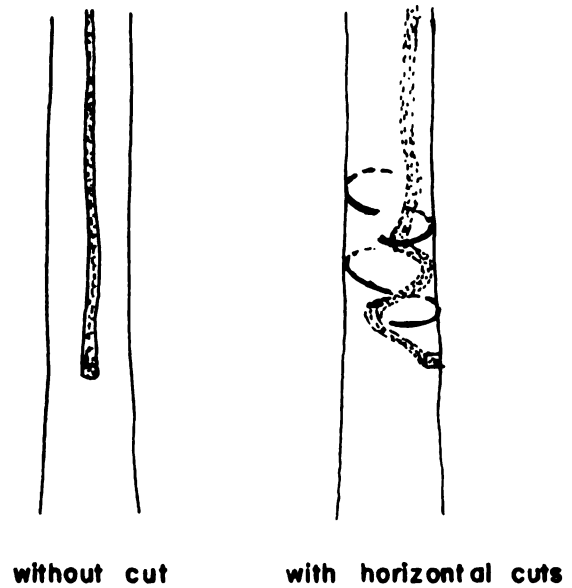


**FIG. 14 - EFFECT OF CUTS ON WATER PATH**

### II-C. Assimilates Translocation:

Salisbury (1966) discussed the translocation of assimilates from point of origin to point of utilization. The point of origin is usually a photosynthesizing cell or a cell that converts insoluble starch to soluble sugar. Substances move by diffusion, but two mechanisms may be considered to increase the rate of translocation. The first is the cytoplasmic-streaming hypothesis, Figure 15, in which a substance can diffuse from the streaming cytoplasm of one cell to the other. This mechanism is untenable for mature sieve tubes, because the cytoplasm does not stream in these phloem cells. The other mechanism was suggested by Münch. This mechanism permits bulk flow of assimilates through the sieve tube. The mechanism itself consists of two osmometers connected by a tube and surrounded by water, Figure 16. One osmometer contains a high concentrated solution, while the other contains a much more dilute solution. The first osmometer will take up water by osmosis, developing a pressure on both osmometers which increases the free energy of the water in the second osmometer and forces water to diffuse from it. This results in a flow of material from the first to the second osmometer.

This pressure flow mechanism can be applied to a plant by considering the producer cell as the high-concentrated-solution osmometer, the consumer cell as the other osmometer, the symplast as the connecting link, and the surrounding solution in the apoplast as that in the Münch mechanism, Figure 17. The plant system never reaches equilibrium because sugars are continually being produced and

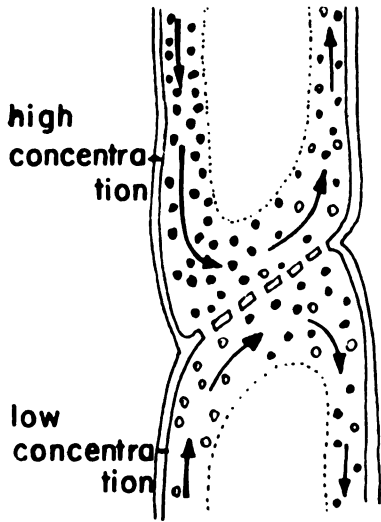


FIG. 15 - CYTOPLASM STREAMING

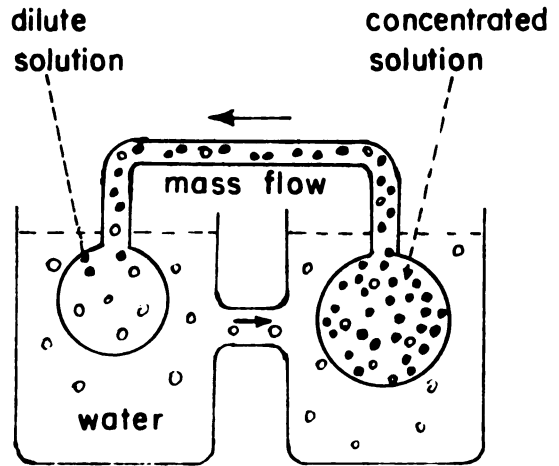


FIG. 16 - MÜNCH MECHANISM

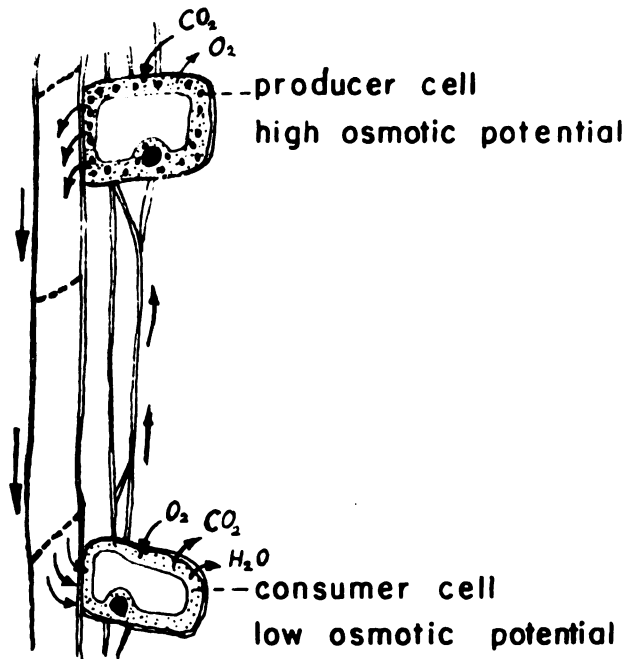


FIG. 17- PRESSURE FLOW MECHANISM (MÜNCH MECH.) IN PLANT

used up.

Manson (1928), showed that the removal of the bark stopped sugar transport whereas separation of bark and wood did not, and that transport took place into the loosened flaps of bark.

Loomis (1945), in a study on translocation of sucrose in maize, stated that neither the active diffusion nor the pressure flow mechanism will explain the polarized type of movement where sugars are moved from leaves containing 0.3 per cent sucrose through tissues containing 7 or 8 per cent sucrose.

Gauch (1953), showed that small concentrations of boron greatly facilitated the absorption and transport of applied sucrose. He proposed that boron reacts with the sugar to form a sugar-borate complex which moves through cellular membranes more readily than nonborated sucrose.

Crafts (1961), pointed out that one weakness of Münchs' and others past work was their failure to realize that the phloem is a distribution system and that its function is not to carry foods only from leaves to roots; its role is to provide organic nutrients for every living nonphotosynthetic cell of the plant.

Spanner (1958), put forward a new theory that involves a bulk flow of the sieve-tube contents actuated by a mechanism located at the sieve plates. The motive force proposed is electro-osmosis. Spanner claimed that the three requirements for electro-osmosis, namely a charged membrane, a membrane potential difference, and a porous structure in the membrane - are present in the sieve plate. Spanner attributed maintenance



of the potential difference to a cycle movement of potassium ions into the sieve tube above the sieve plate and thence out of the tube below the plate. The return motion of potassium ions takes place in companion cells or possibly in phloem parenchyma. The starting device for this mechanism would be:

1. discharge of sugar into the sieve tubes
2. uptake of water osmotically leading to a vertical surge in cells neighboring the sieve tube, and
3. flow of potassium ions along the direction of flow in the sieve tubes and counter to this direction in the neighboring cells.

Once established, this circulation would electrically polarize the sieve plate causing rapid electro-osmosis through the plate. Thus each sieve plate would contribute its energy to the flowing stream.

Crafts (1961) criticized electro-osmosis theory because of the recognized low permeability of tonoplast of companion cells and phloem parenchyma, and the lack of an explanation for the ready reversibility of phloem exudation.

Crafts (1961) mentioned the results of Tammes (1957) in which he gave the composition of sieve-tube sap of Arenga saccharifera as:

Sucrose:	about 15 per cent
Nitrogen:	total 410 mg per liter
Potash:	1200 mg per liter of $K^+$

Phosphate: 98 mg per liter of  $PO^{3-}$   
Magnesium: 96 mg per liter of  $Mg^{2+}$   
Calcium: 10 mg per liter of  $Ca^{2+}$

Hipton (1955), mentioned that when phloem exudation takes place by mass movement of a solution through sieve tube strands, the strands might be sufficiently permeable to allow a flow of solution at a linear velocity of 200 to 500 cm per hour.

#### II-D. Electrical Potential in Plants:

The phenomenon of the existence of a natural electric potential in plants has been observed by many investigators. Fenson (1957), mentioned that Kinkel in 1878 suggested that water transport was the cause of plant electricity. Waller (1925), referred to Haake who in 1892 was the first one to observe alternations of potential in plants due to a change of illumination. Haakes' conclusion was that oxygen respiration and carbonic acid assimilation are prominently considered in the electric current in plant. The movement of water possibly has a share in the causative conditions of the electric current, but its influence is but slight. Waller (1925), gave the same observation. By illuminating one half of the surface of a green leaf and shading the other half, he found that photo-electric response was mainly dependent upon the metabolic activity of chlorophyll. He mentioned that photo-electric current varied in magnitude and direction in different leaves. He also observed that photo-electric current occurred in some cases in the absence of chlorophyll.

Lund (1931), observed that in normal unstimulated condition of Douglas fir, the main apex of a lateral branch maintained an electro-positive conditions to all points below it. After several experiments, Lund (1931 b) concluded that the cortex of the Douglas fir is the origin of the E.M.F. and that the orientation of the radial E.M.F. in the cortex is opposite to that in the wood. On other experiments on the Douglas fir, Lund (1932), found that the electric polarity of the apex could be decreased, reversed or made equal to zero by means of changing its temperature.

In some earlier experiments, Lund (1927) observed the electropositivity of regions of greater growth to more basal regions. March (1928) observed the same phenomenon on growing roots. In his discussion on the possible origin of continuous bioelectric current in root tips, Lund (1928), concluded that it was a result of oxidation-reduction potentials developed by the respiratory mechanism of the cell. These potentials were developed at cell surfaces, internal, external or probably both, resulting in typical polarization phenomena. Scott (1967) mentioned that almost always the interior of the cell is more negative in potential than the external solution by 70 to 150 millivolts.

March (1928) agreed with Lund and adds that the E.M.F. of a given length of onion root is the algebraic sum of E.M.F.'s of the individual cells of such length. Lund (1930), also concluded that the inherent electric potential existing on the leaf of Bryophyllum must be equal to the algebraic sum of a complex system of E.M.F.'s of individual cells.

Burr (1942), observed a potential difference between the base and the apex of the seedling growing root during development, with the base positive and the growing point negative. He mentioned that this potential was complicated by fluctuations which presumably represented the diversion of energy from the electrical reserves of the organisms. On other experiments, Burr (1944) found that as fruits grew larger, the potential gradients tended to decrease.

Burr (1944) in his experiments on young maple trees, where two electrodes were introduced between the bark and the cambium on the trunk of the tree, five feet apart, observed natural electric potential in the trunk with the upper electrode positive. He noticed also that in the early morning from two to four hours before sunrise, the potential difference was maximum, then it dropped without interruption until the afternoon. After sunset the potential increased again.

Burr (1945), in other experiments, observed that during winter months, the upper electrode in the tree was positive. During the summer months, the tree showed a reversal in polarity. By carrying on the same experiments the following year, he found that during December, the upper-electrode was positive, while in January the upper electrode became negative and in February it became positive once again. Burr (1947) observed that in Fall and Winter, when the tree became dormant, the upper electrode became increasingly positive. In early Spring the potential

tended to fall and the polarity reversed. In Spring and Summer, the potential reversed once again, with the upper electrode positive. Before the leaves fell in the Fall, the potential started to rise markedly. Part (1948) concluded that the apex of a healthy tree is usually more positive than the base.

Fensom (1957), after reviewing many of the earlier experiments concluded that these published reports did not show any obvious correlation between transpiration and potentials. He mentioned also that since many of these experiments showed that bio-potentials might be accounted for in terms of membrane permeability as well as by the oxidation-reduction systems of metabolism, there has been a quite reasonable tendency to attribute potentials to transport rather than the reverse. Fensom (1958), on a study on the sunflower, showed that a correlation existed between transport pattern and bio-potential patterns.

Fensom (1963), in his experiments on three kinds of trees, found that there was yearly and daily rhythms of electrical potential. This potential was due to the effect of electro-osmosis or streaming potential, and was influenced by major temperature changes, by heavy rain, and by many other factors inherent inside the living tree. Fensom (1962) showed that artificial flow through open channels of woody tissue produced changes in electrical potential. Fensom (1959) interpreted the electrical potential differences which were found in dead wood when it was wetted, as resulting from local differences in ion concentrations which cause Donnan potential.

The existence of these natural electrical potentials, caused many investigators to try to utilize this phenomenon to affect the biological processes inside the plant. Blackman (1924), showed that by stretching insulated wire above the crop at a height of about seven feet, and positively charging it to a voltage of 40,000 to 80,000 volts with a discharge rate of .5 to 1.0 milliamper per acre, the increase in yield of oats was between 30 and 50 percent. In another experiment carried on Pot-Culture, Blackman (1924 b), found that the percentage of increase in the dry weight of Maize was 27 percent.

Plowman (1909), observed that an electric charge of positive sign inhibited the vital processes of plant protoplasm, while negative electric charge stimulated such processes. Collins (1929), observed that current which was supplied by suspending a charge network above maize plants with current intensity of  $10^{-9}$  amperes per plant did not show any significant response. Murr (1963), by positively charging a suspended wire mesh electrode over the plants with 30 to 75 Kvolt/m, found that the treated plants produced less growth, a leaf tip burning phenomenon occurred, and the whole plant appeared deeper green when compared with the control plants. On further discussion of this effect, Murr (1965) believes that this effect may not be electrostatic but may be attributed to lethal current densities caused by corona discharge from cells near the tip.

On the other hand, several researchers tried to direct current inside the plant. Knight (1914), found that direct

current of a density of  $10^{-6}$  to  $10^{-4}$  amperes had no effect upon the respiration of the germinating peas. Breazeale (1951), showed that ion absorption by plants is an electrical phenomenon. When a negative lead of -2.23 volts was connected to the tomato plant and the positive to the metal container, the cation uptake was greatly increased. When the negative lead was attached to the metal container and the positive to the plant, absorption of cations was not influenced by the electric current. Breazeale (1953), in other experiments, showed that the uptake of Na, K, and Ca was actively stimulated by applying the electrical current.

Berry (1943) observed that the response of the inherent electrical potential of onion roots to an applied direct current depended upon the direction and magnitude of the applied current flow. When the current was directed from the top to the base of the plant the positivity of the natural electrical potential decreased.

Clark (1938), showed that the negative apical polarity of *Avena* coleoptile was increased on stimulation by alternating current. At the same time, he showed that the inherent potential had no apparent causal relation to polar auxin transport in plant. Rosene (1937) noticed that the longitudinal potentials of the branches and stem of the Douglas fir were modified by the application of an electric current from an external source.

Scott (1967), after reviewing many experiments, concluded that many attempts have been made to modify the rate of plant growth either by the application of electrostatic fields or by

the passage of electric current through the tissue. Most of these treatments have either had no effect or have caused reduced growth and sometimes tissue damage.

Fensom (1962) showed that artificially applied voltages produced two effects. First a small and temporary disturbance in sap flow, second a sudden large surge of sap flow into the stem after prolonged electrical stimulation of up to 45 volts. This was accompanied with artificial guttation.

#### II-E. Background Theories:

Collins (1961), explained the phenomena of streaming potential and electro-osmosis. When two chambers containing water are separated by a plate of porous material, and a difference in electrical potential between the chambers is maintained by metal electrodes placed on each side of the porous place, a flow of water occurs from one side to the other. This phenomenon is called electro-osmosis. Liquids other than water also exhibit this behavior.

Conversely, when water or other liquid is forced through a porous plate by a pressure differential, an electrical potential difference across the plate is observed. This potential is called streaming potential.

Both of these phenomena are associated with the existence of charged layers at the solid-liquid interface. These layers behave as two parallel surfaces of opposite electrical charge separated by a distance of molecular dimension. The potential



difference between these two layers is called the zeta potential ( $\zeta$ ).

If the charged double layers are treated as a condenser with parallel plates, a distance  $d_m$  apart, the zeta potential can be related to the charge  $e$  on a plate as

$$\zeta = \frac{ed_m}{D\epsilon_0}$$

where  $D$  = the dielectric constant of the liquid

$$\epsilon_0 = 8.85 \times 10^{-12} \text{ (coulombs)}^2 / \text{newton} - \text{(meter)}^2 \text{ in M.K.S. units}$$

When applying electric potential  $E$  across the plate, the electric force  $F_E$  which will displace the charged layer will be  $\frac{eE}{t}$  per unit area.

where  $t$  = the thickness of the plate

$E$  = applied electromotive force in e.s.u.

and the total force will be given by integrating  $\frac{eE}{t}$  over the pore surface, which is proportional to the bulk volume of the porous plate.

$$F_E = \frac{eE}{t} (cAt) = ceAE$$

where  $c$  = the proportionality constant for pore surface ( $\text{cm}^{-1}$ )

$A$  = area of the plate

As the electric force displace the charge, the fluid is dragged along with the charges. For a steady flow, the displacement force  $F_E$  and the viscous force  $F_\mu$ , which opposes the flow, must be in

equilibrium. But  $F_{\mu}$  is proportional to pore surfaces, velocity  $u$  and viscosity  $\mu$  of the liquid

$$F_{\mu} = B\mu u (At) = B\mu qt$$

where  $B$  = proportionality constant with permeability considered

$$q = uA = \text{volume flow}$$

At equilibrium  $ceAE = B\mu qt$

$$q = \frac{c}{B} \frac{e}{\mu} A \frac{E}{t} = \frac{c\zeta D\epsilon_0}{Bd_m} A \frac{E}{t}$$

This equation gives the magnitude of electro-osmotic flow rate.

Mason (1950), discussed the electrokinetic theory of fibers. He mentioned that the fundamental quantity of this theory is the zeta potential which in the beginning was considered to be of a simple nature, but has since been the center of considerable controversy. The theory says that a solid in contact with polar liquid acquires an electric charge. By the absorption of cations or anions having a specific affinity for the solid, the excess charge of opposite sign accumulates as a diffuse ionic layer in the liquid adjacent to the solid. This mobil charge causes the potential difference which is known as the zeta-potential. If the liquid is caused to flow through a cellulose fiber pad, by the application of a pressure gradient, a flow of electric charge occurs.

Mason (1950) gives the relation between the current  $I$ , capillary path length  $l$ , pressure difference  $\Delta p$ , and pad resistance  $R$  by

Helmholtz-Smoluchowski equation:

$$\frac{I}{\Delta p} = \frac{V}{R\Delta p} = \frac{D\zeta}{4\pi\mu l} \xi$$

where  $\xi$  = pore factor

$V$  = the streaming potential

However, Mason (1950) pointed out that the origin of the electric charge in cellulose in contact with pure water is obscure.

Neale (1946) mentioned that most chemical neutral solids acquire a negative charge in contact with water and concluded that this is due to an intrinsic property of water to expel electrons from itself.

Fensom (1957) indicated that the two expressions commonly used to describe electrokinetic movement of liquids in narrow passages are the Helmholtz-Smoluchowski equations. For electro-osmosis, where an applied E.M.F. produces flow of liquid.

$$q = \frac{A_c D \zeta}{4\pi\mu} \frac{E}{l} \quad (1)$$

where  $A_c$  = the cross section area of a capillary tube.

For streaming potential, where there is a pressure causing flow of liquid which produces a difference in electrical potential between the ends of the flowing column:

$$V = \frac{D \zeta \Delta p}{4 \pi \mu l k_c} \quad (2)$$

where  $k_c$  = specific conductivity of liquid

Fensom (1957) gave the value of these parameters in xylem tissue as:

$$D = 80 \quad \mu = 0.01 \text{ poise} \quad \zeta = 0.013$$

From these values, and by considering the velocity of the liquid to be  $u = \frac{q}{A_c}$ , he solved the first equation for  $u$  as:

$$u = 0.92 \times 10^{-4} \frac{E}{l}$$

This equation means that 4500 volts would be required along 150 cm of tracheal tube to give flow velocity of 10 cm per hour.

To solve the second equation, he used Poiseuille equation:

$$\Delta p = \frac{8q l \mu}{r_c^4} = \frac{128 q l \mu}{D_c^4} = \frac{32 \pi l \mu u}{D_c^2}$$

$$\text{where } q = A_c u = \frac{\pi D_c^2}{4} u$$

$r_c$  = capillary tube radius

$D_c$  = capillary tube diameter

He estimated the value of  $V$  to be:

$$V = \frac{8D\zeta}{k_c D_c^2} = 2.9 \times 10^{-12} \frac{u}{k_c D_c^2}$$

This equation means that a flow rate of 10 cm per hour in tracheal diameter of 20 microns with  $k_c = 2 \times 10^{-6} \text{ ohm}^{-1}$  will give

a streaming potential of 1 millivolt.

From these equations, Fensom (1957) believes that the streaming potential will be significant only if transpiration rates are high, if liquid conductivity is very low, or if the xylem tubes are small in diameter.

Fensom (1957) pointed out that if the observed potentials are assumed to be metabolically maintained, then the electro-osmotic pump can move the water with a speed of 36 cm per hour if the potential difference is 100 millivolts and the flow passes through 10 barriers each of 1 micron thickness. These barriers exist across xylem vessels when they are new, and act as electro-osmotic pumps to move water and small ions.

Lundegardh (1951) explained the existence of electrokinetic potential across a membrane separating two solutions by the activity of hydrogen ions on each side of the membrane.

$$V = \frac{R_g T}{\mu e} \ln \frac{(H^+)_2}{(H^+)_1}$$

where  $R_g$  = gas constant

$T$  = absolute temperature

$e$  = charge

and  $(H^+)_1$  and  $(H^+)_2$  are the activities of hydrogen ions on side 1 and 2 respectively.

According to Osterle (1964), the irreversible thermodynamics of electro-osmotic flow can be summarized by the conversion of electric power into hydraulic power. When a liquid electrolyte

flows through an insulating circular tube, the direction of the potential difference  $\Delta V$ , current  $I$ , pressure difference  $\Delta p$ , and flow rate  $q$ , will correspond to that conversion of electrical power  $I \Delta V$  into hydraulic power  $q \Delta p$ .

The dissipation rate ( $D_r$ ) associated with the mode of conversion is:

$$D_r = I \Delta V - q \Delta p$$

The forces  $\Delta V$  and  $\Delta p$  and fluxes  $I$  and  $q$  will be linearly related as

$$\Delta p = \alpha \Delta V - R_\mu q$$

$$I = C_E \Delta V + \alpha q$$

where  $\alpha$  = cross-coefficients which are identical by Orsager's reciprocal theorem

$$R_\mu = \text{viscous resistance, } R_\mu = \frac{8 \mu l}{Ar^2}$$

$$C_E = \text{electric conductance; } C_E = \frac{\sigma_E A}{l}$$

$$\sigma_E = \text{electric conductivity}$$

If the pressure differential were zero, an applied electric field would move the fluid through the tube with a uniform velocity  $u_o$  expressed by:

$$u_o = b_o \frac{\Delta V}{l}$$

where  $b_o$  = the electro-osmotic mobility of the liquid with respect to the wall

$$b_o = \frac{E (-\Psi_o)}{\mu}$$

where  $E$  = the permittibility of the liquid

$\Psi_o$  = the electro-kinetic potential

With the use of the simple parallel plate condenser relationship,

$$b_o = \frac{q_o d_o}{\mu}$$

where  $q_o$  = the surface density of the charge counter to the charge absorbed on the tube wall

$d_o$  = the apparent thickness of the double layer on the tube wall

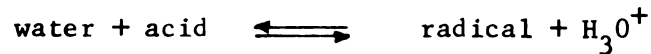
Also  $\alpha$  can be solved by the previous equation to be:

$$\alpha = \frac{8\mu b_o}{r^2}$$

with  $\alpha$ ,  $R$  and  $C$  known, the irreversible thermodynamic description of electro-osmotic flow is complete.

Fensom (1959) related streaming potential and electro-osmosis to the hydrogen ion and hydronium ( $H_3O^+$ ). This ion moves the fastest in plant electrolytes with ( $HO^-$ ) next and ( $K^+$ ) third. The hydronium ion has a diameter of 1.6 Å while that of hydrated potassium ion is 3 Å. Hydronium ion must be present in appreciable concentrations wherever respiratory acids are being produced.

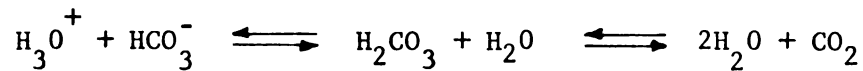
Fensom (1959) summarized the process of producing the hydrogen ion by the following equation.



The hydrogen ion will be increased in any process that:

- a) increases acid concentration as in respiration
- b) decreases the concentration of the free radical
- c) decreased  $\text{H}_3\text{O}^+$ , as happens by the translocation of  $\text{H}_3\text{O}^+$  away from reaction zone by its free migration through the plasmalemma.

On the other hand, hydrogen ion will be absorbed if acid is being removed as happens in evaporation of  $\text{CO}_2$  from the surface of a mesophyll cell in the leaf in the dark



Fensom (1959) showed the role of hydrogen ion in electro-osmosis by considering a system consisted of membrane separating two solutions of 1/10 M (K Cl) and 1/10 M (H Cl). Ions will attempt to get through the holes of the membrane. The ( $\text{Cl}^-$ ) ions will have the same potential on the two sides of the membrane, while ( $\text{H}_3\text{O}^+$ ) and ( $\text{K}^+$ ) will attempt to pass to the opposite side. Because ( $\text{H}_3\text{O}^+$ ) moves faster, it will cause a positive charge on the opposite side (streaming potential). However, since the membrane has negative charge (zeta potential), the previous streaming potential will cause electro-osmotic flow of ( $\text{K}^+$ ) ion on the opposite direction. These two flows, which are opposite in direction will be balanced after short time. But if the holes in the membrane were too small for ( $\text{K}^+$ ) ion to pass, this electro-osmosis flow will be stopped.



Tyree (1968) suggested the use of the Onsager equations of irreversible thermodynamics.

$$J = L_{PP} \frac{dp}{dl} + L_{PE} \frac{dE}{dl}$$

$$I = L_{EP} \frac{dp}{dl} + L_{EE} \frac{dE}{dl}$$

where  $J$  = flux of solution in  $\text{cm}^3 \text{sec}^{-1}$  per  $\text{cm}^2$  of tissue

$I$  = flux of current in amp /  $\text{cm}^2$  of tissue

$\frac{dp}{dl}$  = the hydro-kinetic pressure gradients in  $(\text{Joules cm}^{-3})$   
 $\text{cm}^{-1}$

$\frac{dE}{dl}$  = the electrical potential gradients in volt  $\text{cm}^{-1}$

and  $L_{EP}$ ,  $L_{PE}$ ,  $L_{PP}$  and  $L_{EE}$  are constants. These are called the Onsager coefficients.

Tyree (1968) relates the hydro-kinetic pressure gradients to the electrical current by the equation:

$$\frac{dP}{dl} = \frac{\Delta I}{2 AL_{EP}}$$

and to the electrical potential by the equation

$$\frac{dP}{dl} = \frac{L_{EE}}{L_{EP}} \frac{dE}{dl}$$

and to the velocity front or  $J$  function by the equation

$$\frac{dP}{dl} = \frac{J}{L_{PP}}$$

where  $L_{pp}$  = the hydraulic conductivity of the xylem.

Dainty (1963) also expressed the electro-kinetic phenomena in terms of irreversible thermodynamics and Onsager coefficients. He discusses three models: the Helmholtz-Smoluchowski model, the frictional model, and the model of Schmid. All these models assume linear relations to fit the principles of irreversible thermodynamics.

### III. MATHEMATICAL ANALYSIS OF FLUID TRANSLOCATION INSIDE XYLEM TISSUE

The plant as a biological system is very complicated. However, Figure 18, simplifies the plant system and the physiological processes that occur inside.

Translocation of fluids occurs mainly in two kinds of tissues: the xylem and the phloem. The xylem tissue, which this study concerns itself with, extends from the roots to the leaves. It begins at the root hair zone where the conditions are:

1. The xylem tubes are newly developed.
2. The existing fluid is a low concentrated solution.
3. The water potential of this solution is higher outside than inside xylem vessels.

At its leaf end, the conditions are:

1. The vessel ends are closed and are surrounded with living cells.
2. High rate of transpiration during the day, and therefore, water solution in the surrounding cells exists under negative potential, lower than that inside xylem vessels.

Inside the root and the stem, between the root hair zone and the leaves, xylem vessels are surrounded by living tissues which differ in their water potential during the day and night.

To study the fluid flow process inside the xylem, and to determine its relationship to the natural electrical potential which exists in it, a representative model has been developed.

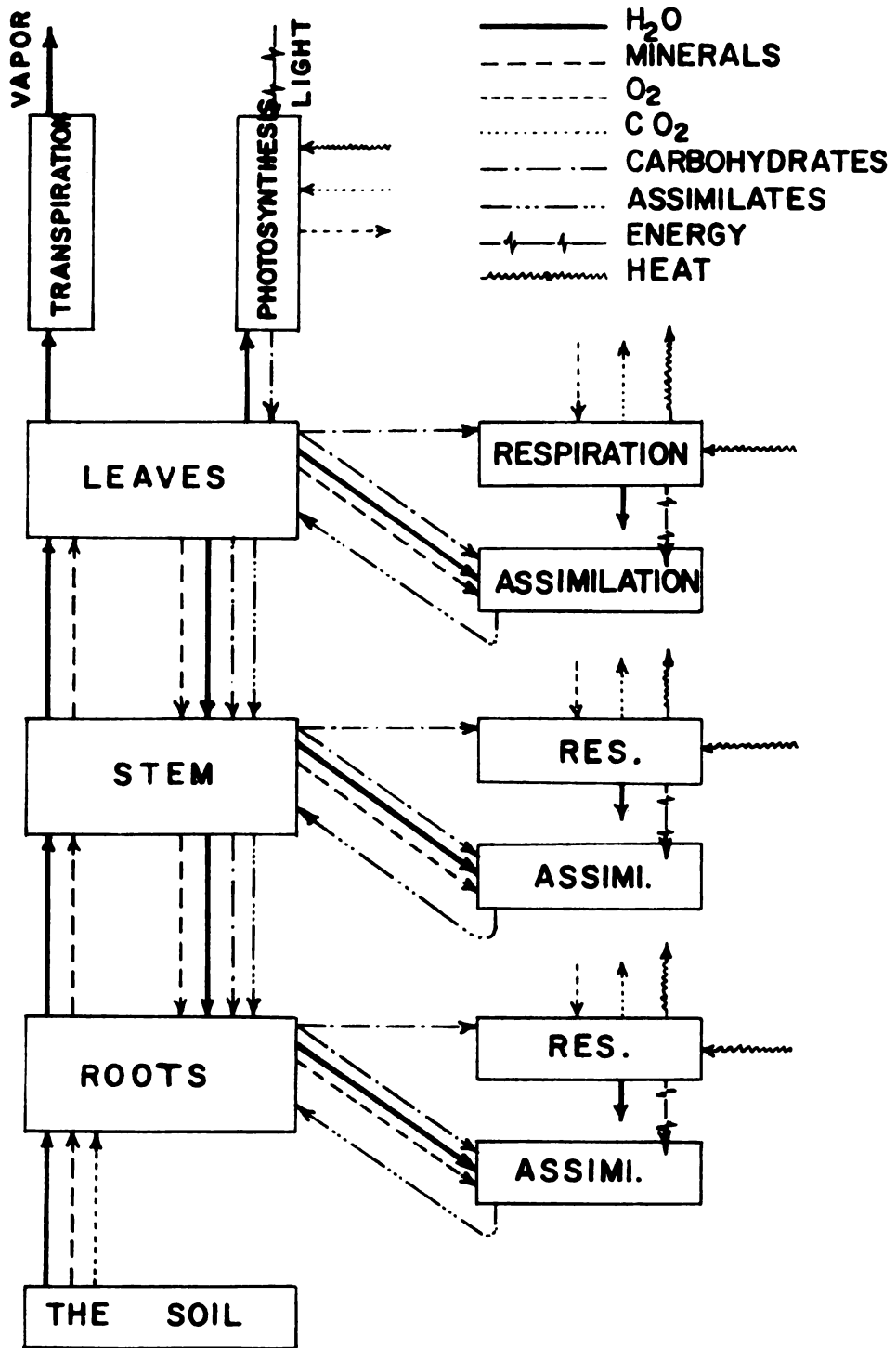


FIG.18. THE PHYSIOLOGICAL PROCESSES IN PLANT.

The model, Figure 19, consists of a long porous and permeable tube closed at both ends. The surrounding of this tube can be divided into three regions. The lower one is the high water potential region, which represents the root hair zone. The middle region is the longest one, and its water potential differs according to the rate of the other physiological processes. This region represents the surrounding parenchyma, fibers, and cambium cells in both the root and the stem. The third one is the low water potential region which represents the surrounding tissues inside the leaf.

It is assumed that the analysis of what occurs in this model holds for all xylem vessels. It is further assumed that what occurs in the xylem tissue is a summation of that which occur in the individual xylem tubes.

The inside and the outside radii of the tube are  $r_i$  and  $r_o$  respectively, therefore, the thickness of the tube wall is  $(r_o - r_i)$ . The length of the tube is represented by  $l$ . The pores in the permeable wall are of two kinds: a) narrow ones which are gaps between the three cellulose layers of the secondary wall. For this study, they are assumed to be circular in cross section with diameter equal to  $\delta_c$ , b) wider ones with diameter  $\delta_p$  which represent the pits in the wall.

If a square segment of the wall is considered, Figure 20, the energy balance through it will be:

Energy in + Energy dissipated or generated

= Change in wall internal energy + Energy out

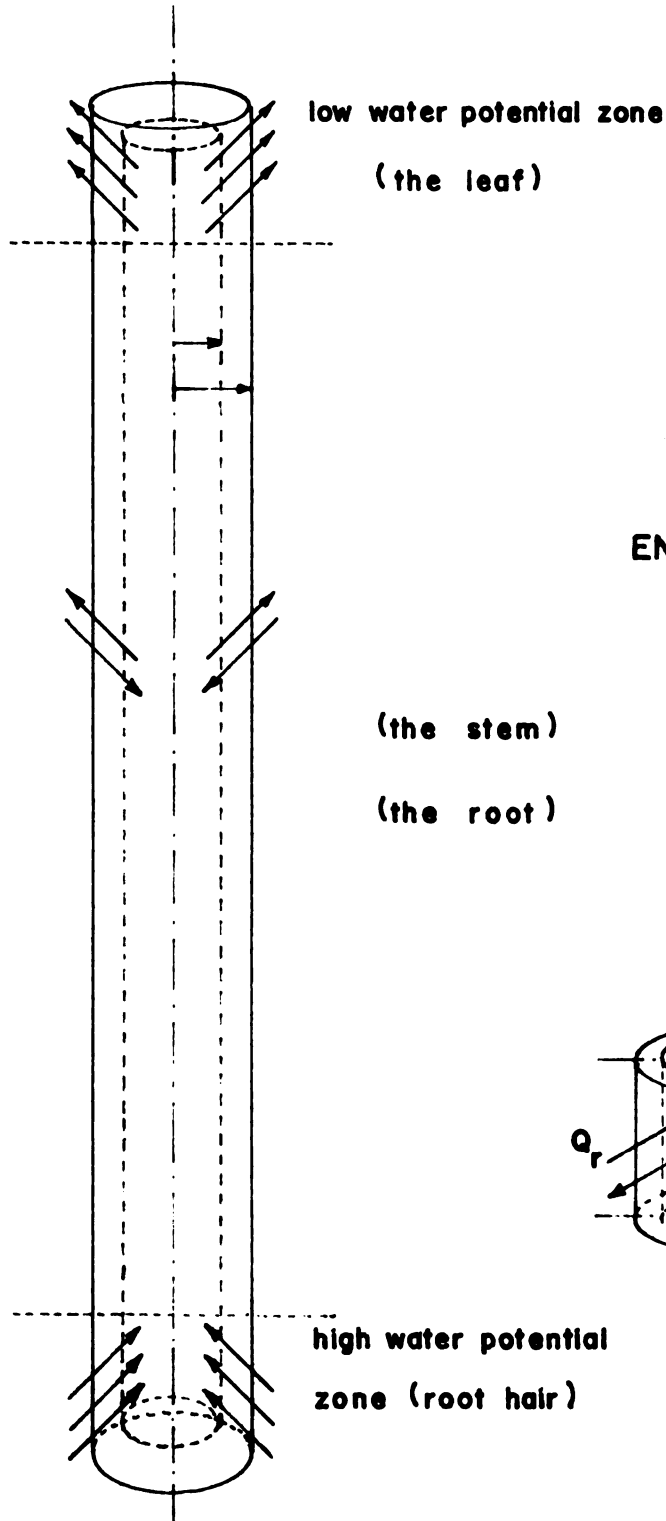


FIG. 19 - XYLEM TUBE MODEL

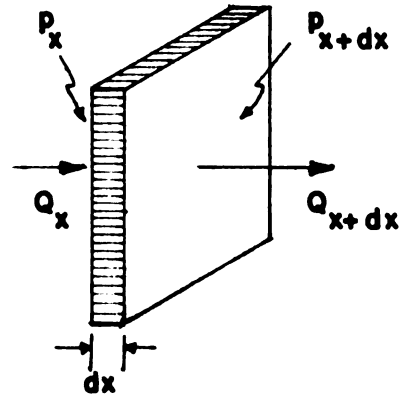


FIG. 20  
ENERGY FLOW THROUGH  
TUBE WALL

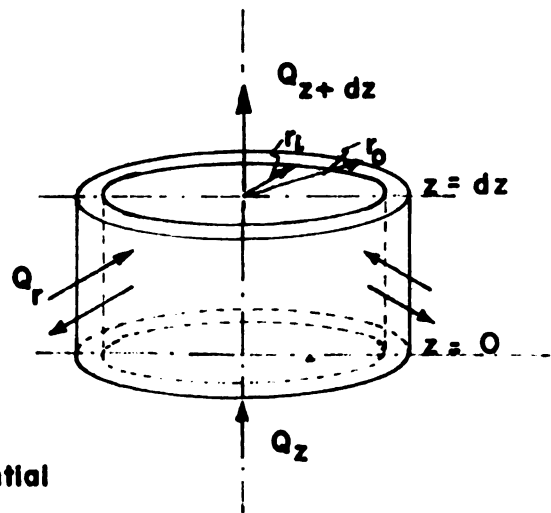


FIG. 21  
FLOW WORK THROUGH A  
TUBE SECTION

The "Energy in" term is  $\Delta Q_x$  and can be defined as:

$$\Delta Q_x = -L_p dA \frac{\partial p}{\partial x}$$

where:  $\Delta Q_x$  = the energy which flows in the x direction per unit time. It can be considered as flow work, with dimension (dyne-cm/sec).

$L_p$  = rate of flow of energy, or rate of flow of work, with dimension (dyne - cm/sec - cm - unit  $\Delta p$ )

$dA$  = area of wall piece, with dimension (cm<sup>2</sup>)

$p$  = water potential with dimension (dyne/cm<sup>2</sup>)

$\frac{\partial p}{\partial x}$  = water potential gradient in the direction x

The term "Energy out"  $Q_{x+dx}$  can be expressed as:

$$\Delta Q_{x+dx} = - \left[ L_p dA \frac{\partial p}{\partial x} + \frac{\partial}{\partial x} (L_p dA \frac{\partial p}{\partial x}) dx \right]$$

There is no source for generating energy from the view point of fluid dynamics, but there is energy dissipation due to the friction between the inside surfaces of the pores and the fluid, and perhaps between solute molecules and water. The dissipation rate per unit volume of pore space in the wall material is  $\Delta \dot{Q}$ . This dissipation rate is a function of fluid viscosity, temperature, and velocity gradient at the inside surfaces of the pores.

$$\Delta \dot{Q} = f \left( \mu, T, \frac{du}{dx}, \dots \right)$$

To simplify the analysis,  $\Delta \dot{Q}$  can be considered as an average rate.

Therefore,

$$\text{Energy dissipated} = \Delta \dot{Q} \phi \, dA \, dx$$

where  $\phi$  = the porosity of the wall material.

The term "Change in internal energy", can be expressed as:

$$\text{Change in internal energy} = dA \, dx \, \phi \, U \, \frac{\partial p}{\partial \tau}$$

where  $U$  = energy needed to change one unit volume of wall pore space, one unit of potential

$\tau$  = time in seconds

Therefore, the energy balance equation becomes:

$$\begin{aligned} -L_p \, dA \, \frac{\partial p}{\partial x} - \Delta \dot{Q} \, \phi \, dA \, dx = \phi U \, dA \, \frac{\partial p}{\partial \tau} \, dx - \left[ L_p \, dA \, \frac{\partial p}{\partial x} \right. \\ \left. + \frac{\partial}{\partial x} \left( L_p \, dA \, \frac{\partial p}{\partial x} \right) \, dx \right] \end{aligned} \quad (1)$$

Canceling, Equation (1) becomes

$$\frac{\partial}{\partial x} \left( L_p \, \frac{\partial p}{\partial x} \right) - \phi \Delta \dot{Q} = \phi U \, \frac{\partial p}{\partial \tau} \quad (2)$$

$L_p$  can be considered as  $L_p = P \cdot \frac{\text{one unit } \Delta p}{\text{one unit length}}$

where  $P$  = the rate of volume flow per unit area under the existing conditions with dimension ( $\text{cm}^3/\text{cm}^2\text{-sec}$ )

To simplify the analysis,  $L_p$  can be considered as a constant under certain conditions. Although, as mentioned previously, it varies according to the rate of volume flow, it can be considered as a constant since the volume of flow does not change as long as the potential differences does not change. This is the case if the analysis is made for a short period of time. On the other hand,



the whole tube wall can be considered as constructed of one material having the same characteristics at any point. Therefore, equation (2) becomes

$$\frac{\partial^2 p}{\partial x^2} - \frac{\phi \Delta \dot{Q}}{L_p} = \frac{\phi U}{L_p} \frac{\partial p}{\partial \tau} \quad (3)$$

For three dimensional model, and by applying the same analysis, the equation becomes:

$$\frac{\partial^2 p}{\partial x^2} + \frac{\partial^2 p}{\partial y^2} + \frac{\partial^2 p}{\partial z^2} - \frac{\phi \Delta \dot{Q}}{L_p} = \frac{\phi U}{L_p} \frac{\partial p}{\partial \tau} \quad (4)$$

For cylindrical coordinates, the equation becomes:

$$\frac{\partial^2 p}{\partial r^2} + \frac{1}{r} \frac{\partial p}{\partial r} + \frac{1}{r^2} \frac{\partial^2 p}{\partial \theta^2} + \frac{\partial^2 p}{\partial z^2} - \frac{\phi \Delta \dot{Q}}{L_p} = \frac{\phi U}{L_p} \frac{\partial p}{\partial \tau} \quad (5)$$

However, the conditions around the tube wall in the horizontal plane, can be assumed symmetrical. Moreover, the flow of energy in the z direction, inside the wall itself, is of lower order than that in the r direction, because  $\frac{\partial p}{\partial z} \ll \frac{\partial p}{\partial r}$

Therefore,  $\frac{\partial^2 p}{\partial \theta^2}$  and  $\frac{\partial^2 p}{\partial z^2}$  can be neglected, and equation (5)

becomes:

$$\frac{\partial^2 p}{\partial r^2} + \frac{1}{r} \frac{\partial p}{\partial r} - \frac{\phi \Delta \dot{Q}_r}{L_p} = \frac{\phi U}{L_p} \frac{\partial p}{\partial \tau} \quad (6)$$

The plant is not in a steady state condition because of the dynamic physiological processes. As mentioned previously, the change in the internal energy of the tube wall, during a short period of time, can be considered negligible, and the term  $\frac{\partial p}{\partial \tau}$  approaches zero. Therefore equation (6) becomes

$$\frac{d^2 p}{dr^2} + \frac{1}{r} \frac{dp}{dr} - \frac{\phi \Delta \dot{Q}_r}{L_p} = 0 \quad (7)$$

This equation can be solved for  $\Delta \dot{Q}_r$  by multiplying it by  $r$  and considering the boundary conditions.

$$r \frac{d^2 p}{dr^2} + \frac{dp}{dr} = \frac{\phi \Delta \dot{Q}_r r}{L_p} \quad (8)$$

with boundary conditions:

$$p = p_o \quad \text{at } r = r_o$$

$$p = p_i \quad \text{at } r = r_i$$

$$\frac{dp}{dr} = 0 \quad \text{at } r = 0$$

$$\text{Since } \frac{d}{dr} \left[ r \frac{dp}{dr} \right] = r \frac{d^2 p}{dr^2} + \frac{dp}{dr}$$

$$\text{Then: } \frac{d}{dr} \left[ r \frac{dp}{dr} \right] = \frac{\phi \Delta \dot{Q}_r r}{L_p} \quad (9)$$

$\dot{\Delta Q}_r$  is an average value, but if  $r < r_i$ ,  $\dot{\Delta Q}_r = 0$

Therefore, integrating equation (9) gives:

$$r \frac{dp}{dr} = \frac{\phi \dot{\Delta Q}_r}{2 L p} (r^2 - r_i^2) + c_1 \quad (10)$$

Dividing by  $r$  and integrating once more gives:

$$p = \frac{\phi \dot{\Delta Q}_r}{2 L p} \left[ \frac{(r^2 - r_i^2)}{2} - r_i^2 \ln \frac{r}{r_i} \right] + c_1 \ln r + c_2 \quad (11)$$

Considering the condition  $\frac{dp}{dr} = 0$  at  $r = 0$

$$0(0) = \frac{\phi(0)}{2 L p} (0^2 - r_i^2) + c_1 \quad \therefore c_1 = 0$$

Considering the condition  $p = p_i$  at  $r = r_i$

$$p_i = \frac{\phi(0)}{2 L p} \left[ \frac{(r_i^2 - r_i^2)}{2} - r_i^2 \ln \frac{r_i}{r_i} \right] + c_2$$

$$\therefore c_2 = p_i$$

Considering the condition  $p = p_o$  at  $r = r_o$

$$p_o = \frac{\phi \dot{\Delta Q}_r}{2 L p} \left[ \frac{(r_o^2 - r_i^2)}{2} - r_i^2 \ln \frac{r_o}{r_i} \right] + p_i$$

$$p_o - p_i = \frac{\phi \dot{\Delta Q}_r}{4 L p} \left[ (r_o^2 - r_i^2) - 2r_i^2 \ln \frac{r_o}{r_i} \right]$$

$$\dot{\Delta Q}_r = \frac{4 L p (p_o - p_i)}{\phi \left[ (r_o^2 - r_i^2) - 2r_i^2 \ln \frac{r_o}{r_i} \right]} \quad (12)$$

Since  $\dot{\Delta Q}_r$  is the dissipating rate within one unit of volume of pore space, therefore the dissipation rate for a section of the tube of length  $d_z$  will be =  $d\dot{Q}_r^{**}$

$$d\dot{Q}_r^{**} = \frac{4 L_p (P_o - P_i)}{\phi \left[ (r_o^2 - r_i^2) - 2r_i^2 \ln \frac{r_o}{r_i} \right]} \phi (r_o^2 - r_i^2) \pi dz$$

$$d\dot{Q}_r^{**} = \frac{4\pi L_p (P_o - P_i)}{2r_i^2 \ln \frac{r_o}{r_i} \left[ 1 - \frac{r_i^2}{r_o^2 - r_i^2} \right]} dz \quad (13)$$

and the dissipated energy for the whole length of the tube will be

$$\begin{aligned} \dot{Q}_r^* &= \int_0^l d\dot{Q}_r^{**} \\ \dot{Q}_r^* &= \int_0^l d\dot{Q}_r^{**} = \int_0^l \frac{4\pi L_p (P_o - P_i)}{2r_i^2 \ln \frac{r_o}{r_i} \left[ 1 - \frac{r_i^2}{r_o^2 - r_i^2} \right]} dz \quad (14) \end{aligned}$$

This dissipated energy occurs as a result of fluid flow in and out of the wall of the tube.

$L_p$  is the rate of flow of energy and it is proportional to the volume flow rate. On the other hand, "Poiseuille" equation relates the volume flow to the potential difference  $(p_o - p_i)$ .

$$p_o - p_i = \frac{8 q l \mu}{r^4} \quad \text{or} \quad q = \frac{(p_o - p_i) r^4}{8 l \mu}$$

Therefore,  $L_p$  can be written in terms of  $(p_o - p_i)$  as:

$$L_p = P \cdot \frac{\text{one unit } \Delta p}{\text{one unit length}}$$

$$P = \frac{(p_o - p_i)}{\mu} C$$

where  $C = \text{constant}$ , with dimension  $\text{cm}^3$

Therefore,

$$L_p = \frac{C}{\mu} (p_o - p_i) \frac{\text{per unit } \Delta p}{\text{unit length}} \quad (15)$$

Inserting this expression for  $L_p$  in equations 12, 13, and 14 gives:

$$\dot{Q}_r = \frac{4C}{\phi \mu} \frac{(p_o - p_i)^2}{(r_o^2 - r_i^2) - (2r_i^2 \ln \frac{r_o}{r_i})} > 0 \quad (16)$$

$$d\dot{Q}_r^{**} = \frac{4\pi C}{\mu} \frac{(p_o - p_i)^2}{1 - \frac{2r_i^2 \ln \frac{r_o}{r_i}}{r_o^2 - r_i^2}} dz > 0 \quad (17)$$

$$\dot{Q}_r^* = \int_0^l \frac{4\pi C}{\mu} \frac{(p_o - p_i)^2}{1 - \frac{2r_i^2 \ln \frac{r_o}{r_i}}{r_o^2 - r_i^2}} dz$$

$$\dot{Q}_r^* = \frac{4\pi C}{\mu} \int_0^l \frac{(P_o - P_i)^2}{1 - \frac{2r_i^2 \ln \frac{r_o}{r_i}}{r_o^2 - r_i^2}} dz > 0 \quad (18)$$

However, there is other energy dissipated due to the friction of fluid with the inside surface of the tube. This energy loss can be estimated by considering a section of the tube, Figure 21, of height  $dz$  located at the bottom of the tube. The energy balance for it will be:

$$\begin{aligned} &\text{Energy in} + \text{Energy dissipated inside the wall} \\ &= \text{Change in the internal energy of the wall} \\ &+ \text{Energy dissipated on wall surface} + \text{Energy out} \end{aligned}$$

The term "Energy in" consists of two items,  $Q_z$  and  $\Delta Q_r$ .  $Q_z$  is the energy flow in  $z$  direction. But  $Q_z = 0$  since the tube is closed at the bottom.  $\Delta Q_r$  is the flow of energy in  $r$  direction.

$$\Delta Q_r = -L_p \, dA \, \frac{dp}{dr} = -2\pi r \, dz \, L_p \, \frac{dp}{dr}$$

$$\int_{r_i}^{r_o} \Delta Q_r \frac{dr}{r} = -\int_{P_i}^{P_o} 2\pi L_p \, dz \, dp$$

$$\Delta Q_r = -\frac{2\pi L_p (P_o - P_i) dz}{\ln \frac{r_o}{r_i}}$$

$$\Delta \dot{Q}_r = - \frac{2\pi C}{\mu \ln \frac{r_o}{r_i}} (p_o - p_i)^2 dz \quad (19)$$

The term "Energy dissipated inside the wall itself," has been computed to be:

$$\dot{Q}_r^{**} = \frac{4\pi C}{\mu} \frac{(p_o - p_i)^2}{1 - \frac{2r_i^2 \ln \frac{r_o}{r_i}}{r_o^2 - r_i^2}} dz \quad (19)$$

The term "Change in internal energy" can be dropped out for the same reasons mentioned previously.

The term "Energy dissipated on the inside surface of the tube,"  $\dot{Q}_z$  is a function of flow temperature, viscosity and velocity gradients at tube inner surface.

$$\dot{Q}_z = f(\mu, T, \frac{du}{dr})$$

However, the dissipated energy is proportional to the inside surface area of the tube, and equals:

$$\dot{Q}_z (2\pi r_i) dz$$

The term "Energy out"  $Q_z + dz$  is expressed as:

$$Q_z + dz = Q_z + \frac{\partial}{\partial z} (Q_z) dz$$

Therefore, the energy equation becomes:

$$Q_z + \frac{2\pi C}{\mu \ln \frac{r_o}{r_i}} (p_o - p_i)^2 dz - \frac{4\pi C}{\mu} \frac{(p_o - p_i)^2}{2r_i^2 \ln \frac{r_o}{r_i}} dz =$$

$$Q_z + \frac{\partial Q_z}{\partial z} + \dot{Q}_z 2\pi r_i dz \quad 1 - \frac{r_o^2 - r_i^2}{r_o^2 - r_i^2} \quad (20)$$

Canceling, equation (20) becomes

$$\frac{dQ_z}{dz} = \frac{2\pi C}{\mu \ln \frac{r_o}{r_i}} (p_o - p_i)^2 - \frac{4\pi C}{\mu} \frac{(p_o - p_i)^2}{2r_i^2 \ln \frac{r_o}{r_i}} \quad 1 - \frac{r_o^2 - r_i^2}{r_o^2 - r_i^2}$$

$$- \dot{Q}_z 2\pi r_i \quad (21)$$

Integrating equation(21) gives:

$$Q_l = \frac{2\pi C}{\mu} \int_0^l \frac{(p_o - p_i)^2}{\ln \frac{r_o}{r_i}} dz - \frac{4\pi C}{\mu} \int_0^l \frac{(p_o - p_i)^2}{2r_i^2 \ln \frac{r_o}{r_i}} dz \quad 1 - \frac{r_o^2 - r_i^2}{r_o^2 - r_i^2} dz$$

$$- 2\pi \int_0^l r_i \dot{Q}_z dz \quad (22)$$

Since  $Q_l = 0$  at  $z = l$ , because the tube is assumed to be closed at both ends, therefore,



$$\frac{4\pi C}{\mu} \int_0^l \frac{(P_0 - P_1)^2}{2r_i^2 \ln \frac{r_o}{r_i} \left[ 1 - \frac{r_o^2 - r_i^2}{r_o^2 - r_i^2} \right]} dz + 2\pi \int_0^l r_i \dot{Q}_z dz =$$

$$\frac{2\pi C}{\mu} \int_0^l \frac{(P_0 - P_1)^2}{\ln \frac{r_o}{r_i}} dz \quad (23)$$

i. e., the total loss of energy inside the tube wall material and on the inside surface of the tube equals

$$\frac{2\pi C}{\mu} \int_0^l \frac{(P_0 - P_1)^2}{\ln \frac{r_o}{r_i}} dz \quad (24)$$

While the energy dissipated only by the friction of fluids on the inside surface of the tube is:

$$2\pi \int_0^l r_i \dot{Q}_z dz = \frac{2\pi C}{\mu} \int_0^l (P_0 - P_1)^2 \left[ \frac{1}{\ln \frac{r_o}{r_i}} - \frac{2}{2r_i^2 \ln \frac{r_o}{r_i} \left[ 1 - \frac{r_o^2 - r_i^2}{r_o^2 - r_i^2} \right]} \right] dz =$$

$$\frac{2\pi C}{\mu} \int_0^l (P_0 - P_1)^2 \left[ \frac{(r_o^2 - r_i^2) - 2r_o^2 \ln \frac{r_o}{r_i}}{\ln \frac{r_o}{r_i} (r_o^2 - r_i^2 - 2r_i^2 \ln \frac{r_o}{r_i})} \right] dz \quad (25)$$

These energy equations were solved for the dissipated energy for an important reason. If the natural electric potential in xylem comes from sap flow process, it must be a result of a conversion of some of the energy to electrical energy. Referring to the model, the sources of this electric energy may be one or more of the following:

- 1) the friction of fluid and the wall
- 2) the chemical concentration gradient inside the tube
- 3) the zeta potential
- 4) some biological processes in the surrounding tissues, i.e., an external source of energy outside the tube.

In all cases, the existence of electric energy within the model is a result of dissipation of some of the available energy.

If the performed experiments show a relationship between the electric energy and the dissipated energy, equations 24 and 25 can be used to determine the magnitude of the generated electric energy.

The proportionality factor between the two kinds of energy will depend on the mechanism responsible of generating this electric energy. This factor can be determined experimentally also.

Practically, equations 24 and 25, can be used to determine the dissipated energy due to the sap flow process in the xylem tissue of the plant. Next, the proportionality factor can be used to determine the generated electric energy. The magnitude

of this electric energy, the flow rate and direction, and the pore diameters, at any location in the xylem tissue, will help in estimating solute movement and the surrounding tissues reaction.

The two expressions:  $(p_o - p_i)$ , and  $L_p$ , which were used in the analysis, can be further defined as follows:

- a) The term  $(p_o - p_i)$  is the water potential difference between the two sides of the tube wall. It is not just the hydraulic pressure difference, but it is a combined term consisting of the hydraulic pressure difference, the osmotic pressure difference, and any other chemical potential differences. The dimension of this term is  $(\text{dyne}/\text{cm}^2)$ .
- b) The term  $L_p$  is the rate of flow of energy, or the rate of flow work. It can be determined experimentally by

$$L_p = \frac{Q/A}{dp/dx}$$

$$L_p = \frac{1}{(p_o - p_i)} \left[ \frac{\text{Thickness}}{\text{Area}} \times \text{volume of flow per second} \times \text{fluid potential} \right] = \frac{1}{\Delta p} \left[ \frac{\text{cm}}{\text{cm}^2} \times \frac{\text{cm}^3}{\text{sec}} \times \frac{\text{dyne}}{\text{cm}^2} \right] = \frac{\text{dyne} - \text{cm}}{\text{sec-cm-one unit } \Delta p}$$

$L_p$  can also be determined by equation (15).

The coefficient C in equation (15) can be estimated by referring to "Poiseuille" equation:

$$C = c^* \left[ \frac{a \delta_c^4 + b \delta_p^4}{(r_o - r_i)} \right]$$

where a, b, and c\* are proportional constants

#### IV. EXPERIMENTAL ANALYSIS

The relation between the dissipated energy, flow rate, and the electrical potential differences, which have been observed by many investigators, can be determined experimentally. The source of this electrical potential, according to the previous review of literature, is due to the zeta potential. This concept can be investigated experimentally.

As the mathematical analysis was done for a model representing the xylem vessels, the experimental analysis will be performed on a model made of material representing the wall of the xylem vessels. Filter paper "Whatman No: 1" was used since it is made of pure cellulose. The reason for using this filter paper is to avoid any interference of the living cytoplasm or any of the biological processes which occur in the natural stem of the plant, thus enabling the study of only the effect of fluid flow on the development and magnitude of this natural electrical potential.

A fluid was forced through a pad of filter paper. Electrodes located on each side of the pad were used for measuring the generated voltage and electric current. Figure 22 shows the schematic diagram of the apparatus used, and Figure 23 shows the actual apparatus.

The pad .9 cm thick, was constructed of 50 sheets of filter paper. It was kept in a plexiglass box, the inside of which was coated with paraffin wax. The box had a circular hole on each side. A glass tube of one inch inside diameter was fixed

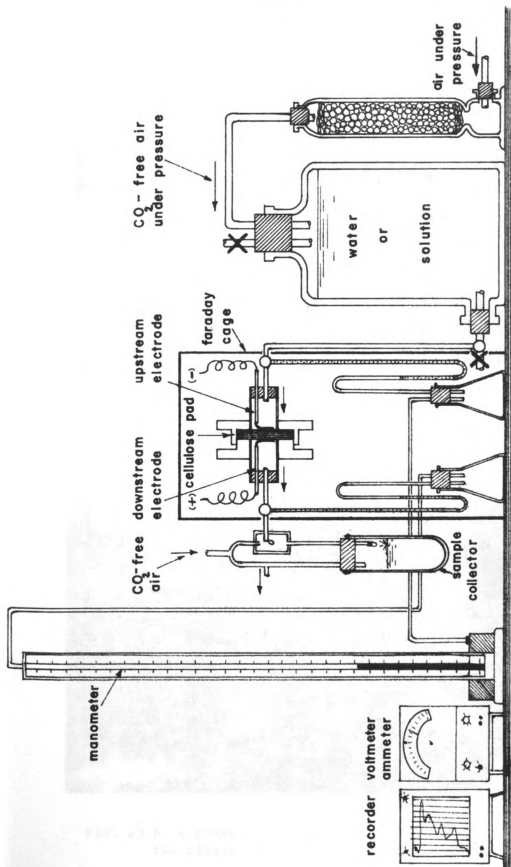


FIG. 22 - SCHEMATIC DIAGRAM OF THE USED APPARATUS

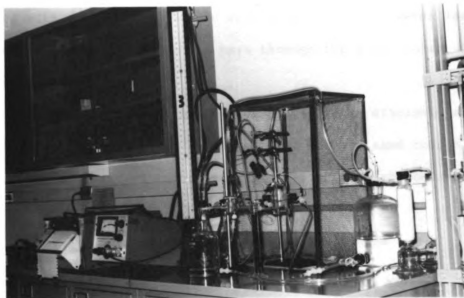


FIG. 23 A. The apparatus used to determine the electrical current and voltage. Showing the general set up, instrumentation, and Faraday cage.

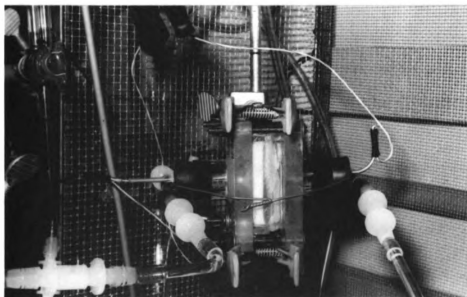


FIG. 23 B. A close up of the cellulose pad in the plexiglass container.

to each hole. With the pad in place the plexyglass box was sealed with the paraffin wax to eliminate any air or water leakage. Therefore, fluid was forced to pass through the glass tubes with the pad between them.

The unit was placed inside a Faraday cage to eliminate any electrical effect from the surroundings. For the same reason, shielded wire was used to connect the electrodes with the measuring instrument.

Tests were performed using the following fluids:

1. Pure distilled deionized water at 23.8<sup>o</sup>c
2. Solution of 0.005 M of KCl
3. Solution of 0.01 M of KCl
4. CO<sub>2</sub> sautrated water
5. Warm distilled deionized water at 30.0<sup>o</sup>c

Provisions were made to allow doing some changes during the performance of the experiments, such as: the change of pressure head, the change of the distance between the electrodes and the surface of the cellulose pad, and the change of the direction of the flow.

Silver - Silver chloride electrodes were used. The coiled wire electrodes were prepared as follows:

1. The base of the electrode was insulated by a thin glass tube filled with paraffin wax.
2. The wire was coiled, then coated with the silver chloride layer. This coating was performed by immersing the coiled end of two electrodes, facing each other, in 1%



HCl acid. The other ends of the electrodes, which were in contact to a  $1\frac{1}{2}$  volt battery, were reversed each 30 seconds for 6 complete cycles.

3. The coiled end was washed with deionized water before the electrode was used.

The electrical measurements were done by a "Keithley 150 B Microvolt Ammeter" having a voltage range from 0.01 microvolt to 1.0 volt, and an amperage range from 0.01 nano ampere (nano ampere =  $10^{-9}$  ampere) to 1.0 milliampere. The values measured were recorder on a "Keithley 370 strip recorder", having speeds of .75, 1.5, 3, 6, and 12 inch per minute, and same speed values per hour.

The pressure head difference was measured by a "Merian mercury manometer".

The distilled deionized water, which was used in all the experiments, was made by passing distilled water through a resin column to eliminate any anion or cations from the water. The resistance of this water was found to be more than 3M $\Omega$ .

The fluids used in the experiments, were kept in CO<sub>2</sub> - free air, and water samples were also collected under CO<sub>2</sub>-free air, except in the cases where CO<sub>2</sub> saturated water was used.

In each experiment, a series of different pressure heads, ranging from 0.2 to 20.0 inches of mercury was used, and voltage, current, volume flow rate, fluid conductivity and pH were measured and recorded.

For each fluid, the experiment was repeated at least three

times, to assure the reproducibility of the results. The electrodes were always reprepared before performing any experiment since the decay or the breakage of the silver chloride layer causes unstable readings.

From the data obtained, the following calculations were made:

$$\text{Pressure head cm H}_2\text{O} = (\text{in Hg}) \times (2.54) \times (13.537) = (\text{in Hg}) \\ \times (34.38)$$

$$\text{Pressure head } \frac{\text{dyne}}{\text{cm}^2} = (\text{cmH}_2\text{O}) \times (.99737) \times (980.67) = (\text{in Hg}) \\ \times (33631)$$

$$\text{Volume flow rate } \frac{\text{cm}^3}{\text{sec-cm}^2} = \frac{(\text{ml})}{(\text{min})} \times \frac{(1)}{(60)} \times \frac{1}{\pi (1.27)^2} \times = \\ \frac{(\text{ml})}{(\text{min})} \times .002583$$

This value equals also the velocity of flow

$$\text{Mass flow rate } \frac{\text{gm}}{\text{sec-cm}^2} = (\text{volume flow rate}) \times (.99737) = \\ \frac{(\text{ml})}{(\text{min})} \times (.002577)$$

$$\text{Potential energy } \frac{\text{dyne} - \text{cm}}{\text{sec}} = \frac{(\text{dyne})}{(\text{cm}^2)} \times (\text{flow velocity}) = (\text{in Hg}) \\ \times \frac{(\text{ml})}{(\text{min})} \times (86.8779)$$

$$\text{Kinetic energy } \frac{\text{dyne} - \text{cm}}{\text{sec}} = (\text{flow velocity})^2 \times (\text{mass flow rate}) \times (1/2) = \\ \frac{(\text{ml})^3}{(\text{min})} \times (.860 \times 10^{-8})$$

Dissipated energy  $\frac{\text{dyne} - \text{cm}}{\text{sec}} \approx (\text{Potential energy})$

$$\text{Electric energy } \frac{\text{dyne} - \text{cm}}{\text{sec}} = (\text{m.V}) (10^{-3}) (\mu \text{ A}) (10^{-6}) (10^7) =$$

$$(\text{m.V}) (\mu \text{ A}) (10^{-2})$$

$$\text{Ratio of } \frac{\text{Electric energy}}{\text{Dissipated energy (in Hg) } \frac{(\text{ml})}{(\text{min})}} = \frac{(\text{m.V}) (\mu \text{ A})}{(\text{m.V}) (\mu \text{ A}) (10^{-2})} \times (1.151 \times 10^{-4})$$

These figures are for water at 23.8°C. In the case of warm water or KCl solutions, the appropriate figures were used for each case.

## V. DISCUSSION OF RESULTS

The source of the natural electric potential in plants is an important question to be answered. The relationship between this electrical potential and fluid flow process is also important.

### V A. The Source of the Natural Electrical Potential:

In an attempt to determine the source of the natural electrical potential, a series of preliminary experiments were performed. Distilled deionized water was forced through a cellulose pad, by applying an external pressure. The generated voltage, due to fluid flow, was measured, and is shown in Figure 24.

In each experiment, it was noticed that a sudden negative electrical potential, of about -250 millivolts appeared when the cellulose pad was completely wetted. This negative potential decreased fast during the first two minutes, then continued to decrease gradually until it reached zero, about 15 to 25 minutes later. The time needed to reach zero voltage, depended upon the rate of water flow. The time required to reach zero decreased as the flow rate increased. In each case, the downstream electrode was the negative one.

After reaching zero, the voltage built up gradually, but it stopped increasing when it reached a certain reading which depended upon the flow rate. This building up voltage reversed the polarity

of the electrodes. Therefore, the downstream electrode became positive.

Whenever the flow of water was stopped, the voltage rapidly decreased to zero  $\pm$  10 millivolts. The longest time required to reach zero was about 10 hours, but in most the cases, it was a few minutes.

On the other hand, when the direction of flow was reversed, the electrical polarity was also reversed. Thus, the downstream electrode was always positive. The magnitude of voltage remained relatively constant, but of opposite sign. When the flow rate was increased, the voltage increased, Figure 25.

As the distance between the upstream electrode (negative) and pad surface was increased, the voltage decreased.

As the distance between the downstream electrode (positive) and pad surface was increased, the voltage increased. However, any increase of the distance more than 4 millimeters did not affect the voltage magnitude.

For either electrode, the current dropped when the distance between the electrode and pad surface was increased.

There are two possible explanations for the existence of this electric potential. Each depends upon a different theory.

#### V A-1. First Theory:

The active (OH) group in cellulose molecule, has the ability to form hydrogen bonds with two water molecules. Water molecule

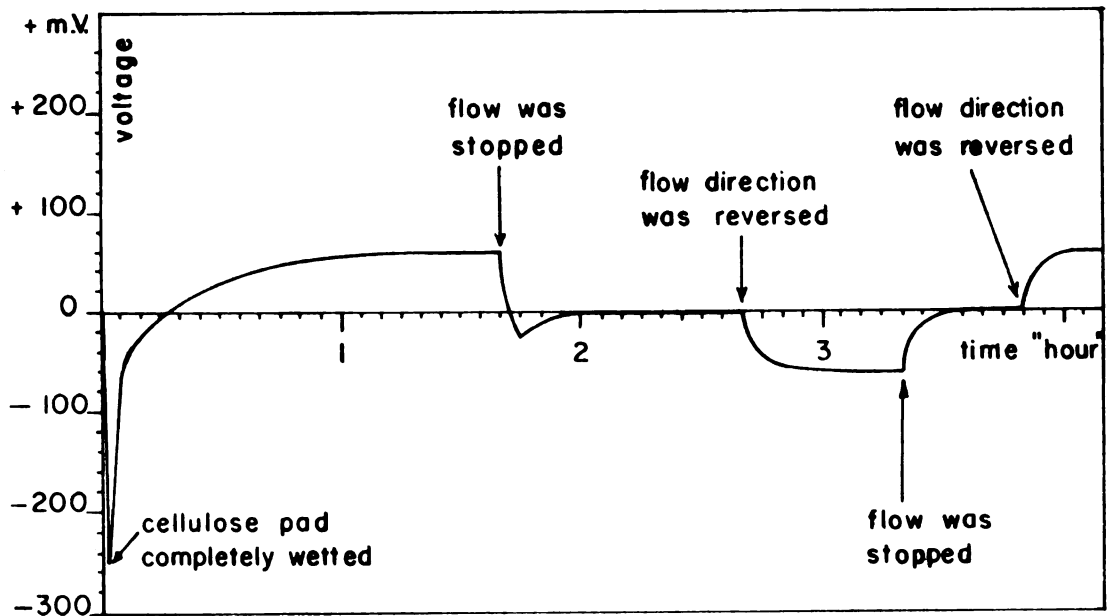


FIG. 24 - THE EFFECT OF WATER FLOW IN CELLULOSE PAD

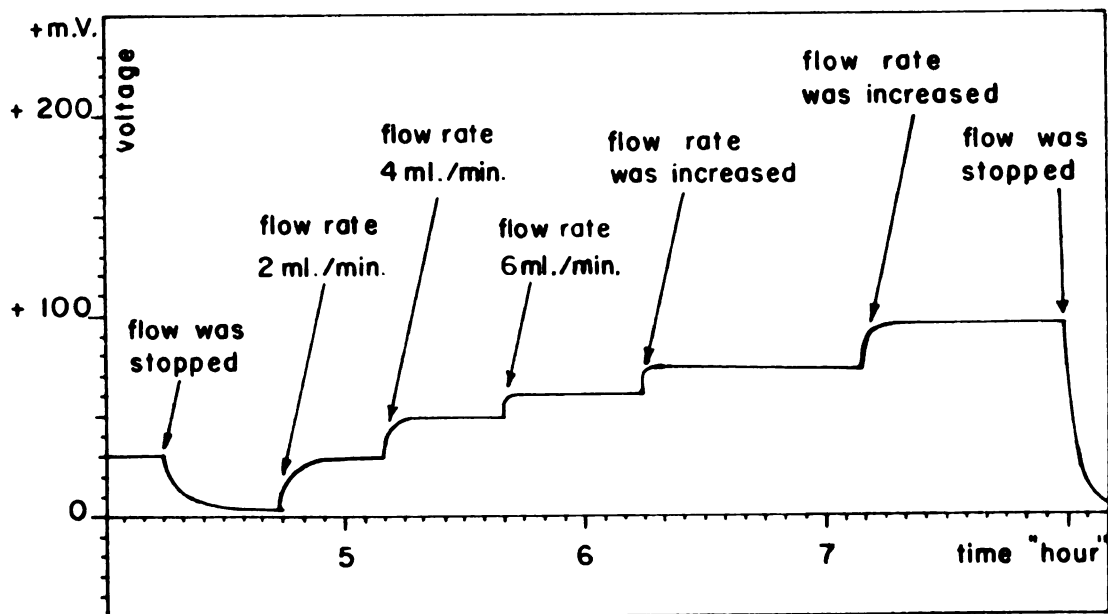


FIG. 25 - THE EFFECT OF WATER FLOW RATE

is a dipole. Therefore, when the cellulose is wetted, water molecules arrange themselves with the positive poles toward the oxygen atom of the active (OH) groups of cellulose molecules. This keeps the negative poles directed outward, which gives the wetted cellulose molecule a negatively charged surface.

Water has  $10^{-7}$  of its molecules dissociated in ( $H^+$ ) and ( $HO^-$ ) ions. ( $H^+$ ) ions are attracted towards this negatively charged surfaces of cellulose, and they form a positively charged layer adjacent to cellulose surfaces.

When water was forced to pass through the cellulose pad, this positively charged layer of ( $H^+$ ) ions was dragged with the flow which caused the observed electric potential.

However, if that is the case, then there is no reason for the drop in voltage when the distance between the upstream electrode and pad surface was increased. There is no reason also, for the increase in voltage when the distance between the downstream electrode and pad surface was increased. Moreover, the sudden negative potential which was noticed when the cellulose pad was completely wetted means that the cellulose caused the ionization of water. The ( $H^+$ ) ions of the ionized water molecules were attracted to the oxygen atoms of the active (OH) groups of cellulose, while the ( $HO^-$ ) ions were washed away with the flow. This process will leave the cellulose with positively charged surfaces, which does not agree with previous work done, Neale, (1946).

This strange observed behavior of the electrical potential lead to the second explanation of the source of this electric phenomenon.

V A-2. Second Theory: "Electron Accumulation Theory":

When water flows in capillary passages, it is subjected to great shear stresses due to the sliding of each molecule layer over the other. This shear stress will be greater near the inner wall surfaces, due to the greater value of velocity gradient there.

The dissipated energy, due to this shear stress, is not completely lost in form of heat. A part of this energy is converted to electric energy.

The sliding of two layers of water molecules over each other, breaks the bonds between these two layers, and causes some electrons to be expelled to the surrounding. When the sliding layers are close to cellulose surfaces, some of these electrons are expelled to these cellulose surfaces.

By the accumulation of electrons on its surfaces, the cellulose becomes negatively charged, while the water molecules, which have expelled the electrons, become positively charged.

Moreover, it is known that the loss of energy from water molecules at the inlet of any passage, is greater than the loss at the exit. The reasons for this are:

1. The changes in flow stream lines at the inlet are greater than the change at the exit.
2. The development of velocity profile, which starts at the inlet, results in the decrease of shear stress magnitude from the inlet towards the exit.



Therefore, this greater energy loss at the inlets of water passages causes more electron accumulation at the upstream side of the cellulose pad. Figure 26 represents that schematically.

V A-3. The Validity of "Electron Accumulation Theory":

The results of the experiments performed support this theory. The validity of this theory can be substantiated by re-examining the behavior of the electric phenomenon with respect to the change of flow and electrode conditions:

1. The downstream electrode was always positive, while the upstream electrode was always negative. This was a result of the greater accumulation of electrons on the upstream side.
2. The voltage dropped when the distance between the upstream electrode and pad surface was increased. This voltage drop occurred, because the upstream electrode did not, any more, measure the difference of the accumulation of electrons on the two sides of the pad. Instead, this electrode acted as one plate of a capacitor, with the pad side as the other plate.
3. The voltage increased when the distance between the downstream electrode and pad surface was increased. This voltage increase occurred, because this electrode got rid of some of the effect of the accumulated electrons on the upstream side of the pad. Therefore, the voltage reading was between the accumulated electrons on the upstream side of the pad, and the partially positively charged water molecules.

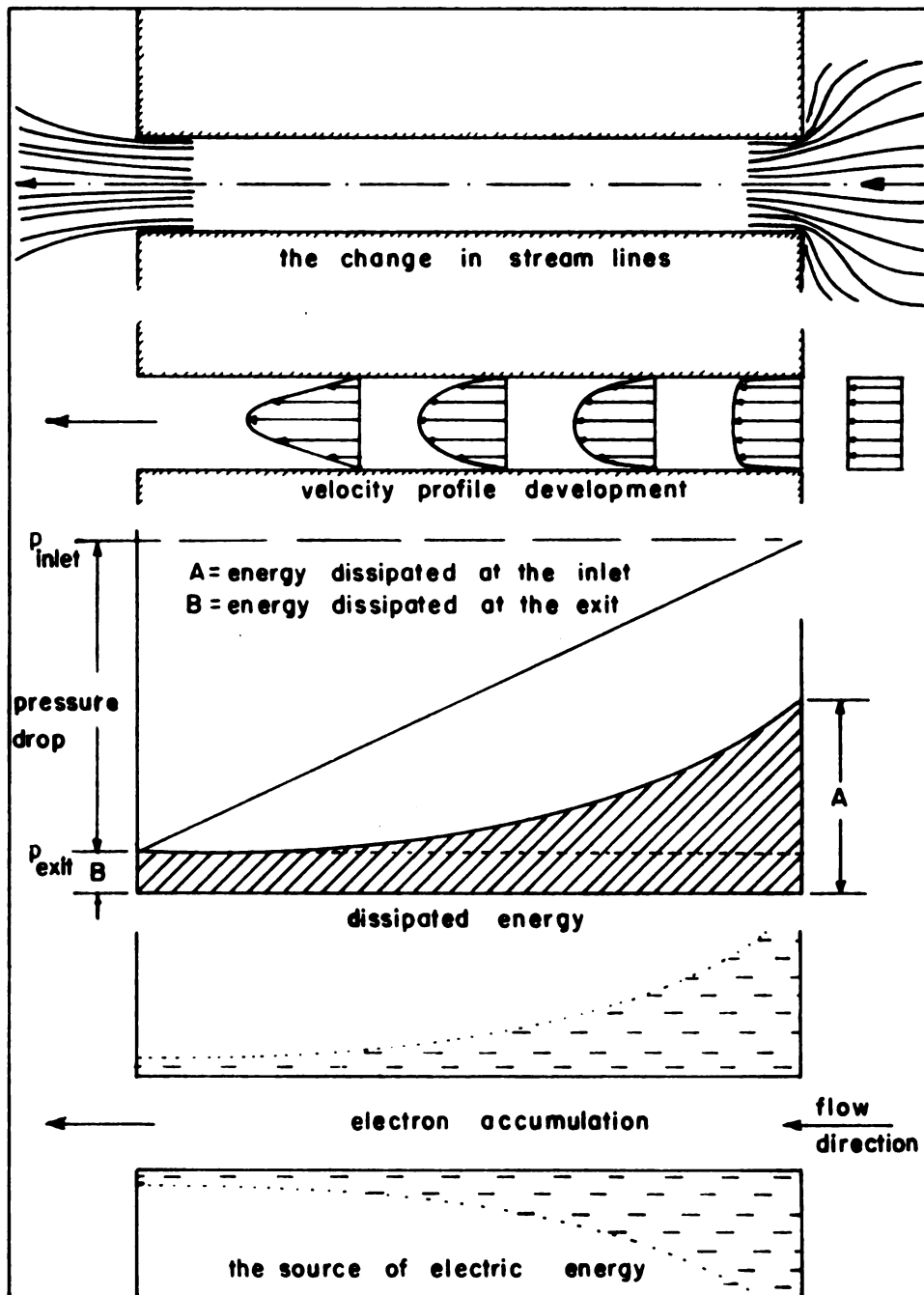


FIG. 26 - SCHEMATIC DIAGRAM REPRESENTS THE SOURCE OF ELECTRICAL POTENTIAL IN THE CELLULOSE PAD.

4. Beyond 4 millimeters, the distance between the downstream electrode and pad surface did not have any effect on the voltage. Beyond this distance, the effect of the accumulated electrons became negligible, thus the voltage stayed constant.
5. The current dropped when the distance between pad surface and either electrode was increased. This is expected because the electrical resistance was also increased. However, the drop in current with the increase in voltage at the same time, supports this theory.

Another test of this theory was made by performing another series of experiments, in which (0.01 Molar) KCl solution was used instead of water.

If the hydrogen-bonds are assumed to be the source of the negatively charged surfaces of cellulose, or if the zeta potential is assumed to be the source of the electric double layer, the voltage should increase, or at least its magnitude should remain constant, when KCl solution was used. However, this did not occur. When KCl solution was used, the voltage dropped to a very small magnitude.

According to "Electron Accumulation Theory", this voltage drop must be expected, because of the high conductivity of this solution. This high conductivity did not permit the accumulation of large quantity of electrons on the cellulose pad. Instead, it caused their discharge.

It can be concluded here, that the source of the electric energy is not an "intrinsic constant quantity" of the material, such as the zeta potential. This electric energy is generated by the dynamics of water flow, which has the ability to convert one form of energy to another. As the dynamics of flow process dissipates some of water's potential energy in form of heat energy, it converts some of the energy to electric energy.

V B. The Relationship Between Fluid Flow and The Electric Phenomenon:

V B-1. Electric Responses to the Tested Fluids:

The preliminary experiments were followed by a series of quantitative experiments. The tested fluids were:

1. Distilled deionized water at 23.8<sup>o</sup>c and 30.0<sup>o</sup>c
2. KCl solution: 0.005M and 0.01M
3. CO<sub>2</sub>-saturated water.

For each fluid tested, the cellulose pad was washed by a flow of distilled deionized water for 48 hours, followed by the tested fluid for 48 hours.

The results of these data are shown in tables: A.1 for water at 23.8<sup>o</sup>c, A.2 for warm water at 30.0<sup>o</sup>c, A.3 for CO<sub>2</sub>-saturated water, A.4 for (0.005M) KCl solution, and A.5 for (0.01M) KCl solution. These data were expressed graphically in Figures 27, 28, 29, 30, and 31 respectively.

For each fluid tested, a series of three experiments were

performed, but only the data of the first of these experiments was tabulated and represented graphically. The other two experiments gave similar data, but the magnitude of this data was always lower due to the decay of the silver chloride layer of the electrodes. The performance of three experiments assured the reproducibility of the obtained results.

Table A.1 and Figure 27, show the effect of water flow on voltage and current across the cellulose pad. Flow rate increased linearly with the increase in water potential difference ( $\Delta p$ ), while the increases in both the electrical potential and current were close, but not exactly linear with respect to ( $\Delta p$ ). The dissipated energy was a parabolic function of  $\Delta p$ . Figure 32-A shows the parabolic relation between the dissipated energy and ( $\Delta p$ ).

The relation between the electric energy and ( $\Delta p$ ) was nearly parabolic. The deviation of this relationship from being parabolic, may be due to a decrease in the rate of electron accumulation on cellulose surfaces as the later became overcharged with these electrons. Voltage and current curves, Figure 27, show that the rate of increase of voltage and current declined as  $\Delta p$  increased.

When warm water at 30.0°C was used, Table A.2 and Figure 28, this reduction in the rate of electron accumulation also occurred.

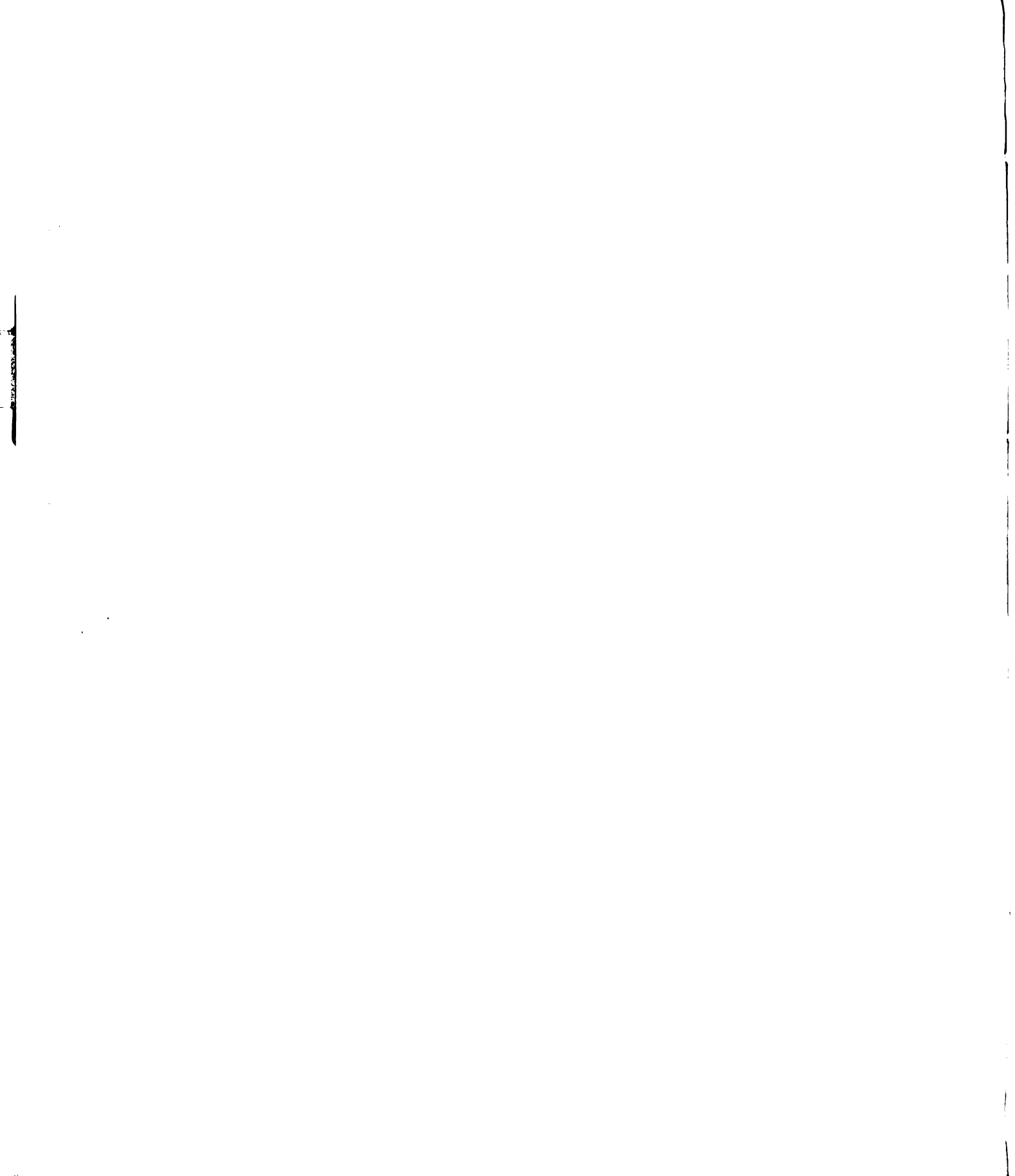
An increase in water temperature, increased the kinetic energy of water molecules. Therefore, the dissipated energy

increased, and so the electric energy. Figure 32-B shows that the dissipated energy was a parabolic function of  $\Delta p$ . It also shows that the electric energy when warm water was used, departed more from being a parabolic function of  $\Delta p$ . This deviation from the parabolic relation may be due to the same previously mentioned reasons.

Table A.3 and Figure 29, show the effect of flow of  $\text{CO}_2$ -saturated water in cellulose pad, on the voltage, current, dissipated energy, and electric energy. Figure 29 shows that the relationship between  $\Delta p$  and voltage, current, and flow velocity was linear. The similarity of both the dissipated energy and the electric energy curves was great. Figure 32-C shows that these two kinds of energies were related to each other, and were parabolic functions of ( $\Delta p$ ).

The magnitude of the electric energy dropped to 1/10 its magnitude when  $\text{CO}_2$ -saturated water was used instead of water. According to the "Electron Accumulation Theory", the higher electric conductivity of  $\text{CO}_2$ -saturated water caused the discharge of electrons from cellulose surfaces. Thus, the voltage dropped to 1/20 its magnitude when  $\text{CO}_2$ -saturated water was used instead of water.

On the contrary, the current reading was doubled. A possible explanation of that, is that some cations of the fluid were attracted towards the negatively charged cellulose surfaces. Some of these cations caused the discharge of some of the accumulated electrons, while others, being dragged with the flow,



caused the high current reading.

The drop in electric energy was due to the decrease in voltage, which was previously mentioned. The magnitude of the electric energy was 1/10 its magnitude, when CO<sub>2</sub>-saturated water was used instead of water. That means that 90 per cent of this electric energy was utilized in moving more cations with the flow. In other words, 90 per cent of the electric energy was converted into kinetic energy for moving these cations.

As previously mentioned, fluid samples were taken before and after the fluid tested passed the cellulose pad. The pH and conductivity of these samples were measured. The data were insignificant because the used pH meter, gave almost the same reading ( $\pm .04$ ) for the sample which were taken before or after passing the cellulose pad. The conductivity meter gave exactly the same readings for both kinds of samples. This was because the sensitivity of the available meters was less than it should be to show this slight changes in cation concentrations. Therefore, these data were neglected.

When (0.005 M) KCl solution was used instead of water, the velocity, voltage and current were in linear relationship with ( $\Delta p$ ), Table A.4 and Figure 30. The current increased five times, while the voltage dropped to about 1/100 its magnitude, when KCl solution was used instead of water. The result was a drop in the electric energy to 1/20 its magnitude for pure water. By



following the same reasoning, it can be said that 95 per cent of the electric energy was utilized in moving more cations with the flow.

The use of (0.01M) KCl solution also caused the drop of the electric energy, Table A.5 and Figure 31. The relationship of flow velocity, voltage, and current vs. ( $\Delta p$ ) was linear. The voltage dropped to about 1/200 of its magnitude when (0.01 M) KCl solution was used instead of water. The magnitude of the current was doubled. Thus the electric energy dropped to about 1/100 of its magnitude for pure water. This means, once again, that 99 per cent of this electric energy was utilized in moving more cations with the flow. Figure 32-D shows the relationship between the electric energy and the dissipated energy for both concentrations of KCl solution. It also shows the parabolic relationship between the two forms of energy and ( $\Delta p$ ).

All energy curves, for all the fluids tested, were drawn together in Figure 33, to show the relative magnitude of the electric energy for all fluid tested.

On the other hand, Table A.6 and Figure 34, represent the effect of the distance between downstream electrode and pad surface on voltage and current magnitude. This was previously discussed.

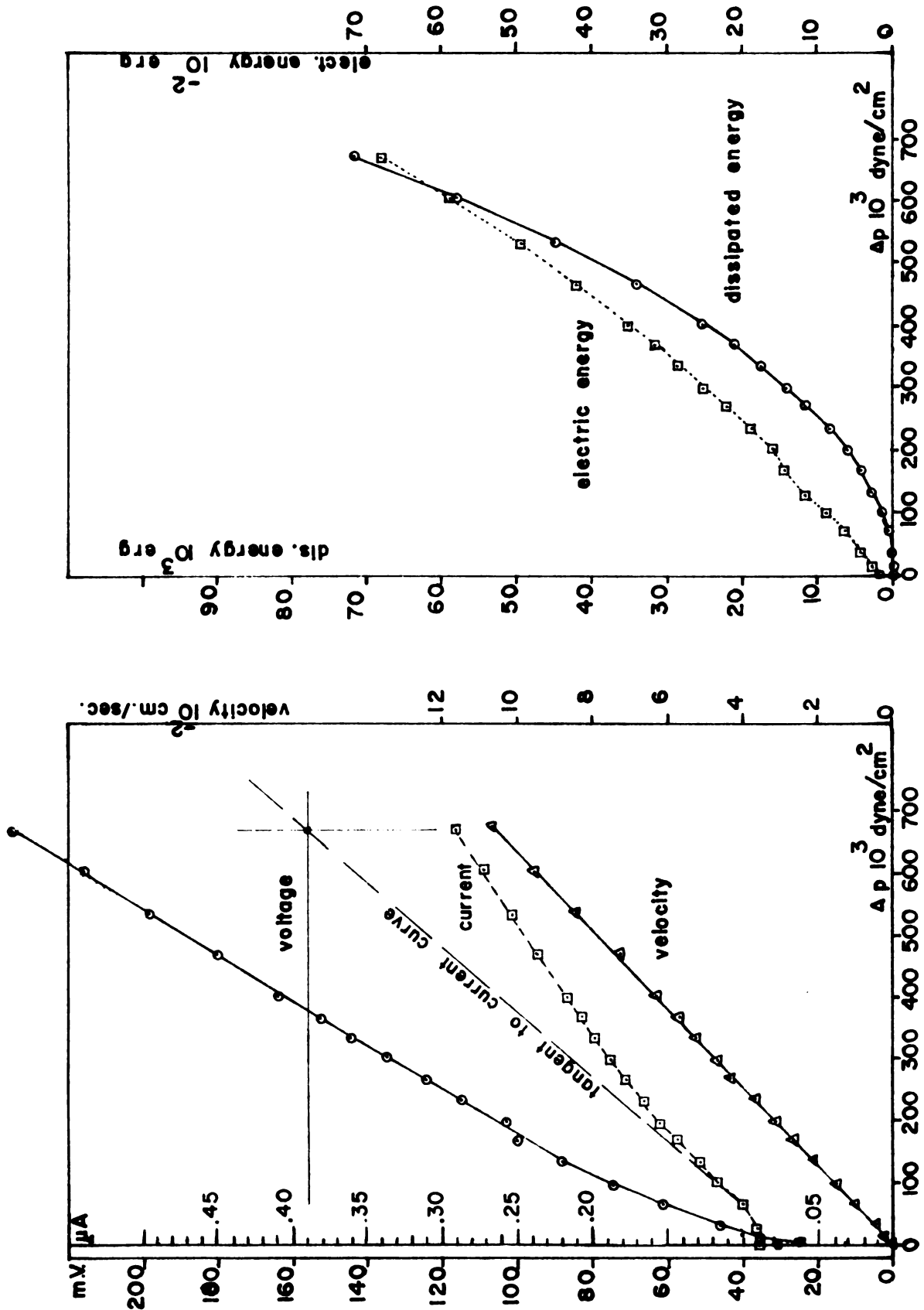


FIG.27- THE EFFECTS OF FLOW OF DISTILLED DEIONIZED WATER (23.8°C) IN CELLULOSE PAD ON VOLTAGE, CURRENT, AND DISSIPATED AND ELECTRIC ENERGY.

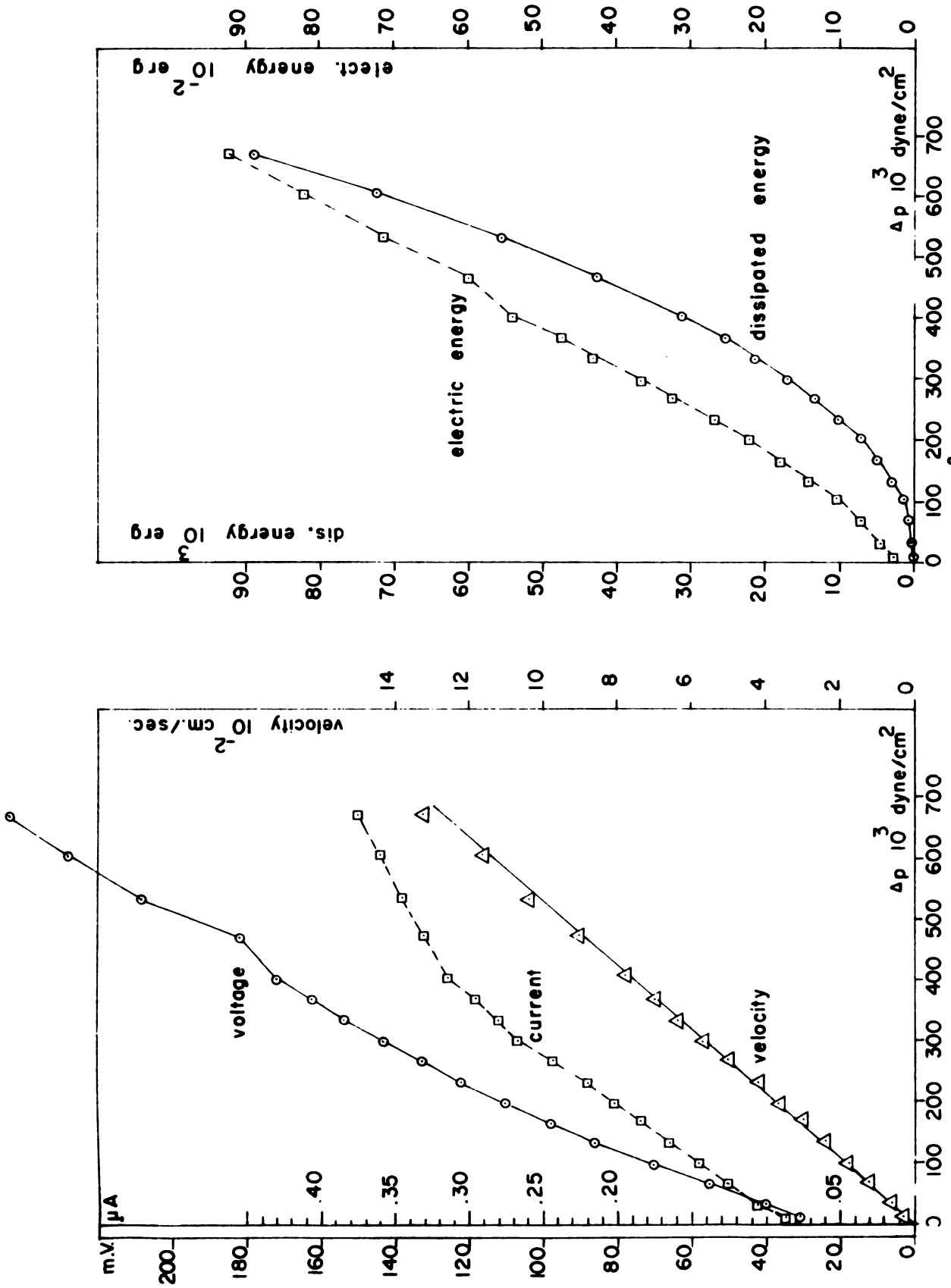


FIG. 28 - THE EFFECTS OF FLOW OF WARM WATER (30.0°C) IN CELLULOSE PAD ON VOLTAGE, CURRENT, AND DISSIPATED AND ELECTRIC ENERGY.

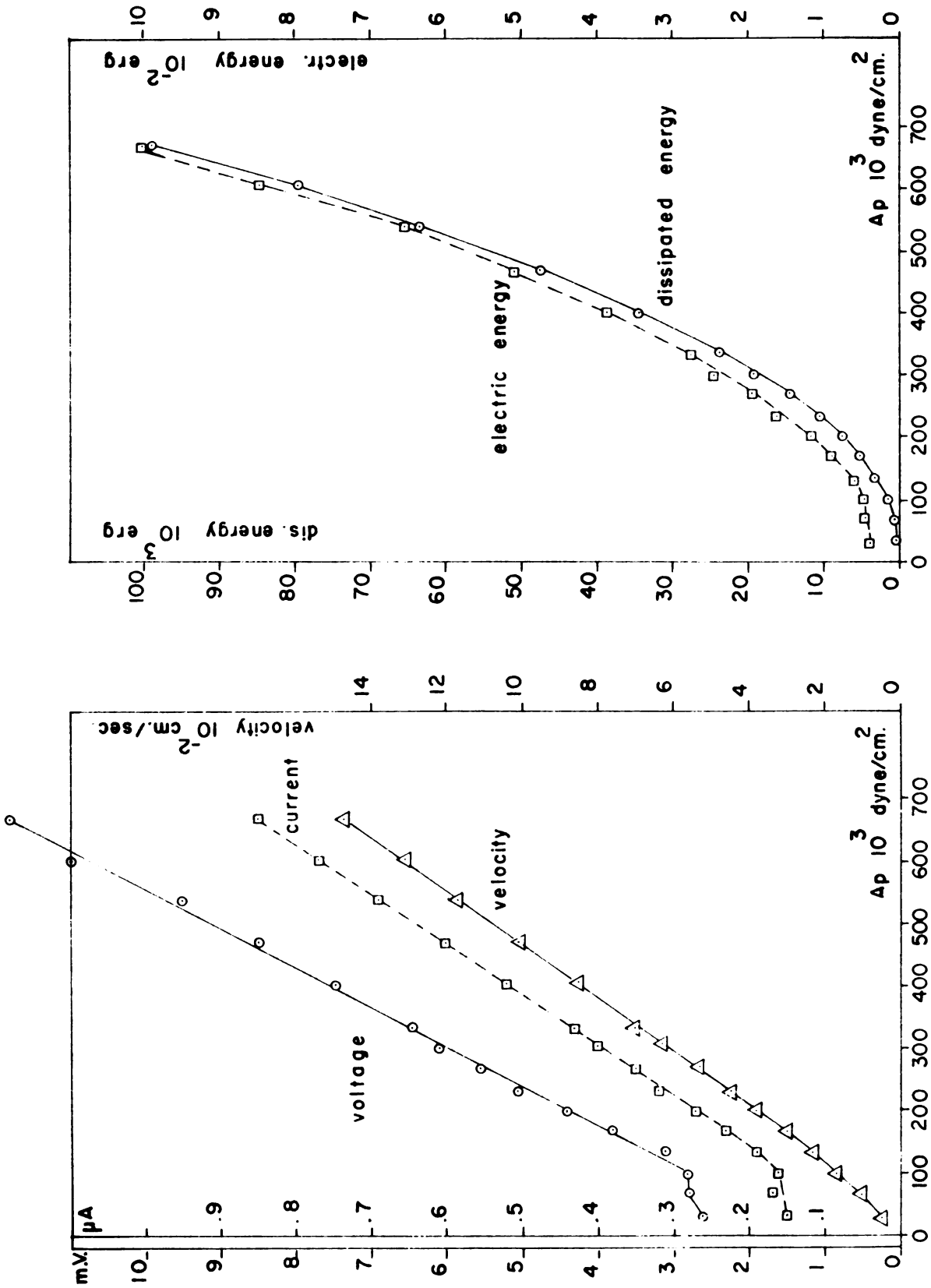


FIG. 29 - THE EFFECTS OF FLOW OF CO<sub>2</sub>-SATURATED WATER IN CELLULOSE PAD ON VOLTAGE, CURRENT, AND DISSIPATED AND ELECTRIC ENERGY.

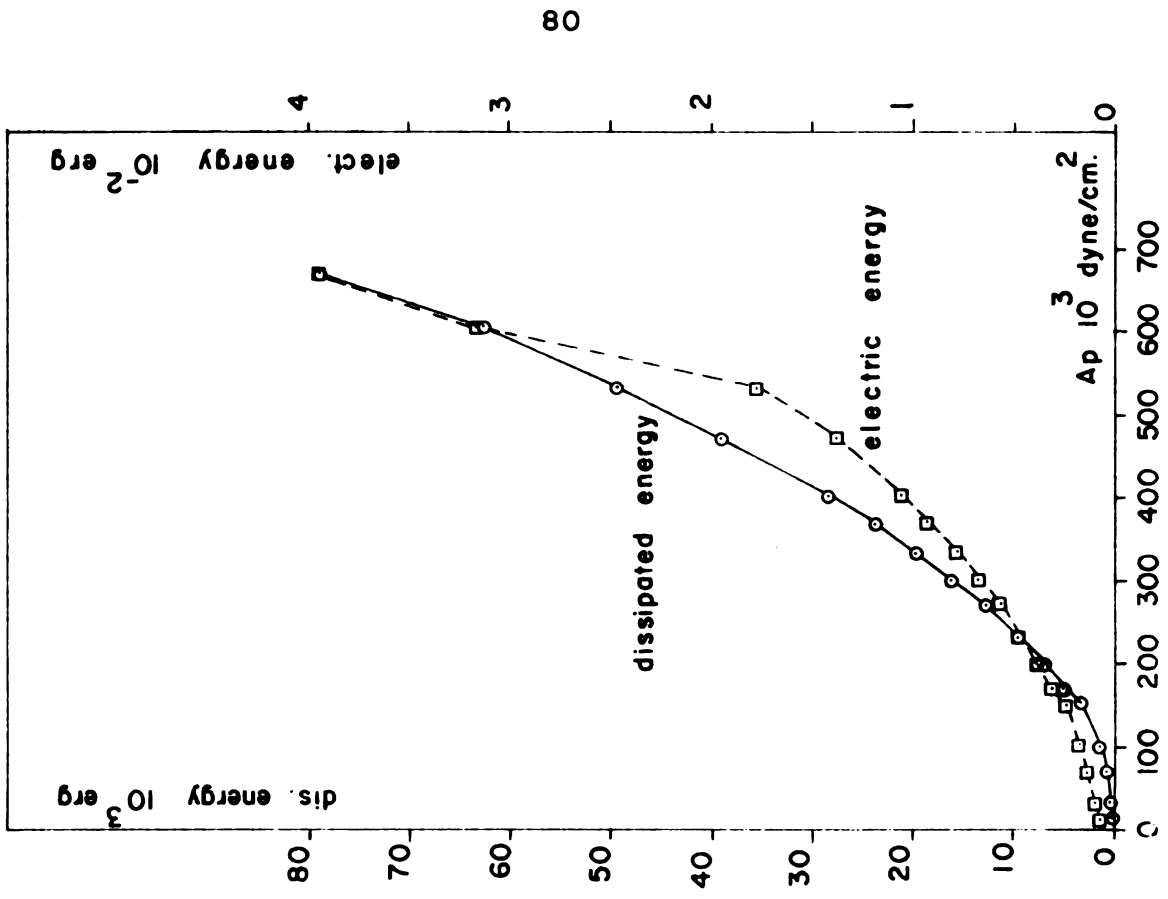
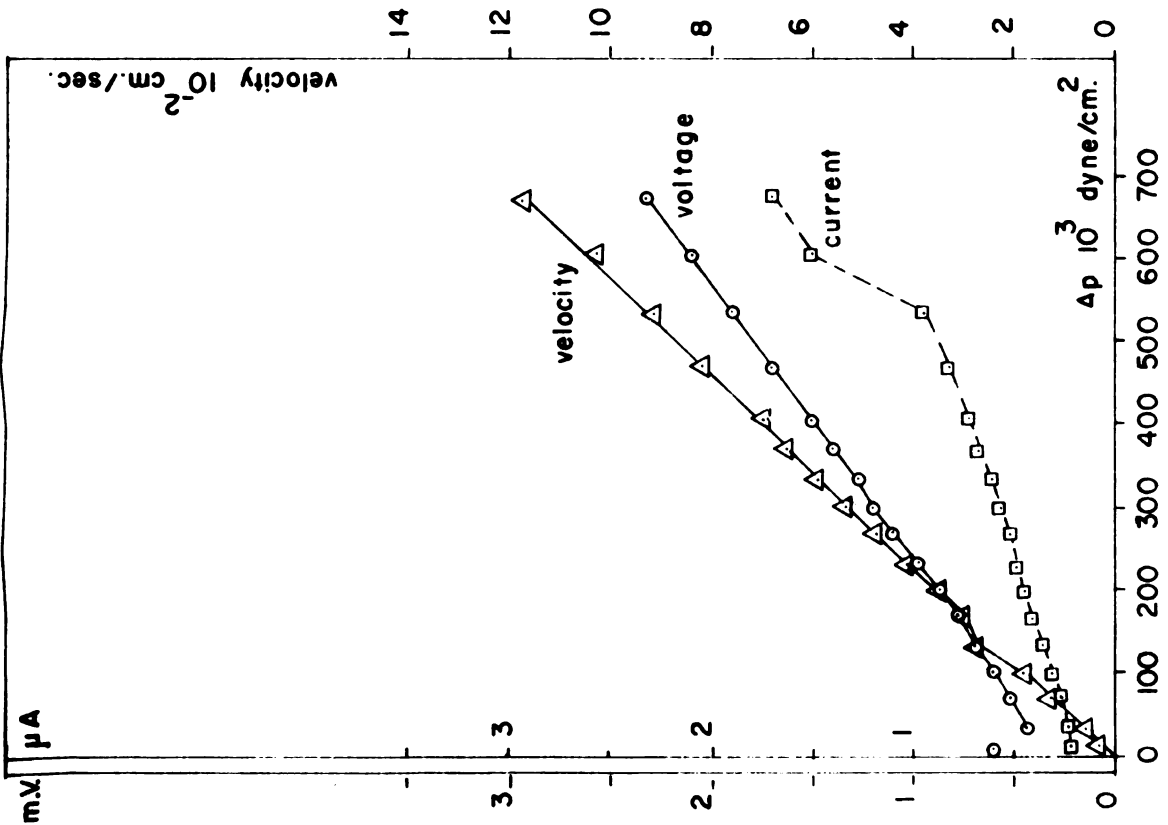


FIG. 30 - THE EFFECTS OF FLOW OF (.005M) KCl SOLUTION IN CELLULOSE PAD ON VOLTAGE, CURRENT, AND DISSIPATED AND ELECTRIC ENERGY.

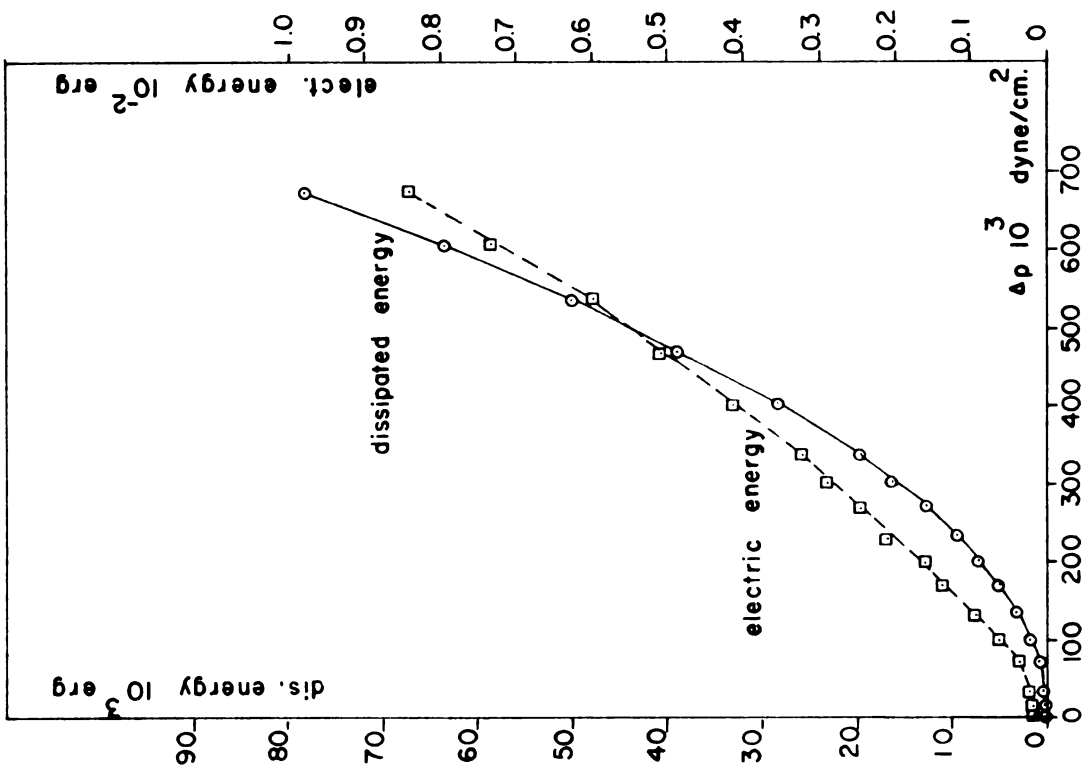
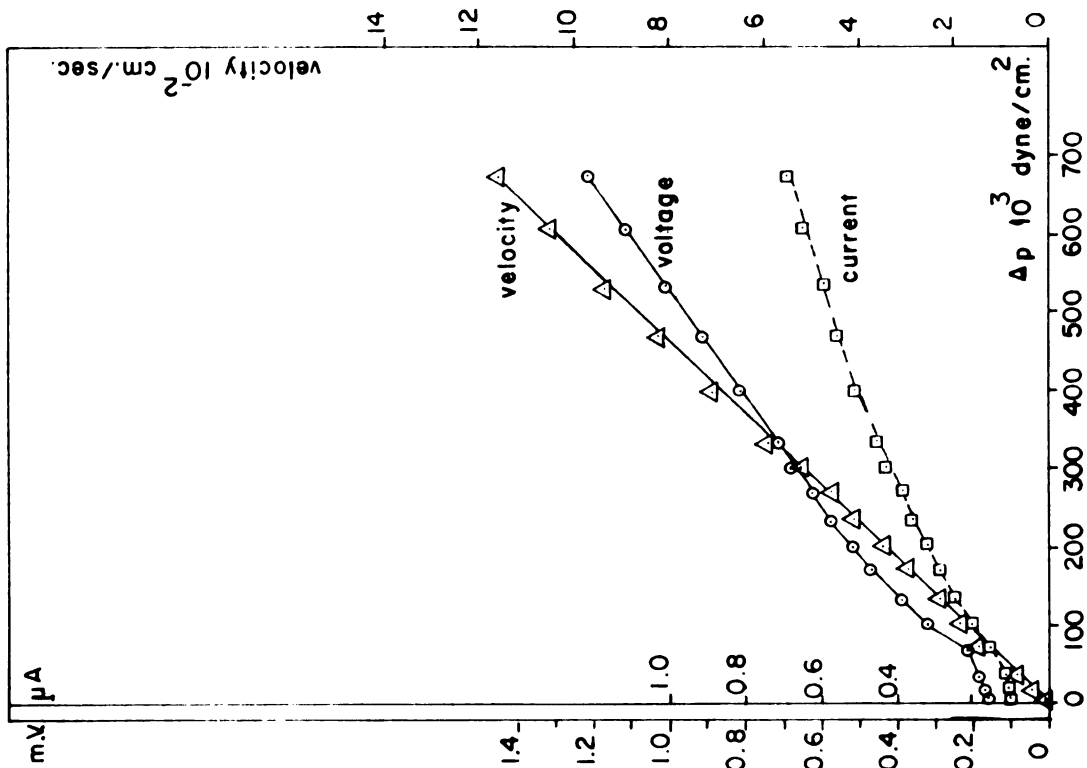


FIG. 31 - THE EFFECTS OF FLOW OF (.01 M) KCl SOLUTION IN CELLULOSE PAD ON VOLTAGE, CURRENT, AND DISSIPATED AND ELECTRIC ENERGY.

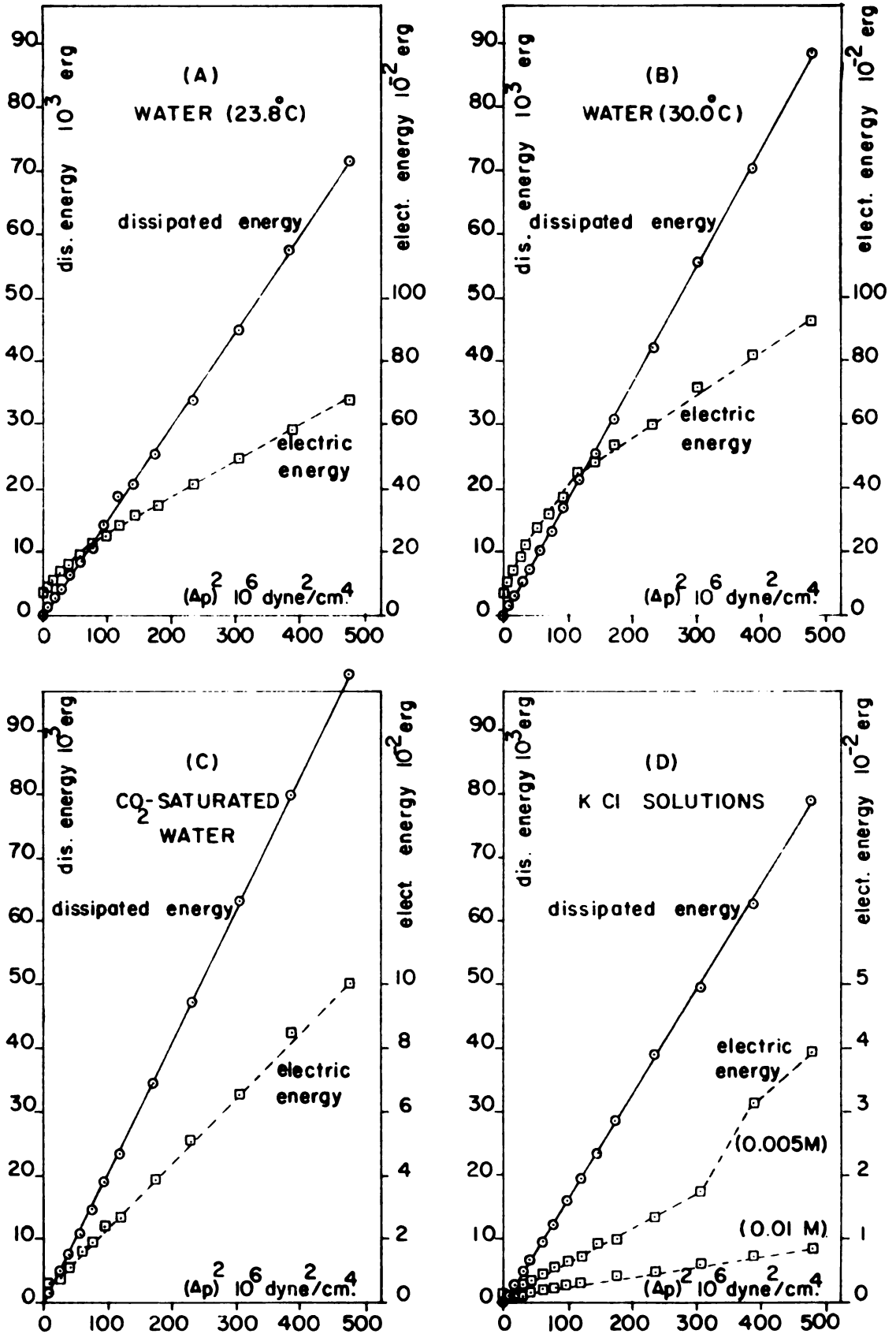


FIG. 32 - ELECTRIC ENERGY AND DISSIPATED ENERGY AS FUNCTIONS OF  $(\Delta p)^2$ .

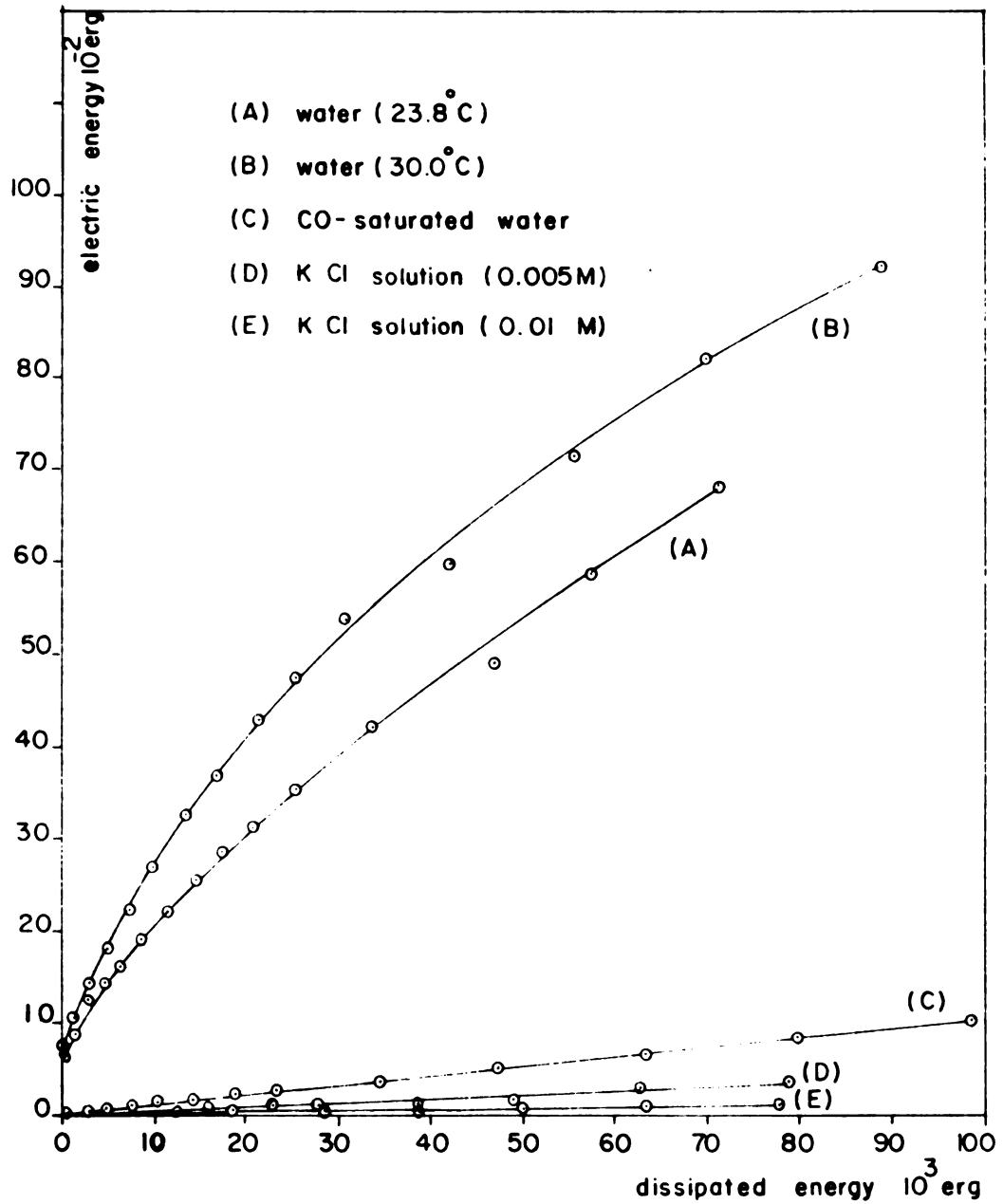
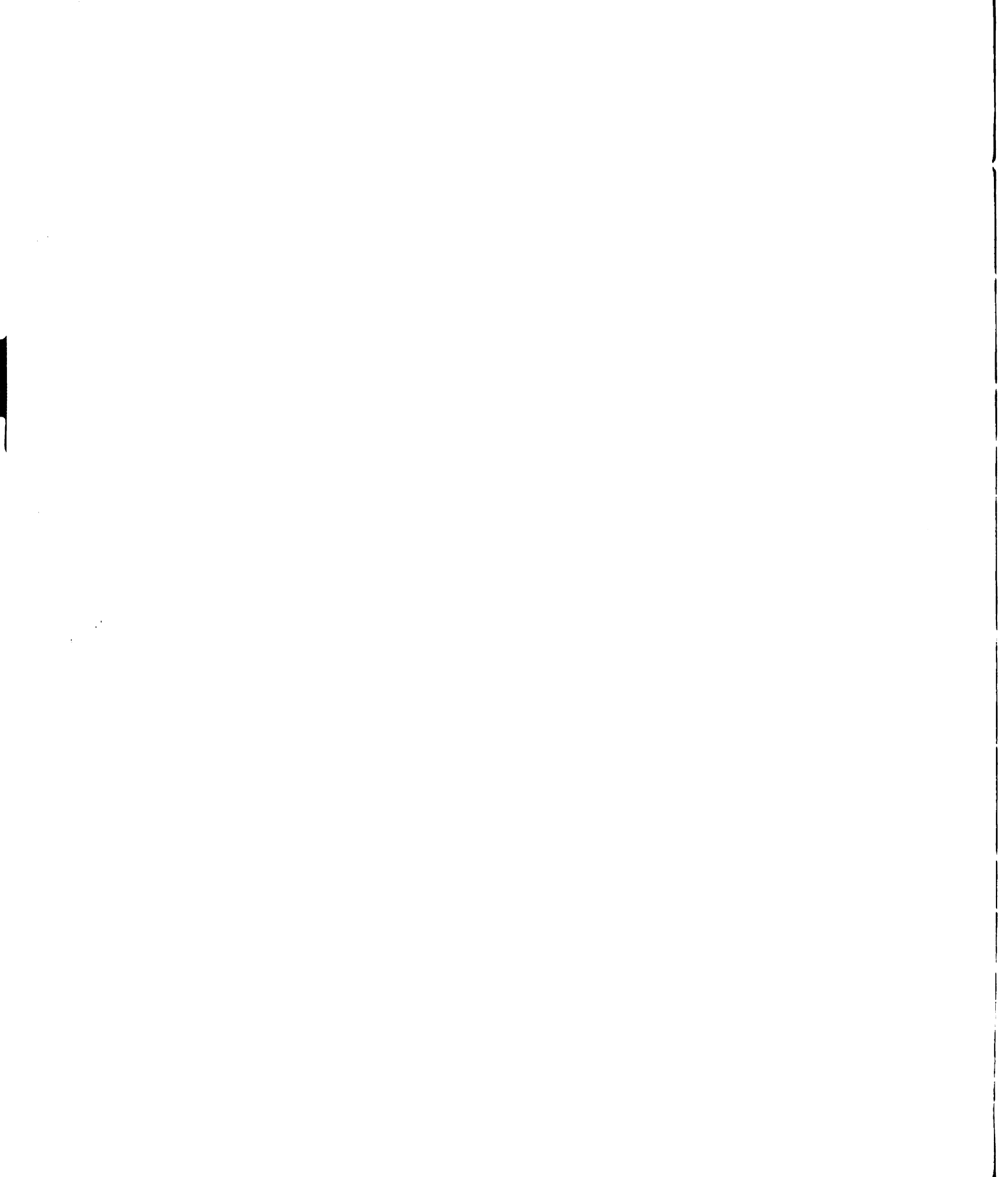


FIG. 33 - THE GENERATED ELECTRIC ENERGY OF THE FLUID TESTED.





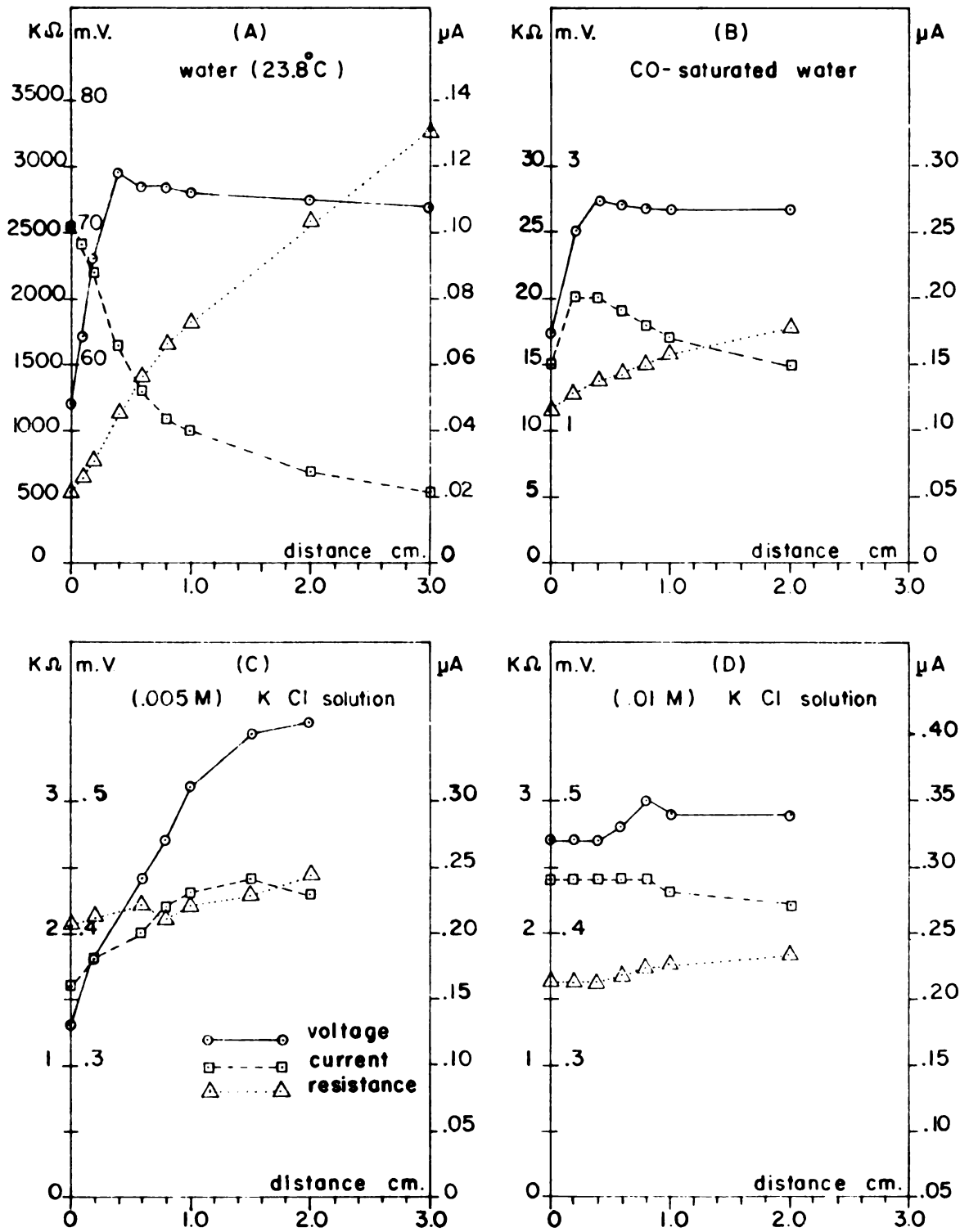


FIG. 34 - THE EFFECT OF THE DISTANCE BETWEEN DOWNSTREAM ELECTRODE AND PAD SURFACE, ON VOLTAGE AND CURRENT.

Another experiment was performed, using glass fiber filter paper instead of cellulose filter paper. In this experiment, a pad constructed of 20 sheets of filter paper was used (filter discs No. 5270-D grade 934 AH, Arthur H. Thomas Company, Philadelphia, Pa.). Distilled deionized water at 22.6<sup>o</sup>c was used with this glass fiber pad. The voltage and current were measured by a "Multi Function Unit," Model 3444A DC, Hewlett Packard, with voltage range from 0.01 millivolts to 1000 volts, and current range from 0.01 microamperes to 1.0 ampere.

The data of this experiment were tabulated in Table A.7, and were expressed graphically in Figure 35.

Table A.7 and Figure 35 show that the use of glass filter paper instead of cellulose filter paper caused the increase of voltage, current, dissipated energy and electric energy. Figure 35 shows that both the electric and dissipated energy are related, and are parabolic functions of  $\Delta p$ .

Table A.1 and Table A.7, show that when  $\Delta p$  was  $\approx 672 \times 10^3$  dyne/cm<sup>2</sup> the voltage and current readings were for a cellulose pad 235 millivolts and 0.29 microamperes; and for a glass fiber pad 4200 millivolts and 6.50 microamperes. Both the voltage and the current were about 20 times greater when glass fiber pad was used in place of a cellulose pad. The two tables show also that the dissipated energy was about  $72 \times 10^3$  ergs when a cellulose pad was used, and about  $159 \times 10^3$  ergs when a glass fiber pad was used. The electric energy was 0.68 erg in case of

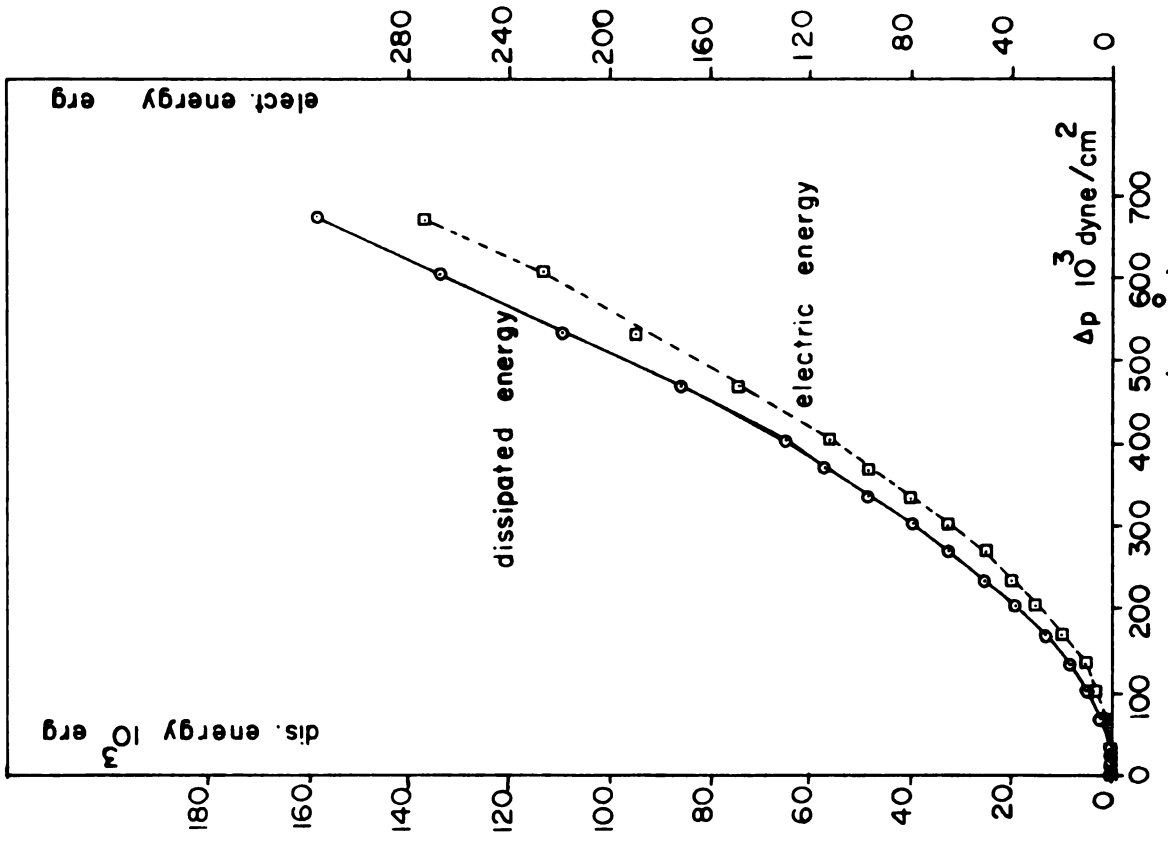
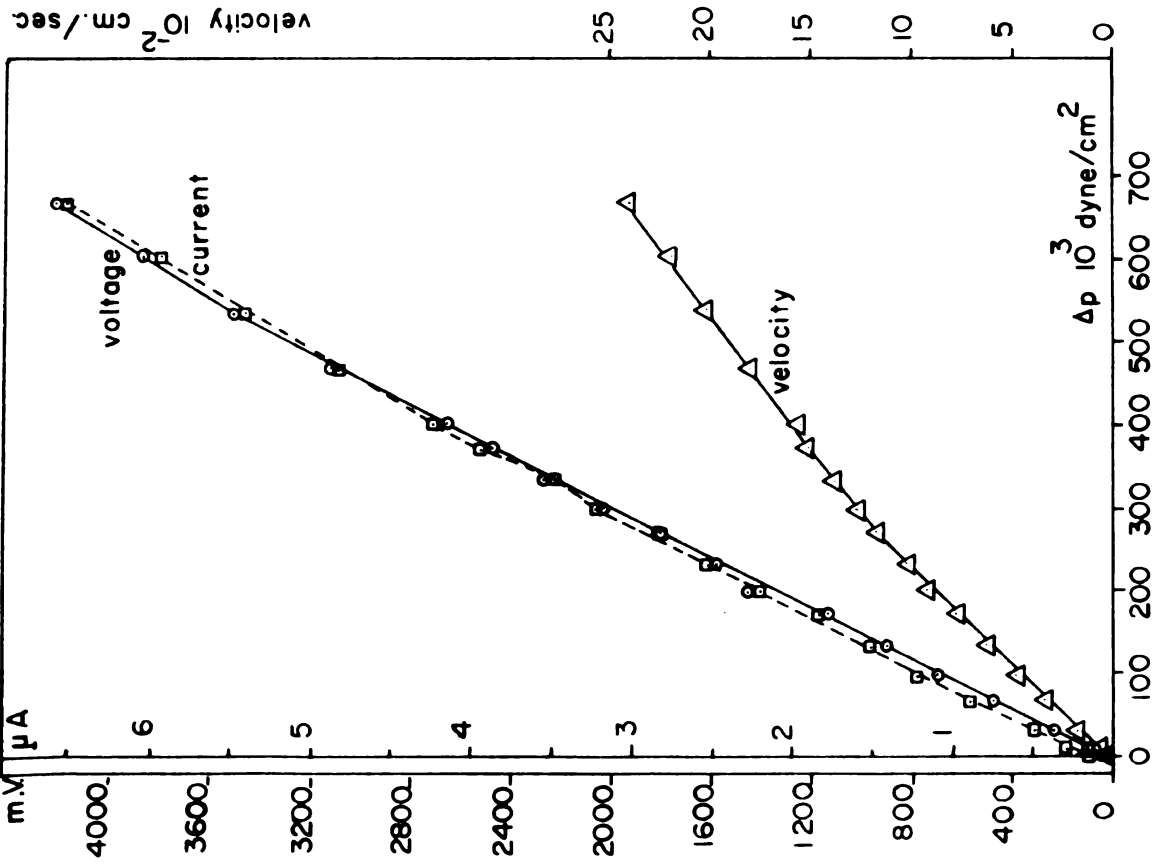


FIG. 35 - THE EFFECTS OF FLOW OF DISTILLED DEIONIZED WATER (22.6C) IN A GLASS-FIBER PAD ON VOLTAGE, CURRENT, AND DISSIPATED AND ELECTRIC ENERGY.

a cellulose pad, while it was 273 ergs in case of a glass fiber pad. Finally, the flow rate was 0.107 cm/sec in case of cellulose pad, while it was 0.236 cm/sec in case of glass fiber pad.

A comparison between the data of the two tables can be explained as follows. The flow passage appeared to be bigger in diameter in the glass fiber pad, which had a higher flow rate. However, the greater flow rate resulted in a larger rate of energy dissipation, probably caused by greater friction losses. The final result was a greater accumulation of electrons on the glass fiber surfaces, which in turn caused the high readings of voltage and current.

V B-2. Numerical Evaluation of Electric Responses to the Tested Fluids:

A further investigation of the response of the generated electric energy was done numerically. In this numerical analysis, the data of the distilled deionized water, Table A.1 was used.

The maximum flow rate, Table A.1, was  $106 \times 10^{-3}$  cm per second. This reading corresponds to flow rate of 6 cm per minute, which is within the range of the actual sap

movement in xylem tissues. The voltage reading corresponding to this flow rate, Table A.1, was 235 millivolts, and the current was 0.29 micro-amperes.

The nonlinearity of voltage and current curves, Figure 27, was considered in the previous discussion, to be a result of the overcharging of cellulose with the expelled water electrons. If there was a means to cancel the repelling effect of the accumulated electrons, voltage and current curves should be linear with respect to  $p$ . That means that the number of the expelled electrons from water, should be greater than what was actually measured.

When KCl solution was used, the conductivity of this solution caused the discharging of the accumulated electrons from cellulose surfaces. Therefore, there was no overcharging with electrons, no repelling effects of electrons, and no limits on the number of electrons which could be expelled from water as it passed in the pad.

To estimate what the current reading should be if its relationship with  $p$  was linear, a tangent line to the first portion of the current curve was drawn, Figure 27. The current

reading on this tangent line, which corresponds to flow rate of  $106 \times 10^{-3}$  cm/sec., is 0.39 microamperes. This reading was converted to a number of positive charges as follows:

$$\begin{aligned}
 1 \text{ electron-charge} &= 1.602 \times 10^{-19} \text{ coulomb} \\
 1 \text{ coul} &= 0.6242 \times 10^{19} \text{ e} \\
 1 \text{ Ampere-sec.} &= 1 \text{ coul.} \\
 &= 0.6242 \times 10^{19} \text{ e} \\
 1 \text{ } \mu\text{A.-sec.} &= 0.6242 \times 10^{13} \text{ e} \\
 0.39 \text{ } \mu\text{A.-sec.} &= 0.6242 \times 10^{13} \times 0.39 = 2.43 \times 10^{12} \text{ e}
 \end{aligned}$$

This indicates that  $2.43 \times 10^{12}$  positive charges should pass through the cellulose pad each second, when the flow rate was  $106 \times 10^{-3}$  cm/sec. However, the actual number of positive charges which passed per second was:

$$0.29 \text{ } \mu\text{A.-sec.} = 0.6242 \times 10^{13} \times 0.29 = 1.81 \times 10^{12} \text{ positive charges/sec}$$

For each positive charge passed through the pad, one electron was expelled to the cellulose pad. The constant reading of the voltage means that there existed an equilibrium condition in which the electrons expelled to the cellulose were balanced by some electrons discharged from the cellulose.

Water has  $10^{-7}$  of its molecules dissociated in ( $\text{H}^+$ ) and ( $\text{HO}^-$ ) ions. The ( $\text{H}^+$ ) ions, being attracted toward the negatively

charged cellulose surfaces, discharged some of the accumulated electrons, then were dragged with the flow without causing any current.

The number of  $(H^+)$  ions which passed through the pad per second were calculated as follows:

$$\text{mass flow rate/sec.} = 0.1067 \times .99737 = 0.10642 \text{ gm/sec}$$

$$\text{Number of } H_2O \text{ molecules/sec} = \frac{0.10642}{18} \times (6.023 \times 10^{23})$$

$$= 3.56 \times 10^{21} \text{ molecules/sec}$$

$$\text{Where the Avocado Number} = 6.023 \times 10^{23} \text{ molecules/mole}$$

$$\text{Number of } (H^+) \text{ ions/sec} = 3.56 \times 10^{21} \times 10^{-7} = 3.56 \times 10^{14}$$

$$(H^+) \text{ ions/sec}$$

$$\text{Ratio of } \frac{(H^+)}{e} = \frac{3.56 \times 10^{14}}{1.81 \times 10^{12}} = 1.97 \times 10^2 \approx 200$$

This ratio indicates that the number of  $(H^+)$  ions which passed through the pad per second, was 200 times the number of the positive charges which passed through the pad per second. This great number of  $(H^+)$  ions should discharge all the accumulated electrons on the cellulose surfaces.

However, no electron could be discharged unless there was an  $(H^+)$  ion passing adjacent to the negatively charged walls of water inlets of the pad. The number of these  $(H^+)$  ions, which were moving along with the water molecule layer adjacent to the inner walls of the passages, was estimated as follows:

If the inlet diameter is  $\delta$ , and water molecule diameter is



$\delta_w$ , the ratio between the number of water molecules which pass, to the number of the molecules which pass adjacent to the inner walls will be:

$$\frac{\pi \delta^2/4}{\pi \delta^2/4 - \pi \left(\frac{\delta}{2} - \frac{\delta}{w}\right)^2} = \frac{\delta}{4 \delta_w \left(1 - \frac{\delta_w}{\delta}\right)}$$

This ratio increases as the diameter of the inlet increases.

Assuming  $\delta = 0.6 \text{ micron}$  and  $\delta_w = 1.5 \text{ \AA}$

$$\delta = 4000 \delta_w$$

The ratio  $\frac{\delta}{4 \delta_w \left(1 - \frac{\delta_w}{\delta}\right)}$  will be  $\frac{4000 \delta_w}{4 \delta_w \left(1 - \frac{\delta_w}{4000 \delta_w}\right)} \approx 1000$

Therefore, the number of ( $H^+$ ) ions which could discharge the electrons from inner wall surfaces, was computed as

$$3.56 \times 10^{14} \times \frac{1}{1000} = 3.56 \times 10^{11}$$

The ratio  $\frac{(H^+)}{e} = \frac{3.56 \times 10^{11}}{1.81 \times 10^{12}} \approx 0.20$

This ratio means that the ( $H^+$ ) ions, which discharged some electrons from the cellulose, were about 20 per cent of the positive charges which were moving along with the flow.

Each ( $H^+$ ) ion discharged one electron, passed with the flow as a neutral (H). At the same time, there was an ( $HO^-$ ) ion passing also with the flow. These ( $HO^-$ ) ions created a current in opposite direction, which when superimposed on the real current,

decreased the reading. The number of these ( $\text{HO}^-$ ) ions, like the ( $\text{H}^+$ ) ions, was also about 20 per cent of the number of the positive charge which were moving with the flow.

Therefore the real current of positive charges can be computed to be:

$$\begin{aligned} & \text{the actual current of positive charges} \times \frac{120}{100} \\ 1.81 \times 10^{12} \times \frac{120}{100} &= 2.172 \times 10^{12} \text{ e} \end{aligned}$$

This number is closer to the number of positive charges which was computed from the tangent of the current curve, and which was  $= 2.43 \times 10^{12} \text{ e}$ .

From these calculations, it can be concluded that the non-linearity of the current curve was due to:

- 1) the repulsive effect of the accumulated electrons on cellulose surfaces.
- 2) the superimposed reverse current.

A calculation was made to examine the effect of the smaller diameters of the gaps between cellulose microfibrils in the cell wall.

$$\begin{aligned} \delta &= 100 \text{ \AA} & \text{and } \delta_w &= 1.5 \text{ \AA} \\ \delta &\approx 60 \delta_w \end{aligned}$$

$$\text{The ratio } \frac{\delta}{4 \delta_w \left(1 - \frac{\delta_w}{\delta}\right)} = \frac{60 \delta_w}{4 \delta_w \left(1 - \frac{\delta_w}{60 \delta_w}\right)} \approx 15$$

The number of ( $\text{H}^+$ ) ions which could discharge the electrons will

be

$$3.56 \times 10^{14} \times 1/15 = 2.37 \times 10^{13} \text{ (H}^+) \text{ ions/sec}$$

$$\text{The ratio } \frac{\text{(H}^+)}{e} = \frac{2.37 \times 10^{13}}{1.81 \times 10^{12}} \approx 10$$

This large ratio indicates that all the accumulated electrons on cellulose surfaces should be discharged by these (H<sup>+</sup>) ions.

This calculation also indicates that the diameters of flow passages limits the ability of the existing positive ions in any solution to discharge the accumulating electrons.

Similar calculations were done for the (0.005 M) KCl solution. Table A.4 shows that at a flow rate of 0.1175 cm/sec., the voltage was 2.32 millivolts and the current was 1.7 microamperes. The current reading was converted to a number of positive charges, as follows:

$$1.7 \mu\text{A./sec} = 0.6242 \times 10^{13} \times 1.7 = 1.0611 \times 10^{13} e$$

The number of (H<sup>+</sup>) ions and (K<sup>+</sup>) ions which were moving adjacent to the inner wall, were computed as follows:

$$\text{mass flow of water/sec.} = .1175 \times .99737 = .11719 \text{ gm./sec.}$$

$$\text{Number of H}_2\text{O molecules/sec.} = \frac{.11719}{18} \times 6.023 \times 10^{23} = 3.92 \times 10^{21} \text{ molecules/sec.}$$

$$\text{Number of (H}^+) \text{ ions/sec.} = 3.92 \times 10^{21} \times 10^{-7} = 3.92 \times 10^{14} \text{ (H}^+) \text{ ions/sec.}$$

$$\text{Number of KCl molecules/liter} = \frac{1}{200} \times 6.023 \times 10^{23} = 3.0125 \times 10^{21} \text{ molecules/liter}$$

$$\text{Number of KCl molecules/sec.} = 3.0125 \times 10^{21} \times 10^{-3} \times .1175 = 3.54 \times 10^{17} \text{ molecules/sec.}$$

$$\text{Number of } (K^+) \text{ ions/sec.} = 3.54 \times 10^{17} (K^+) \text{ ions/sec.}$$

Since  $(H^+)$  ions are  $\frac{1}{1000}$  of  $(K^+)$  ions, the  $(H^+)$  ions can be neglected.

By considering the inlet diameter  $\delta$  and  $(K^+)$  diameter  $\delta_k$

$$\delta = 0.6 \mu \quad \text{and} \quad \delta_k = 3 \text{ \AA}$$

$$\delta = 2000 \delta_k$$

$$\text{The ratio } \frac{\delta}{4 \delta_k (1 - \frac{\delta_k}{\delta})} = \frac{2000 \delta_k}{4 \delta_k (1 - \frac{\delta_k}{2000 \delta_k})} \approx 500$$

The number of  $(K^+)$  ions which passed adjacent to the walls will be  $= 3.54 \times 10^{17} \times \frac{1}{500} = 7.08 \times 10^{14} (K^+) \text{ ions/sec.}$

$$\text{The ratio } \frac{(K^+)}{e} = \frac{7.08 \times 10^{14}}{1.0611 \times 10^{13}} \approx 60$$

Therefore, the number of  $(K^+)$  ions which had the ability to discharge the accumulated electrons, was 60 times the calculated positive charges which caused the current. However, the voltage remained constant with a reading greater than zero. This means that these  $(K^+)$  cations did not discharge all the accumulated electrons. This indicates also that the number of the expelled electrons was greater than the number of  $(K^+)$  cations which were moving adjacent to the cellulose surfaces.

Each ( $K^+$ ) cation discharged one electron. At the same time there was an ( $Cl^-$ ) anion also moving with the flow, since the diameters of the passages were big enough for ( $Cl^-$ ) anion to pass through. This created a current in the opposite direction. Therefore the real number of the positive charges which were moving per second were greater than the actually measured ones. This real number can be estimated as

$$7.08 \times 10^{14} + .106 \times 10^{14} \approx 7.2 \times 10^{14} e$$

This number means that  $7.2 \times 10^{14}$  positive charges were passing per second with the flow, and the number of electrons expelled per second also was  $7.2 \times 10^{14}$ . This is 300 times greater than that calculated for pure water, which was  $2.17 \times 10^{12}$  electrons/sec.

This comparison shows that when the repulse effect of the accumulated electrons was cancelled by their discharge, the water molecules could expel 300 times as many electrons.

If the flow passage diameters were small enough to prevent ( $Cl^-$ ) anion to pass, the cellulose pad will be charged as follows. The upstream side will be negatively charged with both the accumulated electrons and ( $Cl^-$ ) anions. The downstream side will be positively charged with the water molecules which have lost their electrons.

Other calculations were done for the glass fiber pad. Table A.7 shows that at a flow rate of 0.2356 cm/sec., the voltage was 4200 millivolts, and the current was 6.5 microamperes.

The current reading was converted to a number of positive charges, as follows:

$$6.5 \mu\text{A}/\text{sec} = 0.6242 \times 10^{13} \times 6.5 = 4.0573 \times 10^{13} \text{ e}$$

The number of  $(\text{H}^+)$  ions of water which passed through the pad per second were calculated as follows:

$$\text{mass flow rate}/\text{sec} = 0.2356 \times .99764 = .2350 \text{ gm}/\text{sec}$$

$$\text{Number of H}_2\text{O molecules}/\text{sec} = \frac{.235}{18} (6.023 \times 10^{23})$$

$$= 7.86 \times 10^{21} \text{ molecules}/\text{sec}$$

$$\text{Number of } (\text{H}^+) \text{ ions}/\text{sec.} = 7.86 \times 10^{21} \times 10^{-7} = 7.86 \times 10^{14} \text{ } (\text{H}^+) \text{ ions}/\text{sec.}$$

Considering the inlet diameter of glass fiber pores to be 0.8 micron,

$$\delta \approx 5400 \delta_w$$

$$\text{The ratio } \frac{\delta}{4 \delta_w (1 - \frac{\delta_w}{\delta})} = \frac{5400 \delta_w}{4 \delta_w (1 - \frac{\delta_w}{5400 \delta_w})} \approx 1400$$

The number of  $(\text{H}^+)$  ions which passed adjacent to the inner walls of the pores was computed as:

$$7.86 \times 10^{14} \times \frac{1}{1400} = 5.61 \times 10^{11} \text{ } (\text{H}^+) \text{ ions}/\text{sec}$$

$$\text{The ratio } \frac{(\text{H}^+)}{\text{e}} = \frac{5.61 \times 10^{11}}{4.057 \times 10^{13}} \approx 0.013$$

This ratio means that the  $(\text{H}^+)$  ions, which discharged some electrons from glass fiber surfaces were only about 1 per cent of the positive charges which were moving along with the flow. Both the low rate of electron discharge and the high rate of electron accumulation, resulting from a high rate of energy dissipation, may have caused the high voltage reading of 4.2 volts.

V B-3. The Role of Electric Energy in Plant:

The role of electric energy in plant can be seen if the flow pattern of xylem sap is examined.

To simplify the discussion, it is better to start the study of the flow pattern when water potential in both the xylem and the surrounding tissues is nearly in an equilibrium condition.

Equilibrium conditions do not exist in the living plant. Since the water potential is nearly at equilibrium early in the morning, it is convenient to start the study at that time of the day.

During night, water stresses inside xylem vessels decrease, because transpiration drops to its minimum value. Due to the osmotic pressure of cell sap in the surrounding tissues, and the low water stresses inside the vessels, the diffusion pressure deficit of the surrounding cells will be greater than that of the vessels. Therefore, water flows from the inside of the vessels towards those surrounding cells. As this flow continues during the night, the diffusion pressure deficit of the surrounding cells decreases, till it reaches its minimum value about dawn. Therefore, the rate of sap flow to the surrounding tissue reaches its minimum value or may stop completely at dawn. Figure 36.A expresses this schematically.

With the first light of the morning, photosynthesis and transpiration start once again. The rate of these two processes increases as the day advances. The increase of the rate of transpiration affect the stress condition of water inside

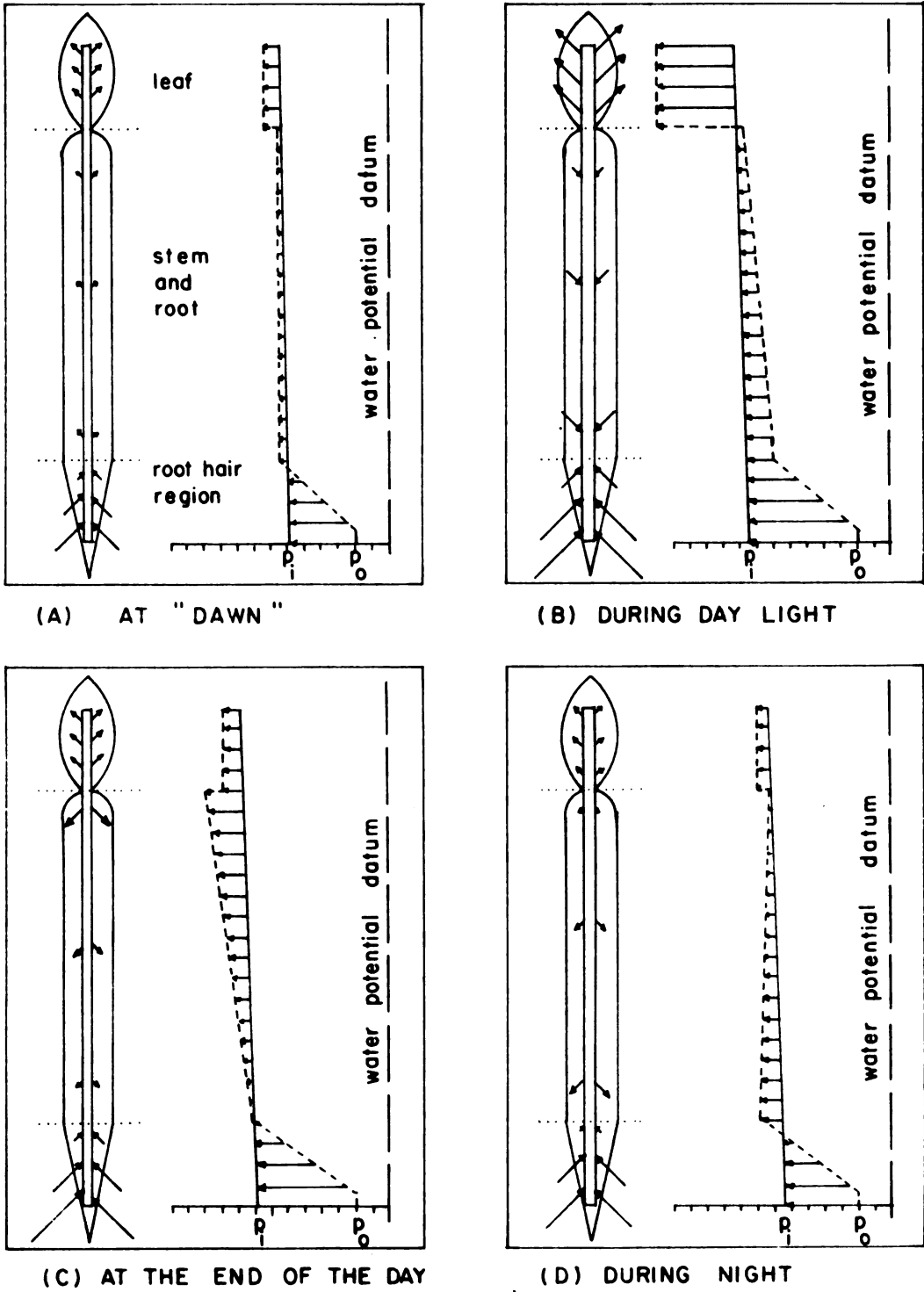


FIG. 36 - FLOW PATTERN DURING THE 24 HOURS OF THE DAY



xylem vessels. When the rate of transpiration becomes greater than the rate of root absorption, the potential of xylem sap drops and its diffusion pressure deficit increases. This disturbs the balance between the potential of xylem sap and that of the surrounding cell sap. The result is the changing of the direction of flow, towards the inside of xylem vessels.

The rate of sap flow in that direction is greater near the lower part of the vessels, because the surrounding tissues of this part are closer to the higher water potential of the root, and further away from the region of higher concentration of sucrose. Figure 36-B shows this flow pattern schematically.

At the end of the day, both photosynthesis and transpiration rates decrease. The sucrose concentration will be greater in the upper part of the stem near the leaf. This keeps water potential of the surrounding tissues of the upper part, at a lower level than that of the tissues near the bottom of the stem. At the same time, the potential of the sap inside xylem vessels increases, due to the continuation of root absorption and the cessation of water losses by transpiration. Therefore, the flow of water reverses once again, from inside the vessels towards the surrounding tissues. The rate of this flow will be higher in the upper part of the stem near the leaf, than in the lower part near the root-hair zone. This difference in the flow rate, may be the cause of the mass flow which occurs in the phloem in the direction of the roots. Figure 36-C shows this schematically.

As the night advances, the flow pattern approaches a condition more close to equilibrium, Figure 36-D.

According to the results of the experiments performed, whenever flow of water occurs through porous media, electric energy is generated. In the case where electrolytes or carbon dioxide are present, which is the case inside the plant, and in the case where water passage are narrow, this electric energy is utilized in moving an extra number of cations with the flow. The cations are first attracted towards the negatively charged inlets, they discharge the electrons, then are dragged off with the flow. The pattern of flow of these cations depends on their concentration, the flow rate, and the diameter of the flow inlets.

The solutes move from the soil to the endodermis, with the absorbed water via the apoplast. Because the passage diameters are big in the apoplast, the cations discharge some of the accumulated electrons, and the greatest portion of the anions move also with the flow. The outer surfaces of root-hairs become negatively charged, which may have a great effect in attracting more cations.

In the endodermis, the narrow gaps of the casparian strip play another role in absorption of ions. A greater number of cations are attracted toward the negatively charged inlets, they discharge the electrons and then pass on with the flow. The anions, cause a negatively charged surge in the central portion

of the passage, due to their attraction toward the positively charged water molecules which have lost their electrons. This may be the reason why solutes sometimes move inside the root with velocity greater than the velocity of water molecules.

There is also a selective absorption of some of the solutes as a result of an active transport by the cytoplasm. This process is considered to be a biological one. Whenever active transport occurs, the role of the electric energy which is generated from the dynamics of the flow, is to help this biological transport, by accumulating the selected cations close to the cytoplasm.

Referring to water flow pattern, Figure 36, water potential was considered nearly at an equilibrium condition, early in the morning. At that time, the cations which have entered the xylem vessels, are transported next toward the surrounding tissues following the flow pattern of water, Figure 36-A. The transportation of the existing anions outwards depends on the flow passage diameters, and the magnitude of the negative charge inside the cells of the surrounding tissues.

During the high rate of transpiration and photosynthesis, some cations are forced to move with water flow, from the surrounding tissues towards the inside xylem vessels. Since the rate of respiration is high in some of the surrounding tissues, especially cambium cells and the companion cells of phloem tissue, the

1

hydronium ions ( $\text{H}_3\text{O}^+$ ) move toward xylem vessels, leaving ( $\text{HCO}_3^-$ ) ions inside these cells, which increase the negativity of these cells. Referring to Figure 36-B, water flow from the surrounding tissues at the lower part of vessels is greater than the flow from the surrounding tissues at the upper part of the vessels. Therefore, the surrounding tissues of the lower part of vessels will be more negatively charged than those of the upper part.

When xylem sap, with the cations in it, reaches the leaf, the generated electric energy helps, once again, in the active transport of these cations by the cytoplasm. Once these cations enter the cytoplasm, they can move via the symplast. Because of their positive charges, they are attracted towards the negatively charged cytoplasm of the companion cells. This helps in moving sugars and assimilates towards the sieve tubes. This movement of sugars and assimilates continues downwards, due to the more negativity of the cytoplasm of the sieve tubes at the lower part of the stem and the root.

Referring to Figure 36-C, the high flow rate of both water and cations in the direction of the surrounding tissue in the upper part of the stem, causes the high rate of downward flow in phloem. It also causes the distribution of sugar and assimilates to regions of their consumption, since these regions are known to be more negatively charged because of their high rate of respiration.

From the previous discussion, it can be concluded that the existence of the electric energy is a product of the flow process. This means that "Electro-osmosis", according to its definition, does not play a role in the flow process in xylem tissue.

It can also be concluded that "Electro-osmosis" does not affect fluid flow in phloem sieve tubes, since the downward surge of cations, which are accompanied by the sugars and assimilates, is due to a process similar to the "Donnan equilibrium" rather than "Electro-osmosis".

#### V C. The Role of Xylem Vessel Wall Structure in Plant:

The structure of the walls of xylem vessels plays three important functions in plants. These functions are:

##### V C-1. The Generation of Electric Energy:

As discussed in sections V.A. and V.B., the porosity of the structure of wall material, provides the means for generating the electric energy. The magnitude of this electric energy depends on the rate of water flow.

This electric energy helps in moving extra cations in the direction of flow. Sometimes, it causes a surge of anions, whose velocity may be faster than that of the water molecules.

In the active transport of ions, the electric energy helps the cytoplasm by accumulating these ions close to the action of this biological process.

V C-2. The Existence of High Tensile Stresses in Xylem Sap:

The second function, is that this structure, which consists of layers of cellulose microfibrils and macrofibrils, is the only guarantee for the existence of high tensile stresses in xylem sap, without permitting evaporation to occur.

When water pressure decreases until it reaches a value equal or less than the vapor pressure at the existence temperature, evaporation occurs.

At 70°F., vapor pressure of water is 0.3631 psi

$$0.3631 \text{ psi} = 2.503 \times 10^4 \text{ dyne/cm}^2$$

At this temperature, negative pressure exists in the xylem tissue of, not only tall trees, but also many of the annual plants like corn. A negative pressure of 10 atm. in xylem sap was estimated in corn plant.

$$1 \text{ atm.} = 1.013 \times 10^6 \text{ dyne/cm}^2$$

Evaporation cannot occur at any point located inside a liquid. In the absence of any gas bubble, vapor bubbles are unstable and collapse.

There are two forces acting on these vapor bubbles:

1) The surface tension force =  $2\pi r\sigma$

where  $r$  = bubble radius

$\sigma$  = surface tension of the liquid

This surface tension acts to collapse the bubble,

Figure 37-A.

2) The force of vapor pressure =  $\pi r^2 (p_v - p_w)$

where  $(p_v - p_w)$  = the difference between water pressure  
and vapor pressure at the existing  
temperature.

This force acts in the direction of increasing the  
size of the bubble, if  $(p_v - p_w)$  is a positive quantity.

At equilibrium

$$(p_v - p_w) = \Delta p = \frac{2\pi r \sigma}{\pi r^2} = \frac{2\sigma}{r}$$

This means that in the absence of other gas bubbles,  $\Delta p$  must  
be greater than  $\frac{2\sigma}{r}$  for any vapor bubble to form and grow.

For water

$$\sigma = .005 \text{ lb}_f/\text{ft} = 72.9695 \text{ dyne/cm} \approx 73 \text{ dyne/cm}$$

The maximum distance between water molecules is  $5 \text{ \AA}$ . By  
assuming that one molecule is evaporated, the radius of the  
starting bubble will be  $5 \text{ \AA} = 5 \times 10^{-8} \text{ cm}$ .

At equilibrium:

$$\begin{aligned} \Delta p &= \frac{2\sigma}{r} = \frac{2 \times 73}{5 \times 10^{-8}} = 2.92 \times 10^9 \text{ dyne/cm}^2 \\ &= \frac{2.92 \times 10^9}{1.013 \times 10^6} \approx 2000 \text{ atm.} \end{aligned}$$

This figure means that  $\Delta p$  must be greater than 2000 atm. for  
evaporation to occur inside water. That is the reason that  
evaporation always starts at the interface between the water  
and the container. The reasons for that are:



1. The roughness of the container wall traps gas. This gas becomes under high pressure because of the adherent force between water and the material of the container walls, Figure 37-B.
2. The surface of container wall is sometimes contaminated with some material having little or no adherence to water, Figure 37-C.

Both cases, allow the radius of the first bubble of vapor to be big enough for its growth.

Applying these principals to xylem vessels, explains the ability of vessel structure of maintaining the high tensile stresses which occur in xylem sap. The cellulose has great affinity for water, and water adheres to it very strongly. Cellulose in cell walls and xylem vessel walls, does not have any contaminates to let water separate from the cellulose macrofibrils.

The distance between cellulose macrofibrils is of the order of 100 Å. For any gas or water vapor bubble to pass through this wall structure,  $\Delta p$  must be greater than:

$$\begin{aligned} \Delta p > \frac{2\sigma}{r} &= \frac{2 \times 73}{50 \times 10^{-8}} = 2.92 \times 10^8 \text{ dyne/cm}^2 \\ &= \frac{2.92 \times 10^8}{1.013 \times 10^6} \approx 200 \text{ atm.} \end{aligned}$$

Xylem vessels have pits in their walls. Gas and water vapor bubbles may pass through these pits. The pit diameters are

of higher order than the distance between cellulose microfibrils. If the diameters of the pits were about 0.2 micron, the difference in pressure ( $p_v - p_w$ ) which is needed for vapor bubbles to pass through it, must be greater than

$$\begin{aligned} \Delta p &= (p_v - p_w) > \frac{2\sigma}{r} = \frac{2 \times 73}{0.1 \times 10^{-4}} + 1.43 \times 10^7 \text{ dyne/cm}^2 \\ &= \frac{1.43 \times 10^7}{1.013 \times 10^6} \approx 10 \text{ atm.} \end{aligned}$$

This order of magnitude of  $\Delta p$  can be found inside xylem vessels. This means that gas and vapor bubbles can move from the intercellular spaces, in which air and gases are found, towards the inside of the vessels through these pits. However, this does not happen. The reasons of that is that xylem vessels are surrounded with living cells, which have no intercellular spaces between them and these vessels. For any gas or vapor bubble to enter any vessel, it must pass through the gaps between cellulose microfibrils of the walls of these cells.

To investigate this role of the cellulose wall structure, an experiment was carried on, to examine the possibility of the existence of tensile stresses in water, without evaporation or separation in water column.

A steel cylinder, 0.635 cm inside diameter, "Diesel fuel pump cylinder", with two lapped pistons, were used in this experiment. The parts were cleaned and dried. In order to get

rid of gas molecules which were adhered to metal surface, these parts were heated to about 200<sup>o</sup>c under vacuum. The heating was done to increase the kinetic energy of the adhered gases, to enable the vacuum to remove nearly all these gas molecules. After heating for 15 minutes, the parts were cooled under vacuum to room temperature.

Distilled water was boiled and cooled under vacuum. This cold water was introduced to the steel part until the water covered them completely. The vacuum then was released.

The two pistons were inserted in the cylinder, one in each end, while all parts were under water.

A tensile test was carried on the assembly, by applying a tensile force on the two piston while the assembly was under water, Figure 38. The maximum tensile stress which was reached before a separation in the water column occurred, was 2.5 atm.

This experiment was performed to examine the possibility of the existence of tensile stresses in water column. However, this experiment must be performed with more sensitive measuring instrumentation, in order to measure the maximum tensile stress of water, which can be reached in cell wall structure.

#### V C-3. The Existence of a Communication System in Plants:

The third function of the structure of xylem vessel walls, is to provide the plant with a communication system. In this system, the sap inside the vessels acts as a communicating cord

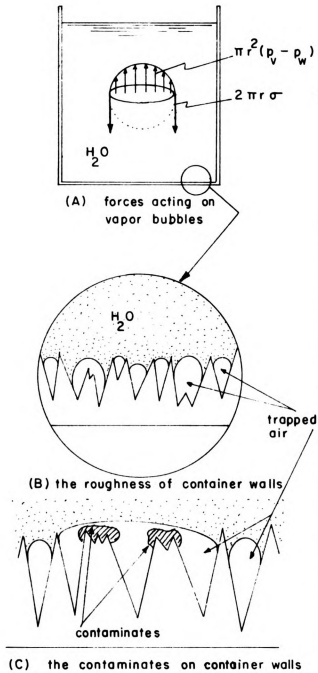
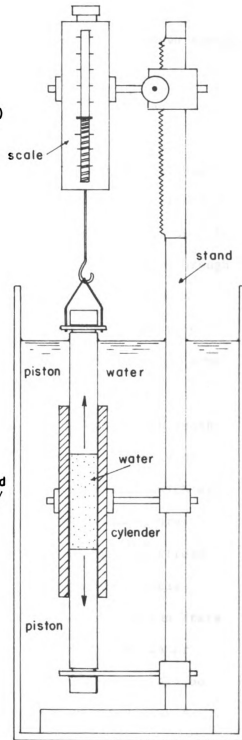


FIG. 37 - VAPOR BUBBLE FORMATION

FIG. 38 - THE APPARATUS  
USED IN TESTING THE EXISTENCE  
OF TENSILE STRESS IN WATER

1

along the whole height of the plant, analogous to the nerve system in the higher classes of animals.

This function, in fact, is a result of the first two functions of vessel wall structure.

The structure of vessel wall permits the existence of high tensile stresses in xylem sap. The state of stress in xylem sap affect the surrounding tissues, as was mentioned in sections V.B. According to the state of stress in xylem sap, water flow through vessel walls and the surrounding tissues in one direction or another, Figure 36. The result is the generation of electric energy which in turn affect ion movements, and subsequently, some of the biological activities of the surrounding tissues.

The tensile stress which occurs in the xylem sap can reach very high values, not only in high trees, but also in many of the annual plants. The differences in water pressure, which are due to the elevation along the height of xylem vessels, are considered negligible when compared to the high tensile stress in xylem sap. Therefore, water column inside xylem vessels, act as a metal cord subjected to a tensile stress. If the state of stress is forced to change at a location  $= Z$  along water column, at time  $= t$ , the change in the state of stress will be transmitted immediately to all locations  $= Z \pm \Delta Z$ , at time  $= t + \Delta t$ , where  $\Delta t$  is the very short time-interval which is needed to transmit stresses along any elastic cord. As a result, all

the surrounding tissue at all locations along the height of the plant, will find a new state of stress, and will react according to it. This reaction will be, not only hydraulic, but also electric. The magnitude of the electrical reaction will depend on the magnitude of water potential change, the change in flow pattern, and the size of pores in the vessels and cell walls.

## VI SUMMARY AND CONCLUSIONS

VI A. Summary

The concept of electro-osmotic flow in plants has been the interest of many scientists. Some investigators related the natural electric potential in plants to the translocation of sap and assimilates. Others considered the translocation of fluid a result of electro-osmosis. Therefore, this study was intended to investigate the engineering bases of fluid flow inside xylem vessels and the nature and role of the electric phenomenon in plants.

A review of the fundamental bases of plant anatomy and physiology was done to examine the limits imposed by them on the vascular tissues and the whole intact plant. The limits imposed by the physical laws were also considered.

The finding of many of the earlier and latest experiments in the area of electro-osmosis were examined, some of these findings disagree with some others. However, the explanation of the results of many experiments were based on the zeta potential concept. This concept assumes that the surfaces of any wetted porous material acquire two layers of opposite electrical charges at the solid-liquid interface. The potential difference between these two layers is called the zeta potential.

To study the engineering bases of fluid flow process inside xylem tissue, a model represents xylem vessels was developed.



The flow of energy through this model was examined and analyzed mathematically. The energy balance equation for this model was solved for the dissipated energy, which was considered the only possible source for the generated electric energy.

To investigate the relationship between the dissipated energy and the electric energy, experiments were performed on a model represents the material of vessel walls. This model consisted of .9 cm cellulose pad constructed of 50 sheets of filter paper "Whatman No: 1". Water was forced to pass through the cellulose pad by applying an external pressure. Voltage and current across the pad, was measured by means of two silver-silver chloride electrodes. Different water heads were applied, and voltage, current, flow rate were measured and recorded. Five fluids were used. They were: distilled deionized water at 23.8<sup>o</sup>c, water at 30.0<sup>o</sup>c, CO<sub>2</sub>-saturated water, (0.005M), KCl solution, and (0.01M) KCl solution. Another matrix was tested also. This matrix was constructed of 20 sheets of glass fiber filter papers.

The data were analyzed and the nature and the role of the electric energy in plants were discussed. The role of the anatomy of vessel walls to plants was also discussed.

#### VI B. Conclusion:

1. Electro-osmosis, according to its definition, does not play a role in sap movement in xylem vessels.



2. The dissipated flow energy and the generated electric energy during water movement through a porous pad are related. Both are parabolic functions of  $\Delta p$ .
3. The source of the electric energy in a system of cellulose and water, may not be an "intrinsic constant quantity" of the solid material and the liquid, such as the zeta potential. The electric energy may result from energy dissipation during the flow process itself due to the sliding of water layers over each other, causing water to expel electrons to the cellulose surfaces. A greater accumulation of expelled electrons on the upstream side, creates an electric potential difference across the pad.
4. Based on the observations of the reduction in the electrical potential and the increase in current when an electrolyte was added to water, it is concluded that the generated electric energy is utilized in moving an additional number of cations more than that which would normally be carried with the flow.
5. An extrapolation of the previous conclusions to water flow in plant is that the flow of water from the soil to the cortex in the root, may cause the outer surfaces of the root hairs to be negatively charged.
6. The final equations (equations 24 and 25) of the mathematical analysis can be solved for the pattern of ion movement in plant, by using numerical techniques.



## RECOMMENDATIONS FOR FURTHER STUDY

1. The relationship between the dissipated energy and the generated energy which are resulted from flow of water through porous material, can be studied further, by using improved equipment and techniques. Such improvements are:
  - a. Performing the experiments under adiabatic conditions to relate the exact magnitude of heat energy to the generated electric energy.
  - b. Performing the experiments on other fluids having different Dielectric constants, and on different porous materials to examine the effects of the electric conductivity of the fluid used, and the effects of the diameters of the pores on the movement of the cations and anions.
  - c. Provide means to measure voltage, current, conductivity, and pH at different locations inside the porous material pad and in the upstream and downstream sides.
2. After part one, above, is studied, experiments can be performed on plant. Such experiments are:
  - a. Using microtechniques to measure the electric potential difference across one of xylem vessel walls.
  - b. Study the response of xylem sap to the applied external electric effects.
  - c. Study the relationship between both transpiration and photosynthesis rates and the electric potential and current

generated in xylem vessels.

- d. Study the relationship between transpiration and photosynthesis rates and the movement of assimilates and sugar in phloem tissues, in order to relate this movement to the generated electric energy.
3. After the studies of parts one and two are done, the effects of the application of external electric voltage and current can be determined experimentally for the whole plant.

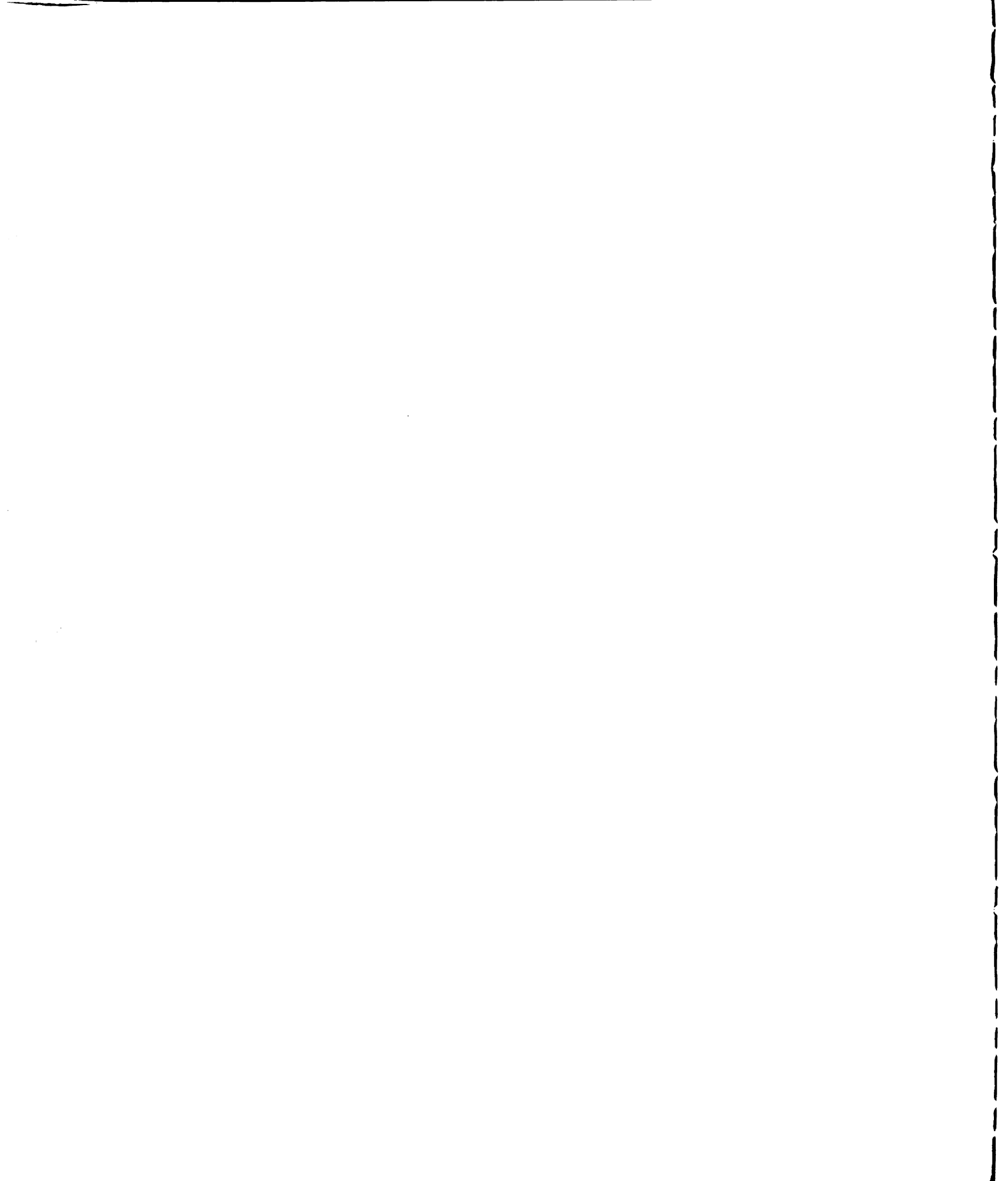
11

Selected References

- Berry, L. J. and Hoyt, R. C. (1943), Simulation of the onion root by alternating current, Plant Physiol., 18 (570-587).
- Blackman, V. H. (1924), Field experiments in electro-culture, Journal of Agricultural Science, 14 (240-267).
- Blackman, V. H. and Legg, A. T. (1924b), Pot-culture experiments with an electric discharge, Journal of Agricultural Science, 14 (268-286).
- Breazeale, E. L., McGeorge, W. T. and Breazeale, J. F. (1951), Nutrition of plants considered as an electrical phenomenon - A new approach, Soil Science, 71 (371-375).
- Breazeale, E. L. and McGeorge, W. T. (1953), Cation uptake by plants as affected by the applied potential, Soil Science, 75 (443-448).
- Burr, H. S. (1942), Electrical correlates of growth in corn roots, Yale Journal of Biology and Medicine, 14 (581-588).
- Burr, H. S. and Sinnott, E. W. (1944), Electrical correlates of form in cucurbit fruit, Am. Journal of Botany, 31, 5, (249-253).
- Burr, H. S. (1945), Diurnal potentials in the Maple tree, Yale Journal of Biology and Medicine, 17 (727-734).
- Burr, H. S. (1947), Tree potentials, Yale Journal of Biology and Medicine, 19 (311-318).
- Clark, W. G. (1938), Electric polarity and auxin transport, Plant Physiol., 13 (529-552).
- Collins, G. M., Flint, L. H. and McLane, J. W. (1929), Electric stimulation of plant growth, Journal of Agric. Res., 38 (585-600).
- Collins, R. E. (1961), Flow of Fluid Through Porous Materials, Reinhold Publishing Corporation, New York, (56-58).
- Crafts, A. S. (1961), Movement of water, salts and assimilates, Translocation In Plants, Holt, Rinehart, and Winston, Inc., New York.
- Dainty, J., Croghan, P. C. and Fensom, D. S. (1963), Electro-osmosis, with some applications to plant physiology, Can. J. Bot., 41(953-966).

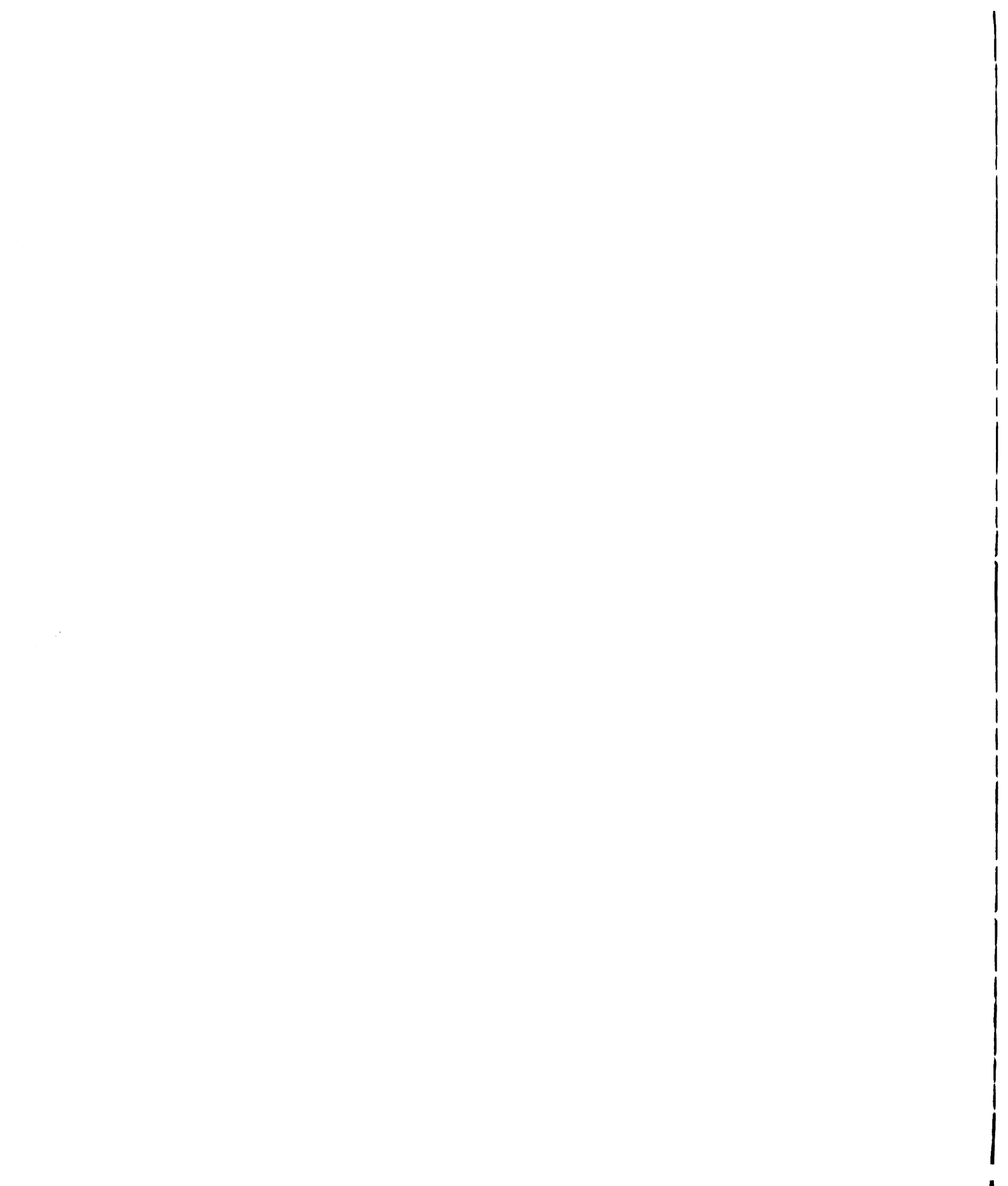


- Esau, K. (1965), Plant Anatomy, John Wiley and Sons, Inc., New York.
- Fensom, D. S. (1957), The bio-electric potentials of plants and their functional significance, I: An electrokinetic theory of transport, Can. J. Botany, 35 (573-582).
- Fensom, D. S. (1958), The bioelectric potentials of plants and their functional significance, II: The patterns of bio-electric potentials and exudation rate in excised sunflower roots and stems, Can. J. Bot., 36 (367-383).
- Fensom, D. S. (1959), The bio-electric potentials of plants and their functional significance, III: The production of continuous potentials across membranes in plant tissue by the circulation of the hydrogen ion, Can. J. Bot., 37 (1003-1026).
- Fensom, D. S. (1962), The bio-electric potentials of plants and their functional significance, IV: Changes in the rate of water absorption in excised stem of *Acer Saccharum* induced by applied electro-motive forces: The flushing effect, Can. J. Bot., 40 (405-413).
- Fensom, D. S. (1963), The bio-electric potentials of plants and their functional significance, V: Some daily and seasonal changes in the electrical potential and resistance of the living trees, Can. J. Bot., 41 (831-851).
- Fisher, J. C. (1949), Fracture of liquids, Sci. Mo., 68, 6, (415-419).
- Fuller, H. J. and Carothers, Z. B. (1963), The Plant World, Holt, Rinehart, and Winston, Inc., New York.
- Gauch, H. G., and Dugger, W. M., Jr. (1953), The role of boron in the translocation of sucrose, Plant Physiol, 28 (457-466).
- Gibbs, R. D. (1935), Studies of wood III: On the physiology of the tree with special reference to the ascent of sap and the movement of water before and after death, Can. J. Res., 12 (761-787).
- Greenidge, K. N. H. (1955), Studies in the physiology of forest trees, III: The effect of drastic interruption of conducting tissue on moisture movement, Am. J. Bot., 42 (582-587).
- Haines, F. M. (1935), Observations on occurrence of air in conducting tracts, Ann. Bot., 49, (367-379).
- Hipton, C. E. L., Preston, R. D. and Repley, G. W. (1955), Electron microscopic observations on the structure of sieve plates in cucurbita, Nature, 176 (868-870).

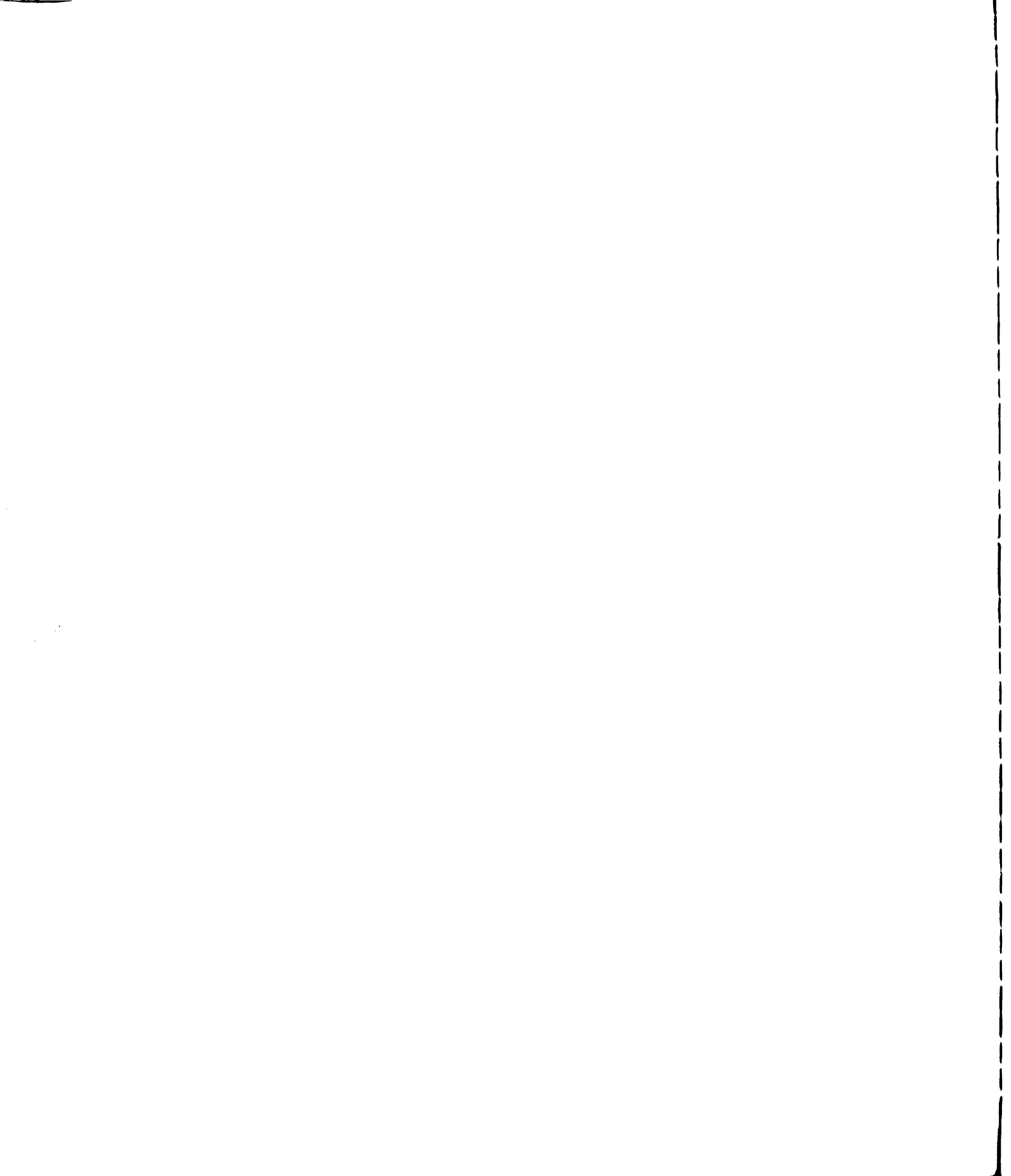


- Knight, R. C. and Priestly, J. H. (1914), The respiration of plants under various electrical conditions, Ann. Bot. Lond., 28 (135-161).
- Kozlowski, T. T. and Winget, C. H. (1963), Pattern of water movement in forest trees, Bot. Gaz., 124 (301-311).
- Kozlowski, T. T. (1964), Water Metabolism in Plants, Harper and Pow Publishers, New York.
- Loomis, W. E. (1945), Translocation of carbohydrates in Maize, Science, 101 (398-400).
- Lund, E. J. and Kenyon, W. A. (1927), Relation between continuous bio-electric currents and cell respiration, I: Electric correlation potentials in growing root tips, Journal Exp. Zool., 48, (333-357).
- Lund, E. J. (1928), Relation between continuous bio-electric current and cell respiration, II, J. Exp. Zool., 51 (265-290).
- Lund, E. J. and Bush, M. (1930), Electric correlation potential in the leaf of Bryophyllum, Plant Physiol., 5 (491-508).
- Lund, E. J. (1931), External polarity potentials in the apex of the Douglas fir before and after mechanical stimulation, Plant Physiol., 6, (507-517).
- Lund, E. J. (1931b), Electric correlation between living cells in cortex and wood in the Douglas fir, Plant Physiol., 6, (631-652).
- Lund, E. J. (1932), Control of the flux equilibrium of electro-chemical processes and electric polarity in Douglas fir by temperature, Plant Physiol., 7, (297-307).
- Lundegardh, H. (1951), Leaf Analysis (Translated by Mitchell, R. L.), Hilger and Watts Ltd., London.
- Manson, T. G. and Maskell, E. J. (1928), Studies on the transport of carbohydrates in the cotton plant, Ann. Bot., 42, (1-65 and 571-636).
- Mason, S. G. (1950), The electrokinetic properties of cellulose fibers, TAPPI, 30, (413-417).
- March, G. (1928), Relation between continuous bio-electric currents and cell respiration, IV: The origin of electric polarity in the root, Jour. Expt. Zool., 51, (309-325).

- Murr, L. E. (1963), Plant growth response in a simulated electric field environment, Nature, 200(490-491).
- Murr, L. E. (1965), Biophysics of plant growth in an electrostatic field, Nature, 206, (467-470).
- Neale, S. M. and Peters, R. H. (1946), Electrokinetic Measurements with Textile Fibers and Aqueous Solution, Trans. Faraday Soc. 42 (478-486).
- Osterle, J. F. (1964), Electrokinetic energy conversion, J. Appl. Mech., 31E, 2 (161-164).
- Part, H. (1948), Histo-physiological gradients and plant organogenesis, Bot. Rev., 14, (603-643).
- Plowman, A. B. (1909), Electrical stimulation of plant growth, Science, 29 (470-471).
- Preston, R. D. (1938), The contents of the vessels of *Fraxinus Americana* L., with respect to the ascent of sap, Ann Bot., N. S. 2 (1-21).
- Preston, R. D. (1965), Biosynthetic Pathway in Higher Plants, Academic Press, New York.
- Rosene, H. F. (1937), Effect of an applied electric current on the external longitudinal polarity potentials of Douglas fir, Amer. Jour. Bot., 24, (390-399).
- Rundinsky, J. A. and Vite' J. P. (1959), Certain ecological and phylogentic aspects of the pattern of water conduction in conifers, Forest Soc., 5, (259-266).
- Salisbury, F. B. (1966), Translocation: The movement of dissolved substances in plant, Plant Biology Today, Wadsworth Publishing Company, Inc., Belmont, California.
- Scholander, P. F., Love, W. E., and Kanwisher, J. W. (1955), The rise of sap in tall grapevines, Plant Physiol., 30 (93-104).
- Scott, B. I. H. (1967), Electric fields in plants, Annual Review of Plant Physiol., 18, (409-418).
- Spanner, D. C. (1958), The translocation of sugar in sieve tubes, Jour. Expt. Bot., 9, (332-342).
- Tammes, P. M. L. (1957), Sieve tube sap, Insect and Plant Food Symposium, Wageningen, Holland.
- Tyree, M. T. and Fensom, D. S. (1968), Methods of measuring hydrokinetic pressure gradients in the xylem of plants in situ, Can. J. Bot., 46, (310-314).



Waller, J. C. (1925), Plant electricity, Annals of Botany, 39,  
(516-538).



## APPENDICES



TABLE A 1

The Effect of Flow of Deionized Distilled Water  
Through Cellulose Pad (23.8°C)

$\Delta p$		Flow Rate		Potential	Volt-	Cur-	Electric
in Hg	$10^3$ dyne/cm <sup>2</sup>	ml/min	$10^{-3}$ cm/sec	Energy $10^5$ erg	+m.V.	+ $\mu$ A.	Energy $10^{-2}$ erg
0.2	6.7	0.22	0.6	0.004	25	.078	1.95
0.5	16.8	1.00	2.6	0.04	35	.089	3.12
1.0	33.6	2.00	5.2	0.17	46	.090	4.14
2.0	67.3	4.00	10.3	0.69	61	.099	6.04
3.0	100.9	6.10	15.8	1.59	75	.116	8.70
4.0	134.5	8.25	21.3	2.87	88	.129	11.35
5.0	168.2	10.25	26.5	4.45	100	.124	14.20
6.0	201.8	12.25	31.7	6.39	103	.155	15.97
7.0	235.4	14.27	36.8	8.67	115	.165	18.98
8.0	269.0	17.00	43.9	11.82	124	.178	22.07
9.0	302.7	18.25	47.2	14.27	135	.189	25.52
10.0	336.3	20.25	52.4	17.59	145	.198	28.71
11.0	369.9	22.00	56.9	21.02	153	.207	31.67
12.0	403.6	24.50	63.4	25.54	164	.216	35.42
14.0	470.8	28.00	72.4	34.06	180	.235	42.30
16.0	538.1	32.50	84.0	45.18	198	.250	49.50
18.0	605.4	37.00	95.7	57.86	216	.272	58.75
20.0	672.6	41.25	106.7	71.66	235	.290	68.15

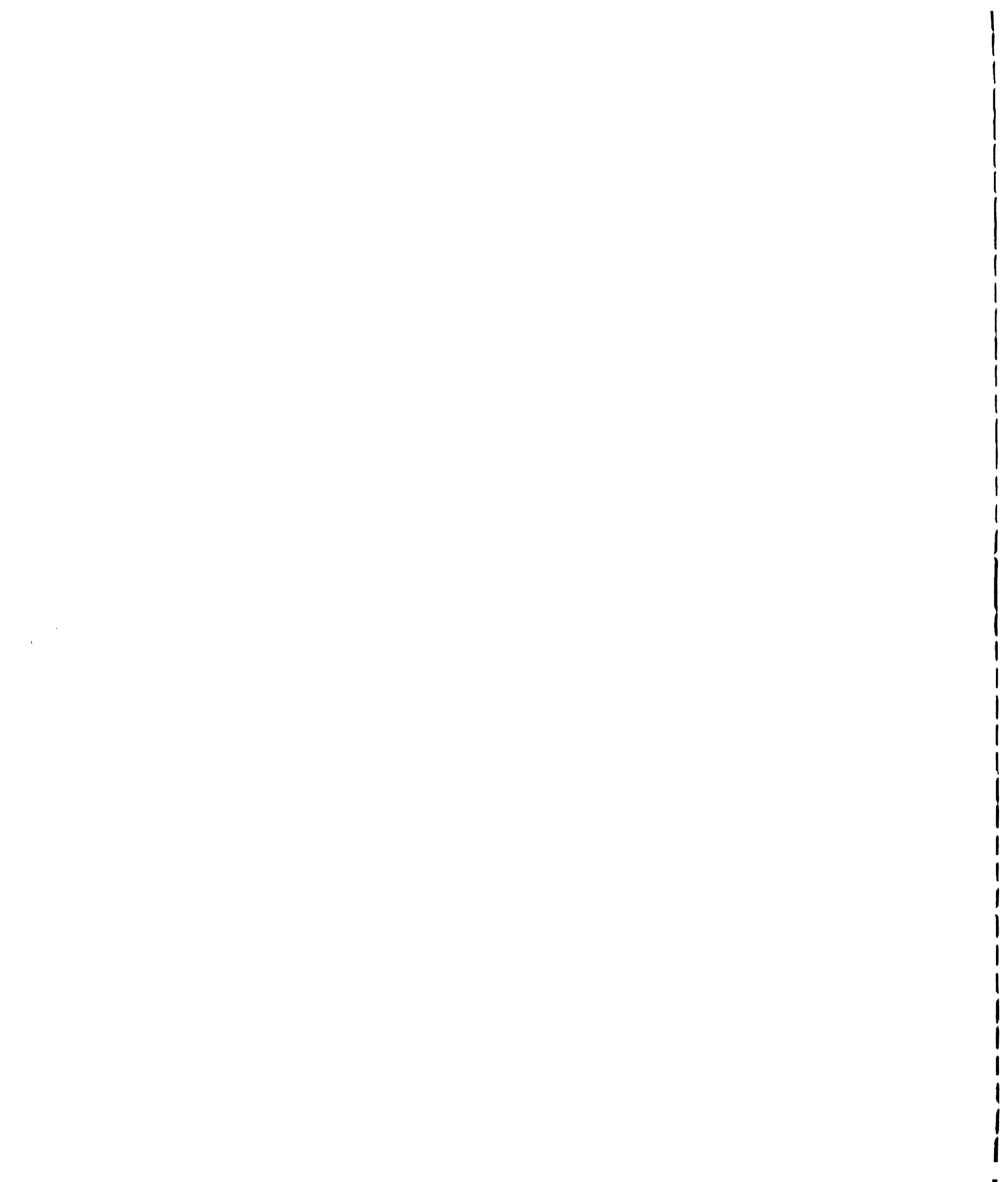


TABLE A 2

The Effect of Flow of Warm Deionized Distilled  
Water Through Cellulose Pad (30.0°C)

	$\Delta p$	Flow Rate		Potential Energy	Volt- age	Cur- rent	Electric Energy
in Hg	$10^3$ dyne/cm <sup>2</sup>	ml/min	$10^{-3}$ cm/sec	$10^3$ erg	m.V.	$\mu$ A.	$10^{-2}$ erg
0.5	16.8	1.10	2.8	0.05	31	.086	2.67
1.0	33.6	2.25	5.8	0.20	40	.105	4.20
2.0	67.2	4.50	11.6	0.78	55	.126	6.93
3.0	100.8	6.75	17.5	1.76	71	.145	10.30
4.0	134.4	9.25	23.9	3.21	86	.165	14.19
5.0	168.0	11.50	29.7	4.99	98	.184	18.03
6.0	201.5	14.25	36.8	7.42	110	.202	22.22
7.0	235.2	16.50	42.7	10.02	122	.220	26.84
8.0	268.8	19.50	50.4	13.53	133	.243	32.32
9.0	302.4	22.00	56.9	17.17	143	.258	36.89
10.0	336.0	24.75	64.0	21.47	154	.280	43.12
11.0	370.0	27.00	69.8	25.76	162	.295	47.79
12.0	403.2	30.00	77.6	31.22	172	.315	54.18
14.0	470.4	35.00	90.5	42.50	182	.330	60.06
16.0	537.6	40.25	104.0	55.85	208	.345	71.76
18.0	604.8	45.00	116.5	70.25	228	.360	82.08
20.0	672.0	51.25	132.5	88.90	246	.375	92.25

TABLE A 3

The Effect of Flow of CO<sub>2</sub> Saturated Water  
 Through Cellulose Pad (23.4<sup>o</sup>c)

	$\Delta p$	Flow Rate		Potential	Volt-	Cur-	Electric
				Energy	age	rent	Energy
in Hg	$10^3$ dyne/cm <sup>2</sup>	ml/min	$10^{-3}$ cm/sec	$10^3$ erg	+m.V.	+ $\mu$ A.	$10^{-2}$ erg
1.0	33.6	2.00	5.2	0.17	2.60	0.15	0.390
2.0	67.3	4.00	10.3	0.70	2.80	0.17	0.406
3.0	100.9	6.40	16.5	1.67	2.80	0.16	0.448
4.0	134.5	9.20	23.8	3.20	3.10	0.19	0.589
5.0	168.2	11.75	30.4	5.10	3.80	0.23	0.874
6.0	201.8	14.75	38.1	7.69	4.40	0.27	1.188
7.0	235.4	17.50	45.3	10.64	5.05	0.32	1.616
8.0	269.0	20.50	53.0	14.25	5.55	0.35	1.943
9.0	302.7	24.50	63.3	19.16	6.10	0.40	2.440
10.0	336.3	27.00	69.8	23.46	6.45	0.43	2.774
12.0	403.6	33.00	85.4	34.41	7.45	0.52	3.874
14.0	470.8	39.00	100.9	47.44	8.50	0.60	5.100
16.05	539.8	45.5	117.5	63.45	9.50	0.69	6.555
18.0	605.4	51.0	131.8	79.76	11.00	0.77	8.470
20.0	672.6	57.0	147.4	99.05	11.80	0.85	10.030

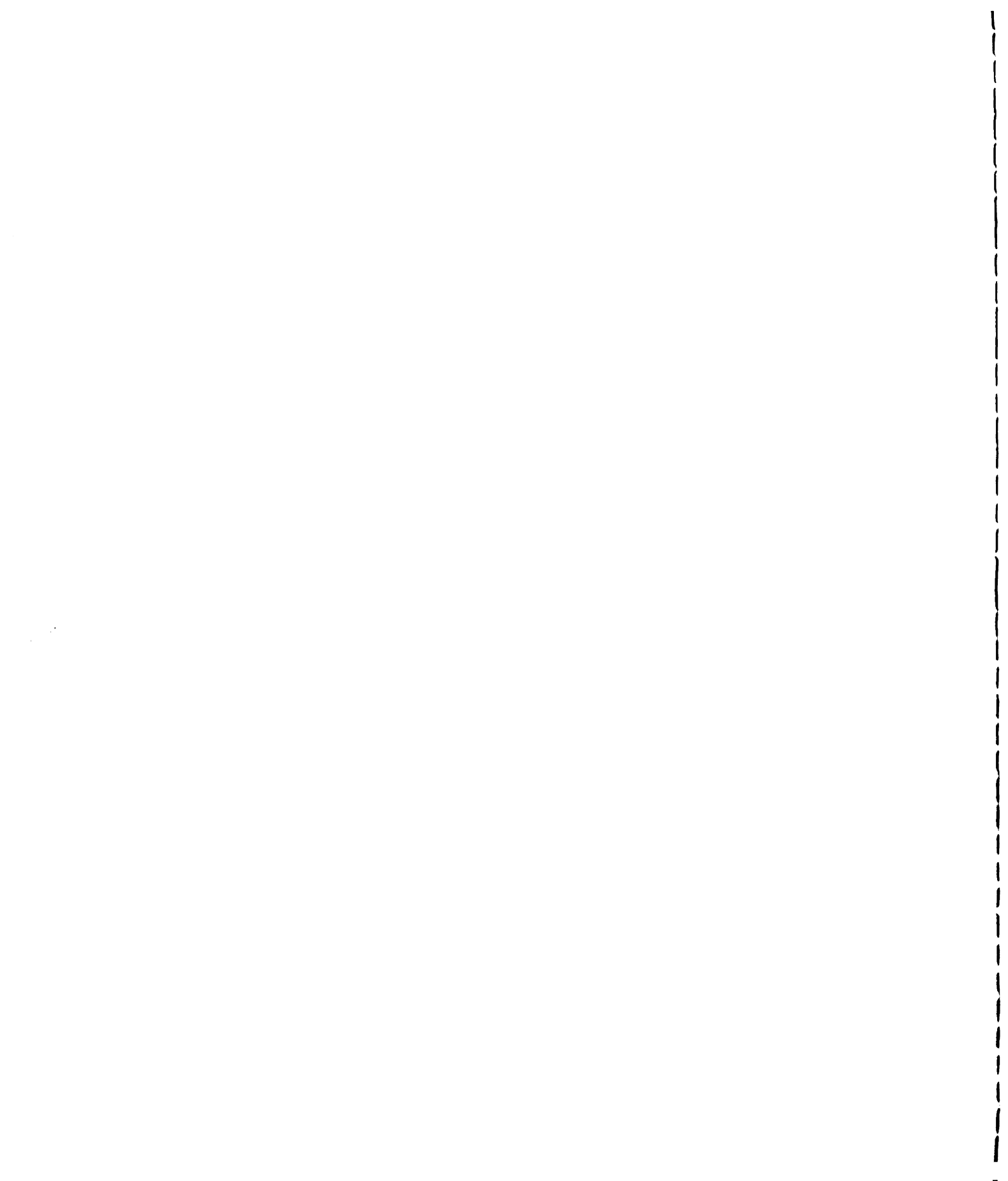


TABLE A 4

The Effect of Flow of (.005M ) KCl Solution  
Through Cellulose Pad (23.8°C)

	$\Delta p$	Flow Rate		Potential Energy	Volt- age	Cur- rent	Electric Energy
in Hg	$10^3$ dyne/cm <sup>2</sup>	ml/min	$10^{-3}$ cm/sec	$10^3$ erg	±m.V.	± $\mu$ A.	$10^{-2}$ erg
0.5	16.8	1.30	3.4	0.06	0.60	0.21	0.126
1.0	33.6	2.25	5.8	0.20	0.44	0.22	0.097
2.0	67.3	4.75	12.3	0.83	0.52	0.26	0.135
3.0	100.9	7.00	18.1	1.82	0.61	0.31	0.189
4.0	134.5	9.25	23.9	3.21	0.70	0.35	0.245
5.0	168.2	11.50	29.5	5.00	0.79	0.40	0.316
6.0	201.8	13.75	35.5	7.17	0.88	0.44	0.387
7.0	235.4	16.00	41.4	9.73	0.98	0.49	0.480
8.0	269.0	18.25	47.2	12.68	1.10	0.51	0.561
9.0	302.7	20.50	53.0	16.03	1.20	0.56	0.672
10.0	336.3	22.75	58.8	19.77	1.28	0.60	0.768
11.0	369.9	25.00	64.7	23.89	1.40	0.67	0.938
12.0	403.6	27.00	69.8	28.15	1.50	0.71	1.065
14.0	470.8	32.00	82.7	38.92	1.70	0.81	1.377
16.0	538.1	35.50	91.8	49.35	1.90	0.94	1.786
18.0	605.4	40.00	103.3	62.55	2.10	1.50	3.150
20.0	672.6	45.50	117.5	79.06	2.32	1.70	3.944



TABLE A 5

The Effect of Flow of (.01 M) KCl Solution  
Through Cellulose Pad (23.8°c)

in Hg	$\Delta p$	Flow Rate		Potential	Volt-	Cur-	Electric
	$10^3$ dyne/cm <sup>2</sup>	ml/min	$10^{-3}$ cm/sec	Energy $10^3$ erg	age +m.V.	rent + $\mu$ A.	Energy $10^{-2}$ erg
0.25	8.4	0.20	0.5	0.004	0.16	0.10	0.016
0.50	16.8	1.25	3.2	0.05	0.17	0.11	0.018
1.05	35.3	2.50	6.5	0.23	0.19	0.12	0.023
2.10	70.6	4.75	12.3	0.87	0.21	0.15	0.032
3.00	100.9	7.00	18.1	1.82	0.32	0.20	0.064
4.00	134.5	9.00	23.3	3.13	0.39	0.25	0.098
5.05	169.8	11.50	29.5	5.05	0.47	0.29	0.136
6.00	201.8	13.75	35.6	7.17	0.52	0.32	0.166
7.05	237.1	16.00	41.4	9.80	0.58	0.36	0.209
8.00	269.0	18.25	47.2	12.68	0.63	0.39	0.246
9.00	302.7	20.75	53.6	16.22	0.68	0.43	0.292
10.00	336.3	22.75	58.8	19.77	0.72	0.45	0.324
12.00	403.6	27.50	71.2	28.67	0.82	0.51	0.418
14.00	470.8	32.00	82.7	38.92	0.91	0.56	0.510
16.00	538.1	36.00	93.2	50.04	1.02	0.59	0.602
18.05	607.0	40.50	104.7	63.51	1.12	0.65	0.728
20.05	674.3	45.00	116.3	78.39	1.22	0.69	0.842



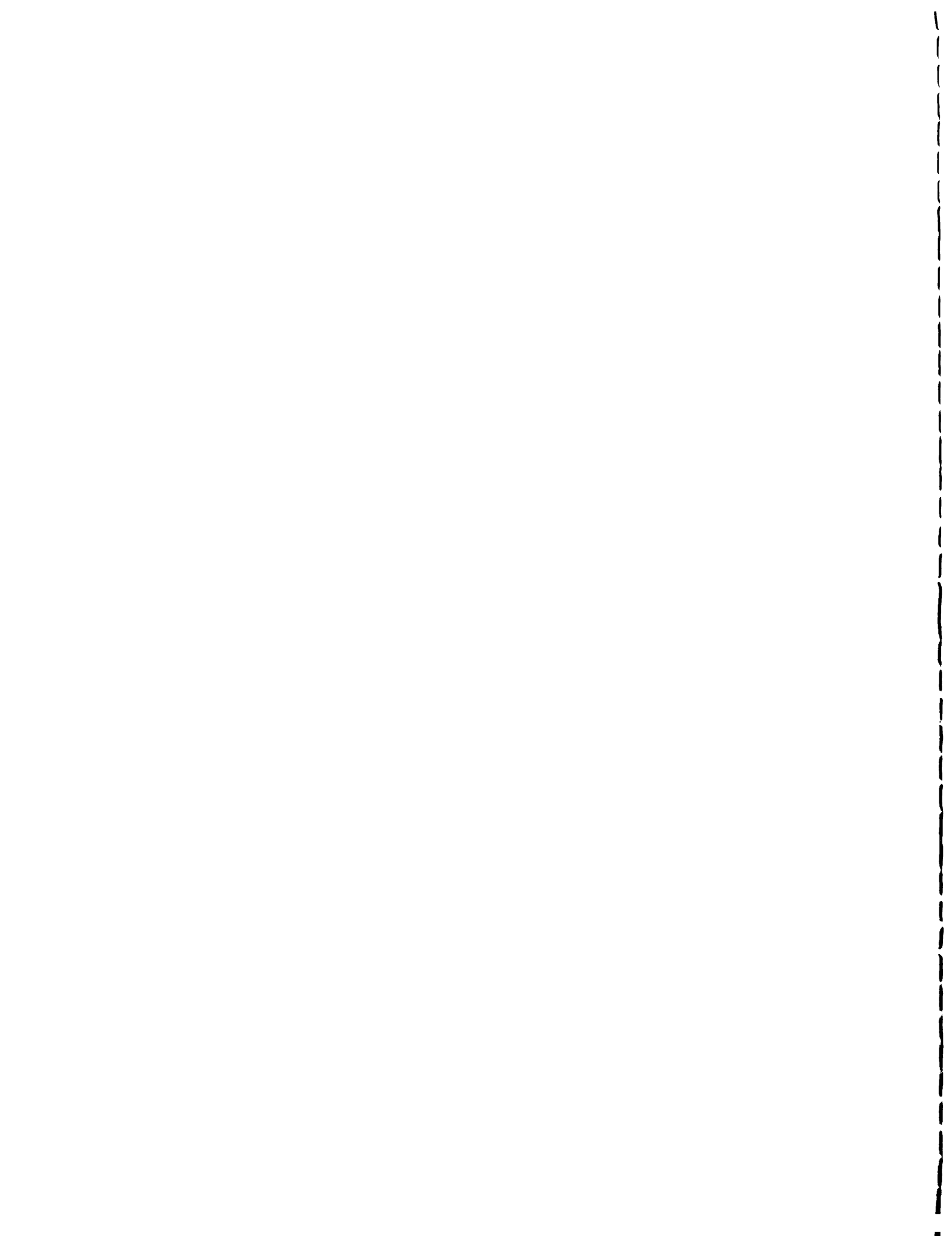


TABLE A 6

The Effect of the Distance of Down Stream Electrode  
From the Pad

Distance From Cellulose cm	Pure Water			CO <sub>2</sub> Saturated Water		
	Voltage m.V.	Current $\mu$ A	Resistance K $\Omega$	Voltage m.V.	Current $\mu$ A	Resistance K $\Omega$
0.0	57.0	.100	559	1.72	0.15	11.47
0.1	62.0	.096	646	---	---	---
0.2	68.0	.088	773	2.52	0.20	12.60
0.4	74.5	.066	1128	2.75	0.20	13.75
0.6	73.5	.052	1413	2.70	0.19	14.21
0.8	73.5	.044	1670	2.68	0.18	14.89
1.0	73.0	.040	1825	2.68	0.17	15.76
2.0	72.5	.028	2589	2.68	0.15	17.87
3.0	72.0	.022	3273	---	---	---

Distance From Cellulose	(.005M) KCl Solution			(.01M) KCl Solution		
	Voltage m.V.	Current $\mu$ A	Resistance K $\Omega$	Voltage m.V.	Current $\mu$ A	Resistance K $\Omega$
0.0	0.33	0.16	2.06	0.47	0.29	1.62
0.2	0.38	0.18	2.11	0.47	0.29	1.62
0.4	---	---	---	0.47	0.29	1.62
0.6	0.44	0.20	2.20	0.48	0.29	1.66
0.8	0.47	0.22	2.14	0.50	0.29	1.72
1.0	0.51	0.23	2.22	0.49	0.28	1.75
1.5	0.55	0.24	2.29	---	---	---
2.0	0.56	0.23	2.43	0.49	0.27	1.82

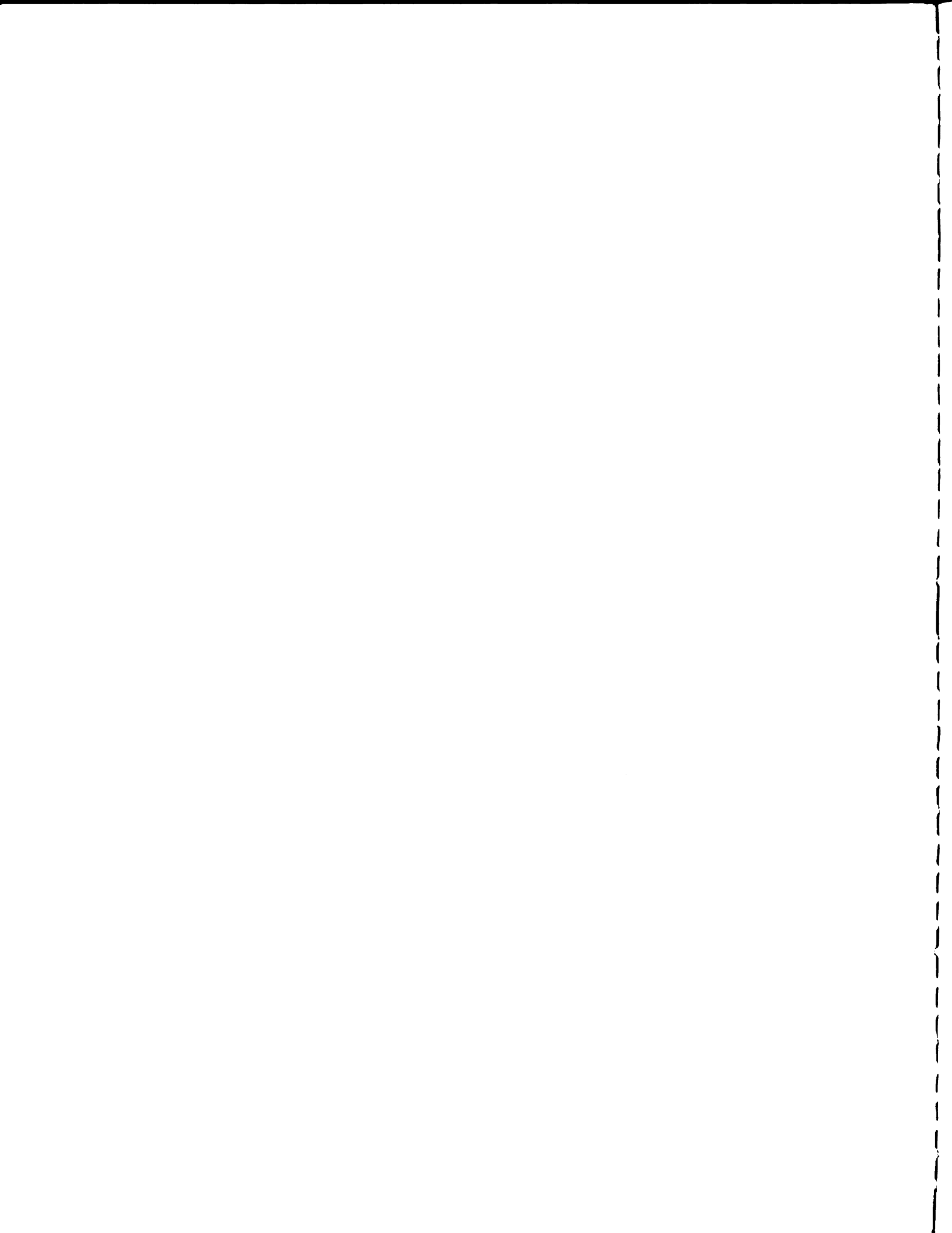


TABLE A 7

The Effect of Flow of Deionized Distilled Water  
Through Glass Fiber Pad (22.6°C)

	$\Delta P$	Flow Rate		Potential Energy	Voltage	Current	Electric Energy
in Hg	$10^3$ dyne/cm <sup>2</sup>	ml/min	$10^{-3}$ cm/sec	$10^3$ erg	+m.V.	+ $\mu$ .A.	$10^{-2}$ erg
0.25	8.4	0.40	4.3	0.036	47	0.12	0.056
0.50	16.8	0.85	9.2	0.155	114	0.28	0.319
1.05	35.3	1.60	17.3	0.612	238	0.48	1.142
2.05	69.0	3.15	34.1	2.35	480	0.87	4.176
3.00	100.9	4.60	49.8	5.03	694	1.20	8.328
4.0	134.6	6.00	65.0	8.75	900	1.50	13.50
5.0	168.2	7.40	80.2	13.49	1128	1.80	20.30
6.0	201.9	8.75	94.8	19.13	1350	2.20	29.70
7.0	235.5	10.00	108.3	25.51	1576	2.50	39.40
8.0	269.2	11.00	119.2	32.07	1805	2.80	50.54
9.0	302.8	12.00	130.0	39.36	2030	3.20	64.96
10.0	336.5	13.25	143.5	48.29	2260	3.50	79.10
11.0	370.1	14.25	154.4	57.13	2475	3.90	96.53
12.0	403.8	14.75	159.8	64.51	2664	4.20	111.89
14.0	471.1	16.75	181.4	85.47	3095	4.80	148.56
16.0	538.4	18.75	203.1	109.34	3490	5.40	188.46
18.0	605.6	20.25	219.4	132.85	3840	5.90	226.56
20.0	672.9	21.75	235.6	158.55	4200	6.50	273.00

Note: The inlet of the flow was 1.4 cm only.

MICHIGAN STATE UNIVERSITY LIBRARIES



3 1293 03142 8628